Metabolism of Antioxidants and Nitrosothiols in Barley (*Hordeum vulgare* L.) Seeds during Germination and Seedling Growth

by

© Zhenguo Ma

A thesis submitted to
the School of Graduate Studies
in partial fulfilment of requirements for the
degree of Doctor of Philosophy

Department of Biology
Memorial University of Newfoundland
January, 2016
St. John's Newfoundland and Labrador

Abstract

In the process of seed germination, antioxidant metabolism in barley seeds is intensified. Production of reactive oxygen and nitrogen species, and activities of enzymes scavenging these reactive species such as ascorbate peroxidase, monodehydroascorbate reductase, dehydroascorbate reductase, glutathione reductase, catalase, superoxide dismutase and *S*-nitrosoglutathione reductase, increased in germinating barley seeds instead of non-germinated more dormant Sundre seeds. Meanwhile the content of total ascorbate and glutathione and the rate of fermentation dropped in germinating seeds. Sharp decrease in glutathione content in embryos of barley seeds led to a dramatic increase in reduction potential of glutathione disulfide/glutathione couple. High levels of adenosine triphosphate and adenosine diphosphate were observed during the first few hours of germination but later their content decreased with a concomitant increase in their ratio in germinating seeds. Expression of the gene encoding alcohol dehydrogenase III declined in Harrington seeds from the onset of germination, while expression of the gene encoding hemoglobin was elevated within the first few hours and later declined, and the expression of the both genes did not change significantly in Sundre seeds. In the process of further transition from imbibition of dry Harrington seeds to seedling growth, glyoxylate cycle and citric acid cycle in scutellum became more active in the first few days, as evidenced by the increased activities of isocitrate lyase and malate synthase in glyoxylate cycle and succinate dehydrogenase and fumarase in citric acid cycle. During this period, the content of malic acid, succinic acid, and overall pH

value declined in both scutellum and endosperm of Harrington seeds. In the endosperm, the content of succinic acid was much lower than malic acid and citric acid. The level of citric acid in scutellum was high and maintained stable while its level in endosperm was low. The increase of H_2O_2 production was observed during the process of seed germination and early period of seedling growth. In summary, the antioxidant metabolism, metabolism of reactive oxygen and nitrogen species, glyoxylate cycle and citric acid cycle were found to be more active during seed germination and early period of seedling growth.

Key words: barley seeds, antioxidants, reactive oxygen and nitrogen species, glyoxylate cycle, citric acid cycle

Acknowledgements

I appreciate my supervisors, Dr. Abir U Igamberdiev and Dr. Natalia V Bykova for their support in my Ph. D education during the past five years in the Memorial University of Newfoundland (MUN). They have given me huge help in scientific research in both their own laboratories and research cooperation with Dr. Frédéric Marsolais, an excellent scientist in Southern Crop Protection and Food Research Center, Agriculture and Agri-Food Canada where I learned some important molecular biotechniques with his guidance. In addition, Dr. Mark Bernards, an outstanding professor in Department of Biology, the University of Western Ontario and Dr. Frédéric Marsolais together gave me essential assistance in GC-MS experiments, both of whom I am grateful to very much. I also have to thank my committee members, Dr. Brian Staveley and Dr. Kapil Tahlan, for their work in my Ph. D programme. In the period of my study in MUN, the help given to me was from multiascpect such as R training, service of the secretary and technician of the Biology Department, MUN and free barley seeds from Crop Development Center Breeder Seed Facility, University of Saskatchewan. Here, I express my sincere appreciation to all of the people giving me assistance.

Contents

List of tables

List of figures

Abbreviation

ABA: abscisic acid

ADH: alcohol dehydrogenase

ADH3: *alcohol dehydrogenase III*

ADP: Adenosine diphosphate

AMP: Adenosine 5'-monophosphate

APX: ascorbate peroxidase

APX: *ascorbate peroxidase*

Asc: ascorbate

ATP: adenosine triphosphate

CAT: catalase

CL: chemiluminescence

cPTIO: 2-(4-carboxyphenyl)-4,4,5,5-tetramethylimidazoline-1-oxyl-3-oxide

cPTI: 2-(4-carboxyphenyl)-4,4,5,5-tetramethylimidazoline-1-oxyl

DCPIP: 2,6-dichlorophenol indophenol

DHA: dehydroascorbate

DHAR: dehydroascorbate reductase

DPI: diphenyleneiodonium

DTNB: 5,5'-dithiobis-(2-nitrobenzoin acid)

DTT: dithiothreitol

EDTA: ethylenediaminetetraacetic acid

ETC: electron transport chain

FID: flame ionization detector

FW: fresh weight

GAs: gibberellic acids

GC: gas chromatograph

GC-MS: gas chromatograph-mass spectrometer

GR: glutathione reductase

GSH: glutathione

GSNOR: *S*-nitrosoglutathione reductase

GSSG: glutathione disulfide

h: hour

Hb: hemoglobin

Hb: *hemoglobin*

ICL: isocitrate lyase

LDH: lactate dehydrogenase

M: marker

MDHA: monodehydroascorbate

MDHAR: monodehydroascorbate reductase

MS: malate synthase

NAD: nicotinamide adenine dinucleotide

NAD(P)H: reduced nicotinamide adenine dinucleotide (phosphate)

NEM: N-ethylmaleimide

NO: nitric oxide

NOS: NO synthase

NR: nitrate reductase

NTC: no template control

PEP: phosphoenolpyruvic acid, (phosphoenolpyruvate)

PEPCK: phosphoenolpyruvate carboxykinase

PMSF: phenylmethylsulfonyl fluoride

PPDK: pyruvate-phosphate dikinase

PPi: pyrophosphate

PVP: polyvinylpyrrolidone

PVPP: polyvinylpolypyrrolidone

RNS: reactive nitrogen species

ROS: reactive oxygen species

RSNO: *S*-nitrosothiol

RT PCR: Real-Time Polymerase Chain Reaction

SDS-PAGE: sodium dodecyl sulfate-polyacrilamide gel electrophoresis

SNP: sodium nitroprusside

SOD: superoxide dismutase

TMS: trimethylsilyl

TNB: 5-Thio-2-nitrobenzoic acid

Appendices

1 Introduction

1.1 Definition of seed germination and dormancy

Seed germination is a complex process starting from water uptake of dry seeds to elongation of embryonic axis (Bewley, 1997). Weitbrecht et al. (2011) divided seed germination into three phases: I, II and III. The early phase (phase I) includes imbibition of dry seeds plus early plateau phase of water uptake. The middle phase (phase II) includes the plateau phase of water uptake and visible radicle protrusion through seed covering layers (Figure 1). The later phase of seed germination (phase III) corresponds to seedling establishment (Figure 1). As dormant seeds can not complete the process of phase II, they will not go to the phase III also called the post-germination phase (Bewley, 1997) to establish seedlings. Seed germination is influenced by many factors such as water, temperature, oxygen, reactive oxygen species (ROS), reactive nitrogen species (RNS), abscisic acid (ABA) and gibberellic acids (GAs) (Bewley, 1997; Šírová et al., 2011). Besides these elements, adenosine triphosphate (ATP) production is essential to seed germination (Perl, 1986). Accumulation of ATP, the most dominant energy currency for biological metabolism in cells, reaches to high levels, compared to dry seeds which contain very low levels of it. At beginning of seed germination, oxygen consumption increased with imbibition (Bewley, 1997). Therefore, the internal environment of seeds would experience hypoxia, during which glycolysis or fermentation plays an important role in the production of ATP.

Dormancy is a key characteristic of seeds and is a vital element in the life cycle of plants (Koornneef et al., 2002). Baskin and Baskin (2004) defined seed dormancy as "Dormant seeds do not have the capacity to germinate in a specified period of time under any combination of normal physical environmental factors that are favorable for germination". Dormant seeds are viable and alive. They will germinate when their dormancy is broken.

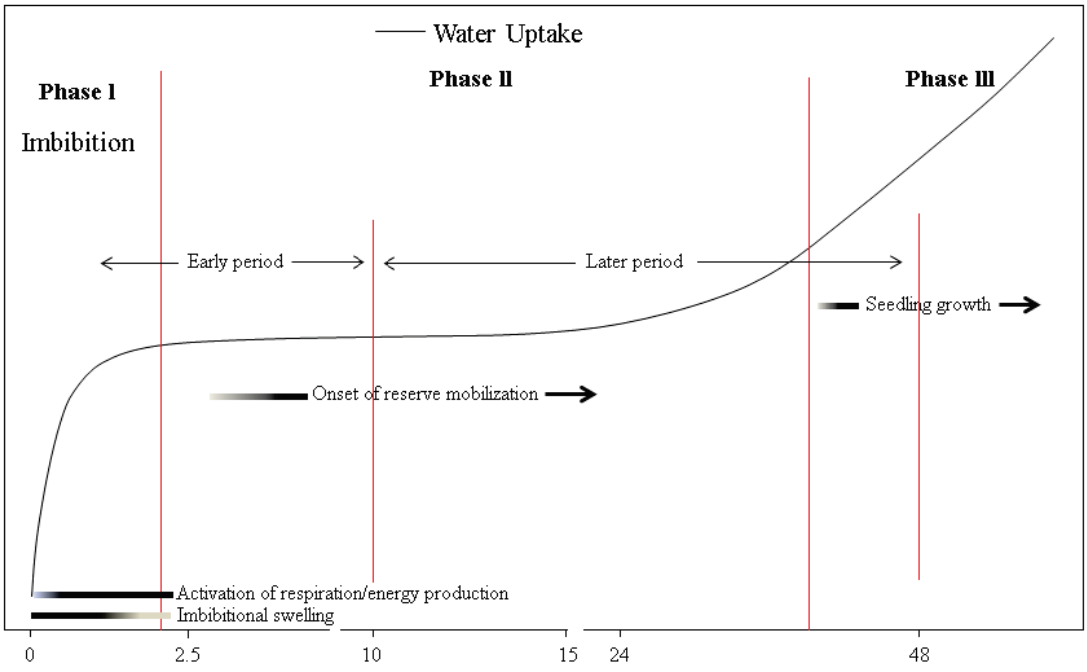

Figure 1 Key processes during germination of typical endospermic eudicot seeds

Weitbrecht et al. (2011)

1.2 The production and role of reactive oxygen species

In the process of seed germination, many ROS are generated such as hydrogen peroxide (H_2O_2), hydroxyl radical ($^{\bullet}OH$) and superoxide anion ($O_2^{\bullet-}$), which exist in all stages of seed development including dry seeds (El-Maarouf-Bouteau and Bailly, 2008; Bønsager et al., 2010). ROS have a dual role in regulation of seed germination. "Oxidative Window" has been used to describe the threshold of their amount for germination. If the concentration of ROS is within the oxidative window, dormancy of seeds will be broken and germination will start. ROS interplay with relative signal molecules such as hormones or RNS to trigger gene expression or redox reactions to initiate seed germination. If the concentration of ROS is lower than the oxidative window, seeds will remain dormant and germination will not occur. On the contrary, if the content of ROS is higher than the oxidative window, they will cause oxidative damage, thereby inhibiting germination or leading to abnormal seedlings (Bailly et al., 2008), demonstrating optimum content of ROS adjusted by homeostasis to seed germination is of huge importance.

1.3 Ascorbate-glutathione cycle

The ascorbate-glutathione cycle, a vital antioxidant system in plants, plays a crucial role in ROS scavenging in plants (Figure 2; Teixeira et al., 2005). In this cycle, ascorbate peroxidase (APX, EC 1.11.1.11) reduces H_2O_2 to H_2O by consuming two molecules of ascorbate, generating two molecules of monodehydroascorbate (MDHA).

MDHA can be reduced to ascorbate directly by MDHA reductases (MDHAR, EC 1.6.5.4) with consumption of reduced nicotinamide adenine dinucleotide (phosphate) (NAD(P)H) (Foyer and Halliwell, 1976). Another way of re-generating ascorbate is reduction of dehydroascorbate (DHA), catalyzed by dehydroascorbate reductase (DHAR, EC 1.8.5.1) with consumption of two molecules of glutathione (GSH). One molecule of glutathione disulfide (GSSG) is produced in this way, where DHA is from nonenzymic disproportionation of MDHA (Foyer and Halliwell, 1976). GSSG is reduced to GSH by NADPH, catalyzed by glutathione reductase (GR, EC 1.8.1.7). In summary, H_2O_2 is reduced to H_2O by electrons derived from NADPH and there is no net consumption of ascorbate and GSH, but they participate in transient redox reactions during the process. The above series of reactions is called the ascorbate-glutathione cycle (Noctor and Foyer, 1998). Besides this cycle, superoxide dismutase (SOD, EC 1.15.1.1) transforming superoxide ($O_2^{\bullet-}$) to O_2 and H_2O_2 (Alscher, 2002), and catalase (CAT, EC 1.11.1.6) transforming H_2O_2 into H_2O and O_2 (Chelikani et al., 2004), are important enzymes for detoxifying ROS. In plants, there are three classes of SOD: Cu/Zn-SOD in chloroplasts and cytosol, Mn-SOD in mitochondria and peroxisomes (Rabinowitch and Fridovich, 1983; Sandalio et al., 1987) and Fe-SOD in chloroplast (Van Breusegem et al., 1999) even though probably not all of them exist in seeds.

1.4 Calculation of reduction potential

With imbibition of dry seeds, reactivation of mitochondrial metabolism, production of ROS, transportation of storage compounds and a great number of redox reactions influence redox state of seeds greatly. Reduction potential is one parameter to demonstrate redox status of cells, which is calculated by the following formula (Schafer and Buettner, 2001):

$$E_{hc} = E^{o\prime\prime} - 2.303RT/(nF) \log Q$$

E_{hc} is reduction potential of the GSSG/2GSH half-cell, the voltage of an electrochemical cell under experimental conditions; $E^{o\prime\prime}$ (-0.240 V) is the voltage of an electrochemical at 25 ºC (T=298.15 K) at pH 7; 2.303 is the conversion factor for ln into $\log_{10}$; R, 8.314 J K^{-1} mol^{-1}, is the gas constant; T is the temperature in Kelvin; n is the number of electrons exchanged in the chemical process (In the reaction transforming GSSG to GSH, n=2); value of F, the Faraday constant, is 9.6485 x 10^4 C mol^{-1}; Q is the mass action expression, which is calculated as follows:

If a chemical reaction is: $aR_1 + bO_1 = cR_2 + dO_2$, then $Q = [R_2]^c [O_2]^d/([R_1]^a [O_1]^b)$.

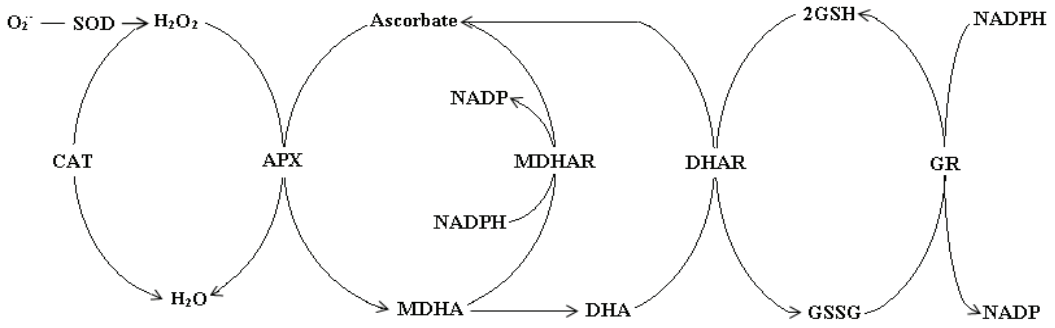

Figure 2 Ascorbate-glutathione cycle for scavenging ROS

GSSG/2GSH couple is abundant in barley seeds. Therefore, in this research it was used to calculate reduction potential in the seeds, by which quantitative redox biochemistry was demonstrated preliminary.

1.5 The role of nitric oxide in regulation of seed germination and dormancy

RNS include nitric oxide (NO) and a group of relative molecules such as peroxynitrite ($ONOO^-$), dinitrogen trioxide (N_2O_3), *S*-nitrosothiols (RSNOs), and all NO derivatives that can affect NO-dependent modifications (Nathan, 2004; Valderrama et al., 2007). In plants, NO, a short-lived inorganic, gaseous free radical, plays a vital role in regulating seed dormancy and germination, diffusing easily through cell membranes (Stamler et al., 1997; Siddiqui et al., 2011). NO is synthesized by nitrate reductase (NR) (Rockel et al., 2002), NO_2^-/NO-reductase (Stöhr et al., 2001), NO synthase (NOS) (Foresi et al., 2010), NO reductase of mitochondrial electron transport chain (ETC) (Gupta and Igamberdiev, 2011) and non-enzymatic conversion of nitrite (del Río et al., 2004; Leitner et al., 2009). NR can reduce both nitrate and nitrite to produce NO with addition of NAD(P)H *in vivo* and *in vitro* (Yamasaki, 2000; Rockel et al., 2002), which is the first confirmed mechanism to generate NO (Crawford, 2006). However, NO production in plants is still controversial.

Results from many experiments demonstrate that NO is involved in germination (Hendricks and Taylorson, 1974) and dormancy release of seeds (Sarath et al., 2006). Generation of NO under seed coat increases upon depletion of oxygen during

germination of apple seeds which supports redox and energy balance together with activation of fermentation processes (Igamberdiev and Hill., 2014). When internal environment of seeds is anaerobic during germination process, NO is actively produced. In addition, nitrite, azide and hydroxylamine promote germination of seeds through putative conversion of these chemicals into NO (Hendricks and Taylorson, 1974). The stimulation effect is similar to exert gaseous nitrogen oxides (Cohn and Castle, 1984). Dormancy of barley seeds is released by sodium nitroprusside (SNP), a NO donor, but strengthened by 2-(4-carboxyphenyl)-4,4,5,5-tetramethylimidazoline-1-oxyl-3-oxide (cPTIO), a NO scavenger, during imbibition of the seeds (Bethke et al., 2004), where SNP releases •NO through light-catalyzed reaction:

$$[Fe^{II}(CN)_5NO]^{2-} \xrightarrow[H_2O]{h\nu} [Fe^{III}(CN)_5H_2O]^{2-} + \bullet NO$$

However, when SNP produces NO, cyanide is generated (Arnold et al., 1984), a toxic chemical which is an inhibitor of complex IV in ETC (Farge et al., 2002). In addition, SNP can not overcome the inhibition effect of ABA on germination of seeds (Bethke et al., 2004). The outcome from decomposition of SNP indicates that its effects on seed germination will be complex, which of them will be dominant will depend on materials and dosage of SNP.

1.6 *S*-Nitrosylation of proteins

The synthesis of RSNO is controversial and discussed by many researchers. Wang et al. (2002) believed that RSNO originates from the reaction of thiol (RSH) and NO

derivatives such as NO_2^-, NO_2 (N_2O_4) and N_2O_3, and NO_2^- is the main form to combine with RSH in acid condition to form RSNO. Stamler et al. (1992) suggested that NO and thiol groups in proteins react directly to form *S*-nitrosothiols but Sundquist (1995) found that pure NO could not react with GSH to form GSNO in deoxygenated solution by bubbling. When oxygen is present, pure NO reacts with GSH to form GSNO and nitrite but not nitrate, where actually GSH reacts directly with N_2O_3 generated from NO and O_2. *S*-nitrosylation of proteins is a post-translational modification (Moreau et al., 2010), which is crucial to adjustment of protein functions.

S-nitrosylation is not catalyzed by enzymes but by acid-base catalysis. Therefore, reactivity and concentration of substrates have obvious influence on the reaction, and the covalent modification of proteins is fragile under physiological conditions (Martínez-Ruiz and Lamas, 2004). Under physiological phosphate buffer (pH 7.4) at 25 ºC, the half-life of *S*-nitrosoproteins was about 24 hours (Stamler et al., 1992). Formation of nitrosothiols in ionisable cysteines or thiolate anion in proteins can be regulated by conformation of proteins and adjacent amino acid groups (Martínez-Ruiz and Lamas, 2004). For example, in relaxed conformation of Hbs, having high affinity for O_2, NO binds with the sulfur in Cysβ93 close to histidine (basic amino acid) spatially, which was called base-catalyzed nitrosylation (Stamler et al., 1997). When conformation of Hbs is tense, having low affinity for O_2, nitrosolated Cys close to aspartate (acidic amino acid) decomposes to Cys and NO• (Arnelle and Stamler, 1995),

which is called acid-catalyzed denitrosylation (Stamler et al., 1997). Thus, the internal environment of cells such as concentration of O_2, pKa of thiols, protein conformation and pH impacts nitrosylation of proteins strikingly.

It is necessary to control NO levels for cell survival as NO could interact with many kinds of molecules because of its highly reactive property (Arc et al., 2013). NO can modify proteins to form nitrosothiols, as NO reservoir, by the processes such as cysteine *S*-nitrosylation or tyrosinenitration (Moreau et al., 2010). *S*-nitrosothiols, as NO carriers, are much more stable than NO itself (Stamler et al., 1992). In addition, *S*-nitrosylated proteins regulating seed germination and dormancy by releasing NO to signal transduction chain (Sen, 2010) could escape from scavenging NO. Thus, *S*-nitrosothiols including *S*-nitrosylated proteins play a crucial role in adjusting NO homeostasis in plants and they joined many physiological reactions. For example, in dry *Arabidopsis* seeds, a β-subunit of ATP synthase complex in mitochondria is *S*-nitrosylated, demonstrating that NO participates in regulation of ATP production in seeds (Arc et al., 2011). When external NO is applied, the quantity of *S*-nitrosylated proteins increases during germination of wheat seeds (Sen, 2010) and seed dormancy is released. On another side, *S*-nitrosylation of cytosol APX is responsible for decrease of its activity (de Pinto et al., 2013). Thus, protein nitrosylation regulates enzyme activities negatively. Maybe positive regulation of it will be discovered in the future or has been addressed.

1.7 Scavenging of NO

External cPTIO was applied to scavenge NO in many experiments (Bethke et al., 2004; Goldstein et al., 2003) by oxidizing NO to form $^{\bullet}NO_2$ radical: NO + cPTIO → $^{\bullet}NO_2$ + cPTI. $^{\bullet}NO_2$ can react with NO to form N_2O_3: $NO_2 + NO \rightarrow N_2O_3$ (D'Alessandro et al., 2013). In plants, GSNOR and hemoglobin (Hb) scavenge NO by corresponding biochemical reactions.

Hb interaction with NO is facilitated by MDHAR and ascorbate, by which NO is transformed into nitrate and NO is removed (Igamberdiev and Hill, 2004; Igamberdiev et al., 2005; Poole, 2005). Igamberdiev et al. (2005) described a Hb/NO cycle (Figure 3), where oxyhaemoglobin [$Hb(Fe^{2+})O_2$] oxygenates NO into nitrate being reduced itself into metHb [$Hb(Fe^{3+})$] (MetHb). MetHb reductase catalyzes transformation of MetHb to [$Hb(Fe^{2+})O_2$] by consuming half molecule of NAD(P)H. Nonsymbiotic Hbs in barley seeds are hypoxia-inducible, whose expression plays an key role in maintaining energy status of cells under hypoxic conditions (Sowa et al., 1998). Namely, if the internal environment in barley seeds is hypoxic in the process of germination, the produced Hbs will scavenge excessive NO, and the much ascorbate and active MDHAR in barley seeds will facilitate the reaction.

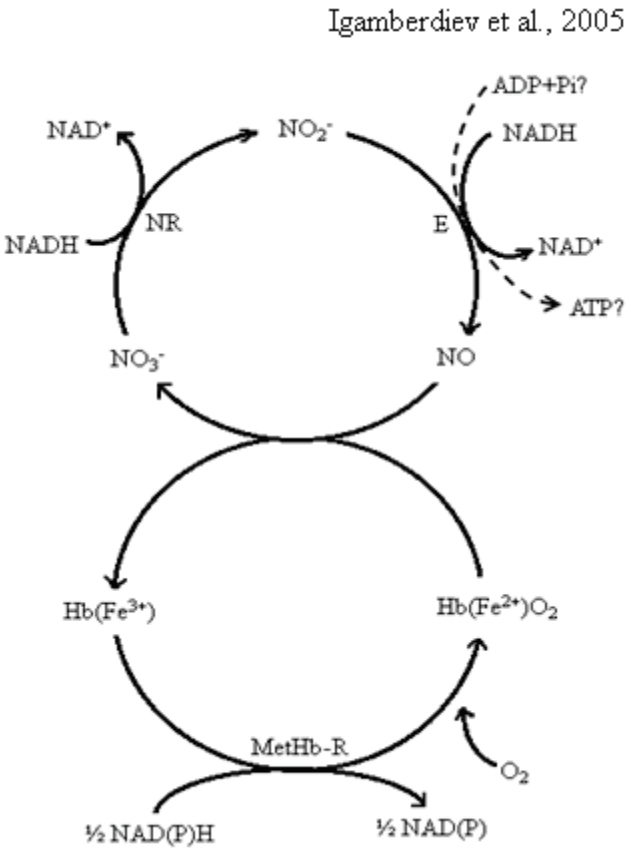

Figure 3 Suggested Hb/NO cycle

NR: nitrate reductase; E: putative NO sources in hypoxia including nitrate reductase, plasma membrane-bound nitrite:NO reductase, NO synthase and mitochondria

Besides reduction of NO by Hbs, denitrosylation of *S*-nitrosoglutathione (GSNO) is another way to metabolize NO, which is catalyzed by GSNOR. GSNO is a storage and transport form for NO in plants and seeds (Sakamoto et al., 2002), which has a crucial impact on content of NO in cells and on seed germination (Sakamoto et al., 2002; Holzmeister et al., 2011; Kwon et al., 2012). When GSNO decomposes to release NO,

GSNO can be reduced into GSSG or glutathione sulfinic acid, depending on concentration of GSH and oxygen in environment (Singh et al., 1996). If GSNO is reduced by GSNOR, one source of NO disappears, by which content of NO in tissue is regulated.

1.8 Tricarboxylic acid cycle and glyoxylate cycle

Once seeds are imbibed, metabolic activities resume. A key metabolic pathway supplying intermediates and energy to support seed germination and seedling growth is tricarboxylic acid (TCA) cycle, also called citric acid cycle (Figure 4; Botha et al., 1992), which provides many organic intermediates and much energy via oxidizing acetate into carbon dioxide. This cycle couples with oxidative phosphorylation to produce ATP (Buchanan and Amon, 1969; Fernie et al., 2004). Several enzymes are involved in the cycle such as succinate dehydrogenase (SDH, EC 1.3.5.1) and fumarase (EC 4.2.1.2).

A variation of the TCA cycle in seeds is glyoxylate cycle occurring in glyoxysomes, which is an anabolic pathway converting acetyl-CoA to succinate in plants (Donaldson et al., 2001). It has two specific enzymes, malate synthase (MS, EC 2.3.3.9) and isocitrate lyase (ICL, EC 4.1.3.1). Three other enzymes, malate dehydrogenase, citrate synthase and aconitase, are shared with TCA cycle. The product of glyoxylate cycle, succinate, is used to synthesize malate in TCA cycle (Popov et al., 2005; Kondrashov et al., 2006). By this pathway, plants can intake simple carbon sources such as acetate

to synthesize complex carbohydrate such as succinate and energy such as NADH and ATP in further steps (Figure 4; Lorenz and Fink, 2002) even though it is not a major metabolic pathway (Bao et al., 1998; Ke et al., 2000). In addition, acetate from β-oxidation of lipid could be used to synthesize glucose at the beginning of seed germination via TCA cycle and glyoxylate cycle in plants, by which seeds are able to use lipids as energy source to support development of shoots (Lorenz and Fink, 2002). Thus, glyoxylate cycle is involved in gluconeogenesis using storage lipid (Bortman et al., 1981). Therefore, glyoxylate cycle bridges lipid and carbohydrate metabolism in germinating seeds, and its activity is indicated by activity of ICL and MS (de los Reyes et al., 2003). Connecting to TCA or glyoxylate cycle, the reaction catalyzed by phosphoenolpyruvate carboxykinase (PEPCK) plays a key role in plant metabolism as it links metabolism of organic acids and sugar.

Except for PEPCK, SDH catalyzing conversion of succinate to fumarate in TCA cycle is crucial too, which is the only enzyme joining both TCA cycle and ETC (Oyedotun and Lemire, 2004). In the process of electron transport and ATP production in mitochondria, ROS are produced unavoidably and ETC is a major place to produce ROS (Moller, 2001). To protect themselves, plants have enzymes or antioxidants such as APX, CAT, SOD, GSH and ascorbate to scavenge ROS.

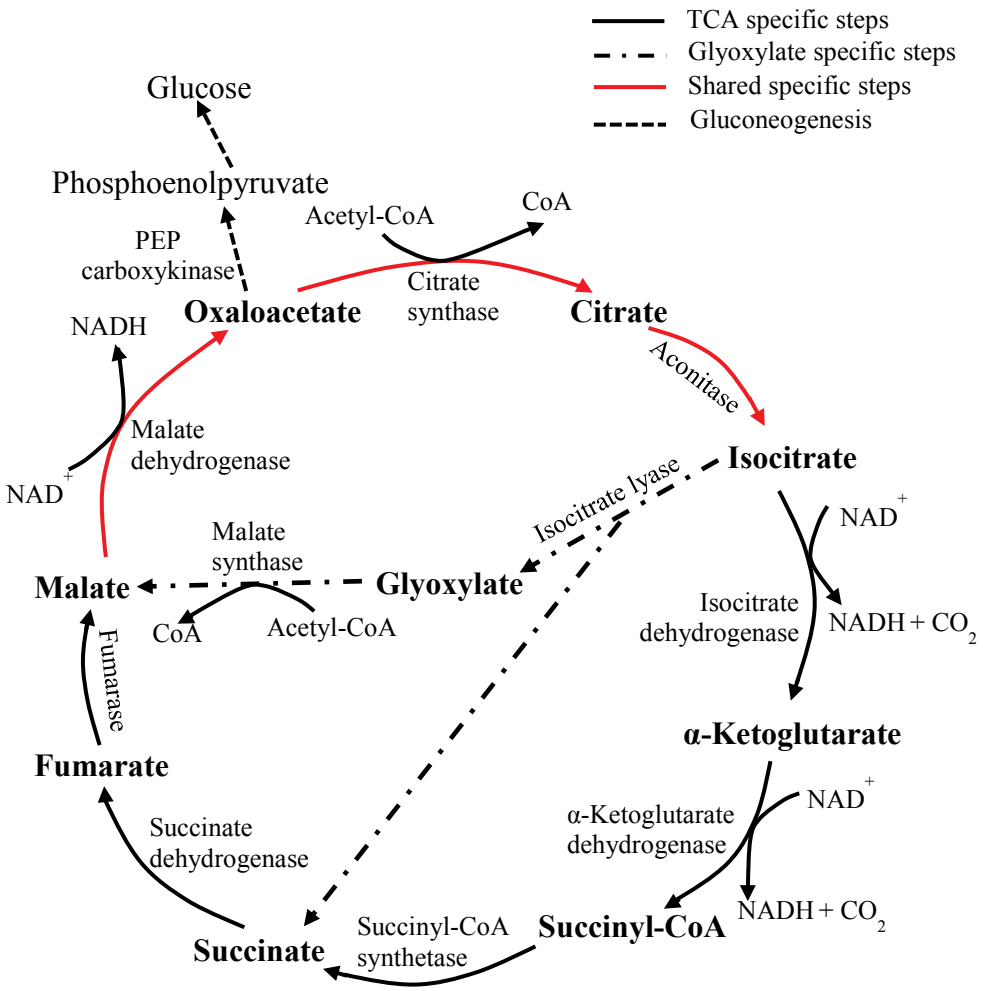

Figure 4 TCA cycle, glyoxylate cycle and gluconeogenesis

Lorenz and Fink, 2002

1.9 Acidification of endosperm

A great amount of energy is required to support physiological activities during seed germination. Before seeds intake nutrient from soil and become photoautotrophic, their energy supplies depend on mobilization of storage reserves, mainly starch, proteins and lipids (Bewley, 1997; Koornneef et al., 2002; Pritchard et al., 2002;

Sheoran et al., 2005). Barley seeds are similar to wheat seeds that energy reserves are mainly stored in the endosperm which is degraded for embryo growth during germination (Yu et al., 2014). Once the process of seed germination initiates, germination is fueled by soluble carbohydrate. Hydrolysis and mobilization of the main reserves in storage organs of seeds generally occurs concurrently (Bewley, 2001). One of the factors influencing digestion of starch is pH value in endosperm. In barley seeds, pH value of endosperm is about 4.5 because of organic acid secretion from surrounding tissue in late phase of seed maturation (Macnicol and Jacobsen, 1992), which is favorable to solubilization of starch (Hamabata et al., 1988) and stability of α-amylase (Bush et al., 1989). In addition, transportation of peptides from endosperm to scutellum is pH-dependent, and optimal value is 3.8-5.0 (Higgins and Payne, 1977). In the TCA cycle and glyoxylate cycle, several organic acids such as isocitric acid, citric acid, malic acid and succinic acid, are produced. In the process of seed germination and seedling establishment, these intermediates and their movements are crucial to growth of embryos and seedlings. With the release of organic acids and phosphoric acids from aleurone layer to endosperm, pH value in endosperm reaches approximately the value of 5 (Martínez-Camacho et al., 2004). Therefore, organic acids play an important role in regulating pH value in endosperm. Acidification of endosperm is favorable to several physiological processes such as starch mobilization, peptide transportation, phytate solubilization, hydrolytic activity of secreted enzymes, cell wall expansion and nutrient transportation (Higgins and Payne, 1977; Hamabata et al., 1988; Rayle and Cleland, 1992). The seeds and cells in the seeds are

compartmented. Thus, low pH value in endosperm will not influence activities of enzymes in other areas even though endosperm occupies the most volume of the barley seeds.

1.10 Anaplerotic role of glyoxylate cycle

When only two-carbon compounds such as ethanol, acetate or acetyl-CoA are available for synthesis of carbohydrate, and glycolytic intermediates and pyruvate are not available either, succinate, the product of glyoxylate cycle will play the anaplerotic role to produce oxaloacetate in microorganisms, and the cycle has a similar role in carbohydrate-starved tissue of plants (Graham et al., 1994; Eastmond and Graham, 2001). In barley seeds, starch is the main storage, and fermentation is very active at beginning of seed germination. Thus, a number of two-carbon molecules such as acetate and ethanol are produced (Lin and Oliver, 2008), which provides enough substrate for glyoxylate cycle. In seeds with storage of oil, the glyoxylate cycle plays a key role in taking advantage of stored oil during seed germination (Kornberg and Beevers, 1957; Beevers, 1980), which was also believed as essential for postgerminative growth and seedling establishment in oil plants (Eastmond et al., 2000). The glyoxylate cycle and gluconeogenesis are important in the process of oilseed germination and seedling establishment (Eckardt, 2005). In addition, the glyoxylate cycle and the TCA cycle must operate simultaneously for the glyoxylate pathway to function anaplerotically (Eastmond and Graham, 2001). However, in seeds with starch as major storage, how important it is has not been described very much yet.

In summary, metabolism of ROS and RNS is important for regulation of seed germination and dormancy, which has not been described thoroughly. The goal of this research, by observing metabolism of antioxidants, ROS and RNS in the two barley cultivars with different dormancy, is to clarify the role of them in regulating seed germination and dormancy, which has not been described systematically. The obtained characters were compared for the non-dormant and more dormant barley cultivars, by which the inherent characteristics of dormant seeds and their possible correlations with dormancy and how the ROS and RNS broke seed dormancy would be discussed. This information would bring some reference to barley breeding. In addition, besides understanding the intensity of antioxidant metabolism, the metabolism of glyoxylate cycle and TCA cycle from seed germination to seedling growth within 8 days was observed. This is helpful to know the difference of antioxidant metabolism and the importance or role of glyoxylate cycle between seed germination and seedling growth, and to prove the existence and activity of glyoxylate cycle in embryos of barley seeds.

2 Materials and methods

2.1 Materials

In experiments from 0 to 48 h, seeds of two barley cultivars, Harrington with fast uniform germination and Sundre with slow un-uniform germination speed (light dormancy) were used in this research. Whole seeds and isolated embryos were ground into fine powder in liquid nitrogen with mortars and pestles respectively. The ratio

between volume of extraction buffer to tissue weight was 1 ml : 20 mg fresh weight (FW) for embryos and 1 ml : 100 mg FW for whole barley seeds, and extraction of enzymes or proteins was performed on ice. The dormant or non-dormant Sundre seeds and embryos isolated from them within 9 h after imbibition could not be distinguished and therefore they represented a mixture of seeds with different germination potential. The data were from embryos of barley seeds or from whole barley seeds unless otherwise indicated.

In the experiments from 0 to 8 days, scutellum (Figure 5 A) and endosperm (Figure 5 B) were isolated from Harrington seeds soaked by sterile ddH_2O. In dry Harrington seeds, the embryos were taken as scutellum. The barley seeds were incubated in dark at 25 ºC for 0 (dry seeds), 1, 2, ……, 7 and 8 days, respectively (Figure 5 C). Endosperm and scutellum were isolated from them and the isolated tissue was ground into fine powder in liquid nitrogen with mortars and pestles. The ratio between volume of extraction buffer and tissue FW was 1 ml : 50 mg unless otherwise notified. In reactions to measure enzyme activities in the whole thesis, 50 µl of crude enzyme solution was added to final 1 ml of the reaction mixture, and on each time point there were three replicates, in each of which 50 seeds were used. The same number of the seeds were used when they were treated by chemicals applied in the research.

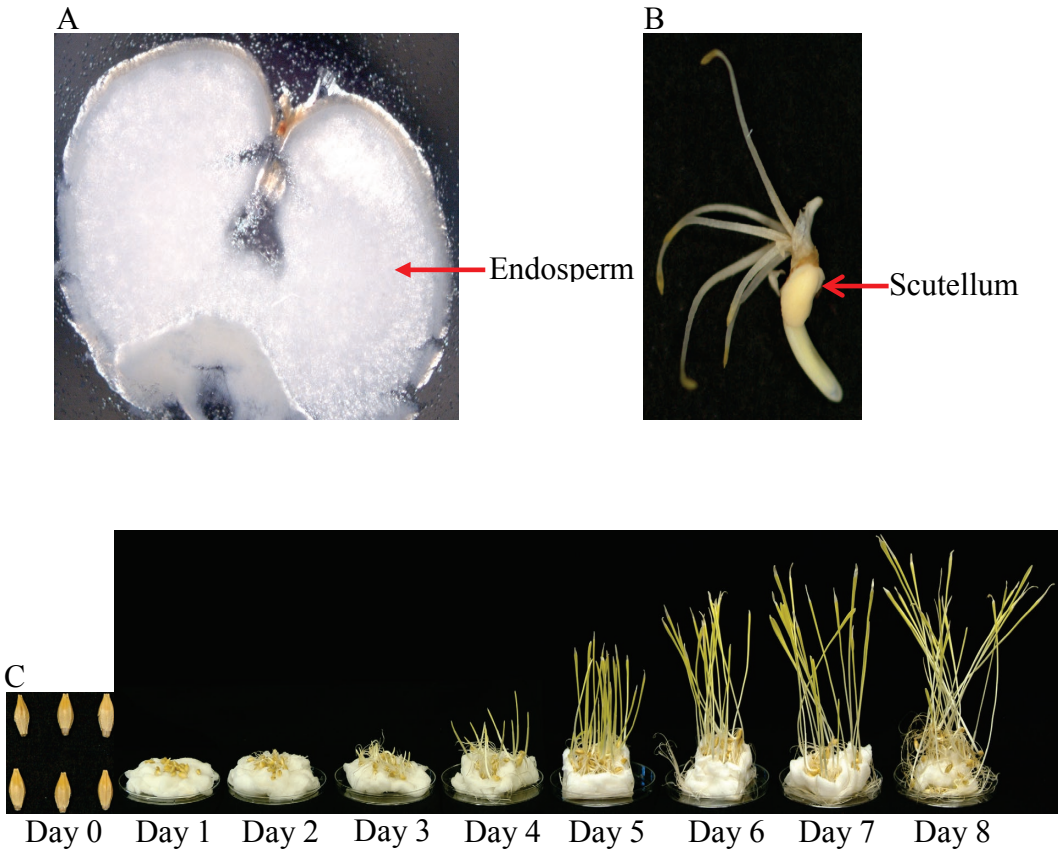

Figure 5 Endosperm and scutellum of Harrington seeds, and Harrington seeds germinating from 0 to 8 days

A: endosperm, B: scutellum, C: Harrington seeds germinating from 0 to 8 days

2.2 Methods

2.2.1 Measurement of germination rate and germination resistance of barley seeds

To measure germination rate of the two kinds of barley seeds, the seeds were imbibed in sterile ddH_2O for 15 minutes. After removing excessive water, 80 seeds of each cultivar were placed in a plastic Petri dish and incubated in an incubator for 24 h in dark at 23 ℃. The number of germinated seeds divided by the total number of seeds treated was used to calculate germination rate of the barley seeds. Embryos isolated from Sundre seeds were treated under the same conditions to observe embryo germination. Sundre seeds treated with 0.5 mM GA were taken as control.

To measure germination resistance, Sundre seeds were sterilized in 1% No DAMP (2.5% Oxine benzoate) for 1 h and 2% sodium hypochlorite for 20 minutes respectively, and they were rinsed with sterile ddH_2O for 4 times. 80 of the sterilized seeds were plated in each plastic Petri dish and extra water was removed from the Petri dishes. The Petri dishes were incubated in an incubator at 15 ℃ in dark for 21 days. The seeds were examined every day and the germinated ones were removed from the Petri dishes daily. Seeds with visible radicle or plumule protruding through seed coat were counted as germinated. The seeds soaked in sterile water and 0.5 mM GA were served as controls. The germination resistance was calculated when half of the seeds geminated using the following formula described by Gordon (1971):

$$\text{Germination resistance} = \frac{\frac{d_1}{2}(n_1) + [\frac{d_2 + d_1}{2}(n_2)] + \ldots + [\frac{d_i + d_{i-1}}{2}(n_i)]}{\mathcal{N}}$$

$d_1, d_2, \ldots, d_i$ are the first, second to ith day of germination counts
$n_1, n_2, n_3, \ldots, n_d$ are the number of seeds germinated on 1st, 2nd, 3rd to d_{th} day
N is the total number of seeds germinated

2.2.2 Measurement of concentration of total soluble proteins

Protein concentration was determined using the Bradford reagent (Sigma). Proteins extracted from fine powder of tissue with 50 mM HEPES buffer (pH7.0) containing 1 mM ethylenediaminetetraacetic acid (EDTA), 0.5% CHAPS and 0.5% SDS. 0.01 ml protein solution was mixed gently with 1.5 ml Bradford reagent (diluted 5 folds) and the mixture was incubated for 10 minutes at room temperature. Absorbance at 595 nm was recorded with a UV/Visible spectrophotometer (Biochrom Ultrospec 4300 spectrophotometer, Amersham, UK). If protein concentration in samples was higher than 1.4 mg/ml, samples have to be diluted by the same extraction buffer to measure. Otherwise, absorbance value will be out of the linear range. Bovine Albumin (MP Biomedicals) was used as a standard to plot the standard curve (Figure A1, Appendices).

2.2.3 Determination of profile of soluble proteins

Proteins were extracted from fine powder of embryo tissue ground in liquid nitrogen with 50 mM HEPES buffer (pH7.0) containing 1 mM EDTA, 0.5% CHAPS, 0.5%

SDS and 1% 2-mercaptoethanol at 4 ºC. Samples were centrifuged at 15000 g (Microfuge 22R Centrifuge, Beckman Coulter) at 4 ºC for 10 minutes and clear supernatants were used for further analysis. Protein profile was analyzed by sodium dodecyl sulfate-polyacrylamide gel electrophoresis (SDS-PAGE). 25 μg of each protein sample was loaded onto polyacrylamide gel consisting of 5% stacking gel and 12.5% separating gel in vertical electrophoretic unit (Mini-PROTEAN Tetra System, BIO-RAD). 150 v and 4 mA for 15 minutes were used to run stacking gel, and 200 v and 4 mA for 50 minutes were used to run separating gel. After fixing the gels in solution [50% methanol (v/v) and 10% acetic acid (v/v)] at room temperature for 45 minutes, they were stained by brilliant Coomassie Blue solution [10% (v/v) acetic acid and 0.006% (w/v) Coomassie blue] for 10 minutes. The stained SDS-PAGE gels were scanned after destaining the gels for half day in solution [30% (v/v) methanol and 10% (v/v) acetic acid].

2.2.4 Measurement of adenosine triphosphate and adenosine diphosphate

Extraction of ATP was conducted according to Joshi et al. (1989) and Yuroff et al. (2003). 25 mg of the tissue powder was lysed in 1ml ice-cold 2.4 M perchloric acid for 60 minutes on ice and the homogenate was centrifuged at 20000 g for 5 minutes at 4 ºC. Supernatant (0.5 ml) was collected and neutralized with 4 M KOH to about pH 6.0 measured by pH test paper. Samples were centrifuged again to collect the clear supernatant for ATP analysis. Quantification of ATP was performed by chemiluminescent analysis using ATP Detection Kit (Invitrogen) and its

corresponding standard curve (Figure A2 A, Appendices). 4 µl of neutralized solution was added into 100 µl standard reaction solution consisting of 1 x Reaction Buffer (Component E), 1 mM dithiothreitol (DTT), 0.5 mM D-Luciferin and 12.5 µg/ml firefly luciferase in deionized water. The reaction was initiated by adding ATP solution and the intensity of luminescence was measured by FB 12 Luminometer (Berthold Detection Systems GmbH, Germany).

Content of adenosine diphosphate (ADP) was determined using EnzyLight^{TM} ADP Assay Kit (EADP-100, BioAssay Systems). 25 mg of fine tissue powder was homogenized in 200 µl of ice cold 50 mM phosphate potassium (pH 7.0) and centrifuged at 12000 g for 5 minutes to pellet debris. Supernatant was used for ADP analysis. 10 µl of supernatant was mixed with 90 µl of ATP reagent and incubated for 10 minutes at room temperature with slight tapping. Intensity of luminescence (RLU A) was read using a luminometer. 5 µl of ADP reagent was added into the above mixture and mixed by tapping. After incubating for two minutes at room temperature, intensity of luminescence (RLU B) was measured. The concentration of ADP was calculated by the following formula:

$$[ADP]_{sample}\ (\mu M) = \frac{(RLU\ B)_{sample} - (RLU\ A)_{sample}}{Slope}$$

The slope was obtained from a standard curve (Figure A2 B, Appendices) plotted using a series of ADP (supplied in the kit) concentrations and corresponding intensity of luminescence.

2.2.5 Measurement of $O_2^{\bullet-}$ and H_2O_2

To extract $O_2^{\bullet-}$, fine powder of fresh tissue was homogenized in 8 M KOH for 20 minutes on ice and centrifuged for 10 minutes at 15000 g at 4 ºC. The concentration of superoxide anion in supernatants was measured by the method modified from Sun and Trumpower (2003) and Dahlgren et al. (2007). 0.1 ml 5 mg ml^{-1} cytochrome *c* was mixed with 1.397 ml of 0.2 M potassium phosphate buffer (pH 8.6) and 3 µl of the extract was added. The mixture was homogenized immediately and incubated for 15 minutes at 25 °C. Absorbance at 550 nm was determined using a spectrophotometer immediately. In the reference set, 50 units of commercial SOD (Sigma-Aldrich) and 100 units of commercial CAT (Sigma-Aldrich) were added to the solution. The value of extinction coefficient, 21.5 mM^{-1} cm^{-1}, was used for the reduced cytochrome *c* (Fe^{2+}). The amount of $O_2^{\bullet-}$ in solution was quantified on the base of a one-to-one molar stoichiometry between $O_2^{\bullet-}$ and cytochrome *c* molecules.

The concentration of H_2O_2 was measured according to the method of Lu et al. (2009). Fine powder of tissue was homogenized in 6% trichloroacetic acid for 30 minutes at 4 ºC, and the homogenate was centrifuged at 15000 g for 10 minutes, followed by the addition of insoluble polyvinylpolypyrrolidone (PVPP) (50 mg ml^{-1}). The samples were centrifuged at 15000 g for additional 3 minutes. The clear supernatant was diluted 1000 folds in 0.1 M sodium carbonate buffer (pH 10.2). The preparation of reagents followed the method of Pérez and Rubio (2006) and Lu et al. (2009). 10 ml of

6.5 mM luminol and 2 ml of 3 mM $CoCl_2$ in the sodium carbonate buffer were mixed, diluted to 100 ml in the same buffer and stored for at least one hour in dark. The solution was further diluted 10 times in the same buffer and stored at 4 ºC in dark overnight before use. 40 µl of each sample was mixed with 10 µl of the sodium carbonate buffer and the mixture was incubated at 30 °C for 15 minutes. 10 µl of 50000 U/ml CAT was added and incubated under the same condition as a control. 10 µl of each sample and 200 µl of the reaction reagent were added into 5 ml SARSTEDT tubes to measure chemiluminescence (CL) using a luminometer. The difference of CL response between each treatment and corresponding control was considered as CL specific for H_2O_2 in samples. The amount of H_2O_2 in tissue was calculated by the standard curve (Figure A3, Appendices) plotted by H_2O_2 solution (Sigma-Aldrich) and corresponding CL.

2.2.6 Measurement of enzyme activities

2.2.6.1 Measurement of enzymes involved in scavenging reactive oxygen species

The method for extracting the enzymes was modified from Murshed et al. (2008). The enzymes were extracted from fine powder of tissue with 50 mM MES-KOH buffer (pH 6.0) containing 40 mM KCl, 2 mM $CaCl_2$ and 1 mM ascorbate (added freshly) on ice. The samples were homogenized and then centrifuged at 15000 g for 10 minutes at 4 ºC. Supernatant was collected as a crude enzyme solution.

Methods for measuring activities of the enzymes in the ascorbate-glutathione cycle were modified from Palma (2006). The assay medium for APX was 50 mM potassium phosphate buffer (pH 7.0) containing 0.25 mM sodium ascorbate and 50 µl of the enzyme solution. The reaction was started by adding H_2O_2 to 0.25 mM and the reaction rate was determined spectrophotometrically by absorbance change at 290 nm (extinction coefficient for ascorbate = 2.8 mM^{-1} cm^{-1}). DHAR activity was measured in assay buffer containing 50 mM HEPES buffer (pH 7.0), 0.1 mM EDTA, 2.5 mM GSH, and 50 µl of the enzyme solution at 265 nm (extinction coefficient for ascorbate = 14 mM^{-1} cm^{-1}). The reaction was initiated by adding freshly prepared DHA to 0.8 mM. MDHAR activity was measured in 50 mM HEPES buffer (pH 7.6) containing 2.5 mM ascorbate, 0.25 mM NADH, and 50 µl of the enzyme solution. The assay was initiated by adding ascorbate oxidase to 2 U ml^{-1} and the reaction rate was monitored at 340 nm (extinction coefficient for NADH = 6.22 mM^{-1} cm^{-1}). GR activity was measured in 50 mM HEPES buffer (pH 8.0) containing 0.5 mM EDTA, 0.25 mM NADPH, and 50 µl of the enzyme solution (extinction coefficient for NADPH = 6.22 mM^{-1} cm^{-1}). The reaction was initiated by adding GSSG to final concentration of 1 mM. CAT activity was measured at 240 nm according to method of Matsumuraa et al. (2002). 25 µl of 1 M H_2O_2 was added to 0.975 ml 50 mM potassium phosphate buffer (pH 7.0) including 50 µl of the enzyme solution to start recording decrease of absorbance at 240 nm (extinction coefficient for H_2O_2 = 0.043 mM^{-1} cm^{-1}). In the above reactions, the change of absorbance was recorded for 3 minutes by a spectrophotometer.

Measurement of SOD activity was carried out according to a method described in Sigma-Aldrich and Gupta et al. (1993). SOD was extracted from tissue with 50 mM potassium phosphate buffer (pH 7.0) containing 0.1 mM EDTA and 1% (w/v) polyvinylpolypyrrolidone (PVPP). After centrifuging at 15000 g for 10 minutes at 4 ºC, the clear supernatant (crude enzyme solution) was used for determination of enzyme activity. A reaction cocktail consisting of 50 mM potassium phosphate buffer (pH 7.8), 0.1 mM EDTA and 50 µM xanthine was prepared. 50 µl of crude SOD solution and 50 µl 5 mg/ml cytochrome *c* on ice were mixed with 0.85 ml of the reaction cocktail and allowed to equilibrate until absorbance at 550 nm was constant and finally 50 µl 0.04 U/ml xanthine oxidase was added and mixed by inversion. The increase of absorbance at 550 nm was recoded for 2 minutes. The same volume of extraction buffer was added to the above reaction system to replace crude SOD solution for blank. The SOD activity in samples was calculated using a regression equation from a standard curve (Figure A4, Appendices). KCN was added into crude SOD solution to 2 mM to measure activity of Mn-SOD because 2 mM KCN can inhibit activity of Cu/Zn-SOD but not Mn-SOD. The activity of Cu/Zn-SOD was calculated by total SOD activity subtracting Mn-SOD activity. Commercial SOD (Sigma-Aldrich) was used to plot standard curve (Figure A4, Appendices) by the same protocol.

2.2.6.2 Measurement of S-nitrosoglutathione reductase

Determination of GSNOR (EC 1.2.1.46), a member of class ADH3 (Jensen et al., 1998), was modified from the method of Wunsche et al. (2011). GSNOR was extracted from tissue by 50 mM Tris-HCl buffer (pH 8.0) containing 0.1 mM EDTA. Supernatant collected after centrifuging for 15 minutes at 18000 g at 4 ºC passed through Sephadex G-10 column to desalt. 50 µl of the desalted enzyme solution was used to measure activity at 340 nm in final 1 ml of 50 mM Tris-HCl (pH 8.0) containing 0.4 mM GSNO and 0.2 mM NADH (Extinction coefficient for NADH = 6.22 mM^{-1} cm^{-1}). The reaction was initiated by adding GSNO and change of absorbance was recorded for 3 min at 25 ºC using a spectrophotometer. The reactions using ddH_2O to replace GSNO were taken as blank.

2.2.6.3 Measurement of enzymes involved in fermentation

Measurement of alcohol dehydrogenase (ADH, EC 1.1.1.1) was modified from Brzezinski et al. (1986). Both ADH and lactate dehydrogenase (LDH, EC 1.1.1.27) were extracted from tissue using buffer containing 0.1 M Tris-HCl (pH7.5), 1 mM EDTA and 5 mM DTT. After centrifuging at 15000 g for 10 minutes at 4 °C, clear supernatant was taken as crude enzyme solution. 0.8 ml 25 mM nicotinamide adenine dinucleotide (NAD) sodium salt in 0.1 M Tris-HCl, 150 µl 1 M ethanol and 50 µl of the crude enzyme solution were added into a cuvette and homogenized by inversion to measure enzyme activities. Ethanol was replaced with the same volume of ddH_2O for the blank. Determination of LDH activity was carried out according to the method of

Hoffman et al. (1986). 50 µl the crude enzyme solution was mixed together with 0.95 ml reaction buffer containing 0.1 M Tris-HCl (pH 7.5), 0.05 mM EDTA, 0.2 mM NADH and 20 mM sodium pyruvate by inverting three times. Sodium pyruvate was replaced by ddH_2O for the blank. For measuring both ADH and LDH, absorbance at 340 nm and 25 °C was recorded for 2 minutes using a spectrophotometer and extinction coefficient for NADH was 6.22 mM^{-1} cm^{-1}.

2.2.6.4 Measurement of phosphoenolpyruvate carboxykinase

Determination of PEPCK (EC 4.1.1.49) was modified from methods of Walker et al. (1999) and Delgado-Alvarado et al. (2007). The enzyme was extracted by homogenizing tissue powder with ice-cold buffer containing 200 mM Bicine-KOH (pH 9.0), 3 mM EDTA, 5% (w/v) polyethylene glycol (PEG) and 25 mM DTT. Samples were centrifuged at 12000 g at 4 °C for 15 minutes. Supernatant was collected and went through Sephadex G-10 columns as crude enzyme solution. The activity of PEPCK was determined in carboxylation direction. The assay mixture contained enzyme solution, 100 mM Hepes-KOH (pH 6.8), 100 mM KCl, 0.14 mM NADH, 0.25 mM DTT, 6 mM $MnCl_2$, 1 mM ADP, 90 mM $KHCO_3$ and 6 U/ml malate dehydrogenase. Reaction was initiated by adding PEP to the final concentration of 6 mM. The decrease of absorbance at 340 nm was recorded for 3 minutes at 25 °C using a spectrophotometer. In blank, PEP was replaced by ddH_2O. Extinction coefficient for NADH in the reaction was 6.22 mM^{-1} cm^{-1}.

2.2.6.5 Measurement of enzymes involved in citric acid cycle and glyoxylate cycle

The measurement of SDH was referred to Igamberdiev et al. (1995) and Popov et al. (2010). The enzyme was extracted with 50 mM Tris-HCl (pH 7.8) containing 1 mM EDTA and 2 mM DTT from fine powder of tissue on ice. Samples were centrifuged at 14000 g at 4 °C for 10 minutes. Supernatant was collected and passed through Sephadex G-10 columns to be taken as crude enzyme solution. Succinate prepared freshly was added up to 5 mM in the reaction mixture containing crude enzyme solution, 50 mM Tris-HCl (pH 7.8), 5 μM 2,6-Dichlorophenolindophenol (DCPIP), 0.1 mM phenylmethylsulfonyl fluoride (PMSF) and 1 mM KCN. The change of absorbance at 600 nm was recorded for 3 minutes using a spectrophotometer. In reduction of DCPIP, its extinction coefficient is 20.6 mM^{-1} cm^{-1} at 600 nm (Armstrong, 1964). Samples added ddH_2O to replace succinate in reactions were taken as blank.

Measurement of fumarase also called fumarate hydratase was referred to Jones (1980), Gibon (2004), and Zhang et al. (2011) and protocol of Sigma-Aldrich. Enzyme extraction was same to that of SDH. 50 μl of enzyme solution was mixed with 0.95 ml 50 mM L-malic acid in 50 mM Tris-HCl buffer (pH7.8). Increase of absorbance at 240 nm at 25 ºC was recorded for 3 minutes using a spectrophotometer. Reactions added ddH_2O to replace the enzyme solution were taken as blank. Extinction coefficient for fumarate at 240 nm is 2.44 mM^{-1} cm^{-1}.

Extraction of ICL was improved from the method of Schmidt et al. (1996). ICL was extracted from fine powder of samples with buffer containing 50 m M Tris-HCl (pH 7.0), 5 mM $MgCl_2$, 1 mM EDTA and 2 mM Cysteine on ice. Samples were homogenized and centrifuged at 15000 g at 4 ºC for 10 minutes. Supernatant was collected and passed through Sephadex G-10 columns as crude enzyme solution. Determination of the enzyme activity was referred to Meister et al. (2005). DL-isocitrate was added up to 10 mM in the reaction mixture containing 50 mM Tris-HCl (pH 7.2), crude enzyme solution, 5.0 mM $MgCl_2$, 2 mM L-Cysteine and 4 mM phenylhydrazine hydrochloride. Increase of absorbance at 324 nm was recorded for 3 minutes at 35 ºC using a spectrophotometer. In blank, DL-isocitrate was replaced by ddH_2O. Extinction coefficient for glyoxylic acid phenylhydrazine is 14.6 mM^{-1} cm^{-1}.

Measurement of MS (EC 4.1.3.2) was referred to the method of Beeckmans et al. (1994) and the protocol of Sigma-Aldrich. The enzyme was extracted by homogenizing fine powder of the tissue with extraction buffer containing 0.1 M HEPES (pH 7.8), 5 mM $MgCl_2$, 1 mM EDTA and 2 mM DTT on ice. Samples were centrifuged at 15000 g at 4 ºC for 10 minutes. Supernatant was collected and filtered through Sephadex G-10 columns as crude enzyme solution. The crude enzyme solution was mixed together with 6 mM $MgCl_2$, 5 mM sodium glyoxylate, 2.5 mM acetyl CoA and 2 mM DTNB in 0.1 M HEPES buffer (pH7.8) by inversion. Increase of absorbance at 412 nm was recorded for 3 minutes at 30 ºC using a spectrophotometer. In blank samples, sodium glyoxylate was replaced by ddH_2O.

Extinction coefficient for 5-Thio-2-nitrobenzoic acid (TNB) is 13.6 mM^{-1} cm^{-1} at 412 nm.

2.2.6.6 Measurement of pyruvate-phosphate dikinase activity

Pyruvate-phosphate dikinase (PPDK, EC 2.7.9.1) was measured according to the method of Aoyagi and Bassham (1983). PPDK was extracted from powdered tissue using 0.1 M Tris-HCl buffer (pH 7.5) containing 10 mM $MgCl_2$, 5 mM sodium pyruvate, 2 mM K_2HPO_4, 1 mM EDTA, 50 mM sodium ascorbate, 5 mM DTT and 1% PVP. After centrifuging at 15000 g at 4 ºC for 10 minutes, supernatant was collected for assaying the enzyme activity. 0.1 ml enzyme solution was added into 0.9 ml ATP production reagent containing 0.1 M Tris-HCl buffer (pH 7.5), 5 µM adenosine 5'-monophosphate (AMP) sodium salt, 304 µM sodium pyrophosphate (PPi), 560 µM phosphoenolpyruvic (PEP) acid trisodium salt, 1 mM DTT and 10 mM $MgCl_2$. The mixture was incubated at 37 ºC for 10 minutes. The reaction was stopped by adding 50 µl 1 M HCl. After neutralization of the ATP solution by 1 M KOH, determination of ATP content followed the protocol of ATP determination kit. Activity of the enzyme was calculated by the production of ATP.

2.2.6.7 Calculation of enzyme activity

Activities of enzymes were calculated according to the following formula unless otherwise indicated.

$$\text{Activity } (\mu\text{mol min}^{-1}\ \text{mg}^{-1}\ \text{protein}) = \frac{(A_{end} - A_{start})}{P \times T \times EC \times V_{reaction}}$$

A_{end}: absorbance at end of reaction, A_{start}: absorbance at beginning of reaction, $V_{reaction}$: volume of enzyme solution added into reaction (ml), P: concentration of proteins in enzyme solution (mg ml^{-1}), T: time of reaction between enzyme and substrate (minute), EC: extinction coefficient (mM^{-1} cm^{-1}). If absorbance in reactions decreased, (A_{start} - A_{end}) would be used to calculate the enzyme activities.

2.2.7 Measurement of ascorbate and glutathione

Ascorbate and GSH were extracted from 0.1 g tissue powder by 6% (v/w) trichloroacetic acid from tissue powder. The homogenate was centrifuged at 12000 g at 4 ºC for 20 minutes. Supernatant as extract of ascorbate and glutathione was used for determining content of them in tissue.

Content of ascorbate and DHA was determined according to the method of Gillespie and Ainsworth (2007). In the first step, total ascorbate including the part from reduction of DHA was measured. 100 µl 75 mM phosphate buffer (pH7.0), 100 µl 10 mM DTT and 200 µl of each extract were added into a 2 ml tube, which were mixed by slight vertex and incubated at room temperature for 10 minutes. 100 µl of 0.5% N-ethylmaleimide (NEM) in ddH_2O was added to the tubes and incubated for at least 30 seconds to remove the excess DTT. 500 µl 6% trichloroacetic acid, 400 µl 43% H_3PO_4, 400 µl 4% α,α'-bipyridyl and 200 µl 3% $FeCl_3$ were added into each tube. The samples were homogenized and incubated at 37 °C for 1 h. The absorbance of samples at 525 nm was determined using a spectrophotometer. 200 µl of extract was replaced by the same volume of 6% trichloroacetic acid in the same protocol to be set

up as blank. In the second step, the actual content of ascorbate in tissue was determined by the same protocol except that DTT was replaced by ddH_2O. Content of DHA in tissue was the difference between total ascorbate and actual content of it. The content of ascorbate was calculated using a standard curve (Figure A5 A, Appendices) plotted by a series of concentrations of (+)-Sodium L-ascorbate (Sigma-Aldrich) and their absorbance.

The measurement of GSH and GSSG followed the method described by Queval and Noctor (2007). In the first step, the total GSH in tissue including GSH converted from GSSG was determined. 1 ml of extract was neutralized with 1.5 ml 0.5 M potassium phosphate buffer (pH7.5). The final pH of all samples was between 5 and 6, which was measured by pH indicator paper. 10 mM 5,5'-dithiobis-(2-nitrobenzoin acid) (DTNB) was prepared in 0.1 M potassium phosphate buffer (pH7.5). 0.6 ml 0.1 M potassium phosphate buffer (pH 7.5) containing 5 mM EDTA, 0.1 ml 10 U/ml GR, 0.1 ml 5 mM NADPH in water and 0.1 ml 10 mM DTNB were mixed together. The reaction was initiated by adding 0.1 ml neutralized extract. After samples were homogenized by inverting cuvettes 2 or 3 times, they were monitored in a spectrophotometer at 412 nm for 1 minute. In blank, 0.1 ml neutralized extract was replaced by the same volume of neutralized extraction solution. Concentration of GSH was calculated using a standard curve (Figure A5 B, Appendices) plotted by L-cysteine (Sigma-Aldrich) and corresponding absorbance. The quantity of GSH in

tissue was the difference between quantity of GSH in the first step and the quantity of it in the second step.

In the second step, quantity of GSSG in tissue was measured. 0.5 ml neutralized extract was homogenized with 25 µl of 2-vinylpyridine and the mixture was vortexed vigorously for about 1 minute to form emulsion. Samples were incubated at room temperature for 60 minutes to remove GSH in solution with pH value higher than 5.5. To remove excess 2-vinylpyridine, the mixture was centrifuged twice and 100 µl of clear solution was used to measure GSH following the same protocol to the first step. One molecule of GSSG could produce two molecules of GSH by reduction reaction. Therefore, [GSSG] = [GSH]/2.

Calculation of redox potential of GSSG/2GSH couple followed to the formula described by Schafer and Buettner (2001) for half-cell reaction of the GSSG/2GHS couple at pH 7:

$$E_{hc}\ (mV) = -240 - (59.1/2) \log ([GSH]^2/[GSSG])$$

2.2.8 Determination of expression of ascorbate peroxidase, alcohol dehydrogenase III and hemoglobin during germination of barley seeds by Real-Time Polymerase Chain Reaction

2.2.8.1 Design of primers

Primers for *APX* (GenBank: AF411228.1), *ADH3* (GenBank: X12734.1) and *Hb* (GenBank: U94968.1) and *mub1* (GenBank: M60175.1) for Real-Time Polymerase Chain Reaction (RT PCR) were designed using NCBI/Primer-BLAST according to known cDNA sequence of the four genes (Figure A6, A7, A8 and A9, Appendices), where *mub1* was a reference gene. Specific primers of *APX*, *ADH3*, *Hb* and *mub1* were listed in table 1, which were synthesized by Eurofins. The sequence of *ADH3* was used to represent that of *GSNOR* in barley seeds as cDNA sequence of *GSNOR* in barley was not found in GenBank.

Table 1 Primers for the genes in RT PCR

Gene	Forward primer 5' to 3'	Reverse primer 5' to 3'
APX	AGCCCATCAAGGAGCAGTTC	CTGAGGTGGTCAGAGCCTTG
ADH3	GTCTCTCAACTGGACTTGGTG	CTTAGCTTGTTCGTATTTTGCAGG
Hb	ACCAACCCCAAGCTCAAGAC	CTGCCACGCCGTATTTCAAG
mub1	CACCGGCAAGGTAACCAG	GACATAGGTGAGTCCGCAC

2.2.8.2 Extraction of total RNA

Extraction of total RNA was carried out using the RNeasy Plant Mini Kit (QIAGEN) and all of the steps followed the standard protocol of its manufacturer. About 30 mg of embryo tissue frozen in liquid nitrogen was placed into RNase-free mortar containing 0.6 ml of buffer RLT. The tissue was ground with RNase-free mortars and pestles immediately. The suspension was transferred into RNase-free 1.5 ml tubes and was incubated for 3 minutes at 56 °C. The lysate was transferred to a QIAshredder spin column (lilac) placed in a 2 ml collection tube. The column was centrifuged for 2 minutes at 15000 rpm and supernatant of flow-through was transferred to a microcentrifuge tube without disturbing cell-debris pellet in the collection tube. 0.5 volume of the ethanol (100%) was added into the cleared lysate and mixed immediately by pipetting. The samples including precipitate in the tube were loaded onto an RNeasy spin column (pink) placed in a 2 ml collection tube and centrifuged for 15 seconds at 8000 g. The flow-through was discarded. 700 µl of Buffer RW1 was added into the RNeasy spin column and centrifuged for 15 seconds at 8000 g to wash the spin column membrane. The flow-through was discarded. The column membrane was washed twice by adding 500 µl of Buffer RPE to the RNeasy spin column and the spin column was centrifuged for 15 seconds at 8000 g. After discarding the flow-through, the RNeasy spin column was put in a new RNase-free 1.5 ml collection tube and 50 µl RNase-free water was added directly to the spin column membrane to elute RNA. After centrifuging at 12000 g for 1 minute, RNA solution was collected. Concentration of total RNA was measured using NanoDrop 1000 instrument (Thermo

Scientific) and 1.5 µg RNA was loaded onto 1% agarose gel and ran for 50 minutes at 100 voltage to observe the quality of the extracted RNA.

2.2.8.3 DNase I treatment of RNA

DNase I treatment of RNA followed the protocol of Ambion Kit (Life Technologies). Total reaction volume was set up as 50 µl and 10 µg RNA was treated even though 1 µg RNA was enough for the later experiments. 5 µl 10 x DNase I Buffer, 1 µl DNase I (2 U) and 10 µg RNA were mixed by slight vortex and final volume was adjusted to 50 µl by nuclease-free water. The samples were centrifuged briefly at 1000 rpm for 2 seconds to collect all of the components at bottom of the reaction tubes which were incubated at 37 °C for 30 minutes. After this, EDTA was added to 5 mM in the RNA solution, followed by heating for 10 minutes at 75 ºC to inactivate DNase I. The concentration of RNA was determined again using a NanoDrop 1000 instrument.

2.2.8.4 Reverse transcription of RNA

Reverse transcription of RNA followed the manufacturer's protocol for the qScript™ cDNA SuperMix (Quanta Biosciences). 1 µg RNA and 4 µl of qScript™ cDNA SuperMix were mixed into final volume of 20 µl adjusted by nuclease-free water. The samples were incubated on Thermometer (Mastercycler nexus gradient, Eppendorf) using the following program: 25 °C for 5 minutes, 42 °C for 30 minutes, 85 °C for 5 minutes and 4 °C for holding. The single strand cDNA was used as a template in the

following RT PCR. The cDNA synthesized in this step was diluted into a series of cDNA solutions (from 2 to 2056 folds) to determine efficiency of the primers.

2.2.8.5 Real-Time Polymerase Chain Reaction of ascorbate peroxidase, alcohol dedrogenase III and hemoglobin

RT PCR of *APX*, *ADH3*, *Hb* and *mub1* followed the manufacturer's protocol for the SsoFast™ EvaGreen® Supermix (Bio-Rad). 0.5 µl 10 µM forward primer, 0.5 µl 10 µM reverse primer, 1 µl cDNA (diluted 8 folds) and 5 µl SsoFast™ EvaGreen® Supermix were mixed and adjusted to 10 µl using nuclease-free water. Samples were transferred to 96-well plate and sealed tightly using a transparent membrane. No template control (NTC) was set up for each biological sample. The program for the RT PCR reactions was set up as enzyme activation at 95 °C for 30 seconds, followed by 40 cycles of 95 °C for 10 seconds and 58 °C for 30 seconds, performed with CFX96 Touch™ Real-Time PCR Detection System. Three different RNA samples were used as three biological replicates, and each biological replicate has three technical replicates. The relative changes of each gene were calculated using the $2^{-\Delta\Delta C}{}_{T}$ method [$-\Delta\Delta C_T$ = (Ct of target gene in samples – Ct of reference gene in samples) – (Ct of target gene in control – Ct of reference gene in control)]. PCR products were viewed by electrophoresis on 2% agarose gel running for 40 minutes at 100 voltages.

2.2.9 Determination of effect of sodium nitroprusside on root growth of Harrington seeds

Harrington seeds were put into Petri dishes (diameter = 11.5 cm) with 2 layers of filter paper (Whatman). A series of SNP solutions were prepared: 10, 25, 50, 100, 250, 500 and 2000 μM. 20 ml of each SNP solution was added to soak Harrington seeds for 15 minutes. Excessive SNP solution was removed and the Petri dishes were incubated in an incubator with light (approximately 100 μmoles/m^2/s) at room temperature for 48 h. Root length was measured and average of it was taken to determine the effect of SNP on root growth. In control, the seeds were treated by sterile ddH_2O.

2.2.10 Interaction of sodium nitroprusside and abscisic acid during the root growth of Harrington seeds and their effect on activity of ascorbate peroxidase and catalase

ABA was mixed with SNP to make a series of solutions: 10 μM ABA + 10 μM SNP, 10 μM ABA + 25 μM SNP, 10 μM ABA + 50 μM SNP, 10 μM ABA + 100 μM SNP, 10 μM ABA + 200 μM SNP and 10 μM ABA + 500 μM SNP. Harrington seeds were soaked in each of the solutions for 15 minutes in Petri dishes and excess of solution was removed. The seeds were incubated at room temperature for 48 hours under light (approximately 100 μmoles/m^2/s). Sterile ddH_2O and 10 μM ABA were set up as control. Activities of APX and CAT in whole Harrington seeds treated by ddH_2O (control), 10 μM ABA, 50 μM SNP, 100 μM SNP, 10 μM ABA + 50 μM SNP, 10 μM ABA + 100 μM SNP were measured and the method was referred to 2.2.6.1.

2.2.11 Effect of sodium nitroprusside and KNO_3 on germination of Sundre seeds

A series of SNP and KNO_3 solutions were prepared. The concentrations of SNP solutions were 10, 25, 50, 100, 200 and 500 μM. The concentrations of KNO_3 solutions were 10, 25, 50, 100, 200, 500 and 2000 μM. Sundre seeds were imbibed by each of the solutions in Petri dishes for 15 minutes. After removing the excessive solution, the seeds were incubated in an incubator at 20 °C with light (approximately 100 μmoles/m^2/s) for 48 h. The seeds treated by sterile ddH_2O and 10 μM GA, respectively, were set up as control. The number of germinated seeds was counted, and germination rate of the seeds was calculated by the formula: the number of germinated seeds/the number of total seeds x 100.

2.2.12 Measurement of NO content

Preparation of Hb solution and NO measurement were referred to Murphy and Noack (1994). 50 mg of commercial Hb (Sigma-Aldrich) was dissolved in 10 ml 50 mM Tris-HCl (pH 7.0). 15 mg sodium dithionite ($Na_2S_2O_4$, excessive) was added directly into the fresh Hb solution (MetHb, dark red, brown) and reacted for 3 minutes to reduce MetHb (Fe^{3+}) to Hb (Fe^{2+}) (dark red and purple). Thereafter, Hb became HbO_2 (bright, light red) quickly because of its high affinity for O_2. The prepared Hb solution was desalted through PD-10 columns (GE Healthcare, UK). Final concentration of HbO_2 was determined by absorbance at 415 nm (extinction coeffecient = 131 mM^{-1} cm^{-1}) and adjusted to ~10 μM. The prepared HbO_2 solution was stored in dim light.

NO was extracted from powder of tissue with buffer containing 50 mM Tris-HCl (pH 7.0) and 0.6% (w/v) PVP by ratio 1 ml/0.01 g tissue on ice. Supernatant was collected as NO solution after centrifuging for 10 minutes at 15000 g at 4 ºC. 0.5 ml of NO solution was mixed with 12.5 µl 4000 U/ml SOD and 12.5 µl 10000 U/ml CAT and incubated for 2 minutes at room temperature to remove ROS. 0.475 ml of the desalted HbO_2 solution was added into the treated NO solution and the mixture was incubated for 5 minutes at room temperature. Absorbance of the reaction at 401 and 421 nm was recorded respectively to calculate the concentration of NO in tissue by the following formula ($\varepsilon = 77\ mM^{-1}\ cm^{-1}$): NO ($\mu mol\ g^{-1}$ FW) = $(A_{401} - A_{421}) * \varepsilon^{-1} * W^{-1}$.

2.2.13 Measurement of protein S-nitrosylation levels

Measurement of protein *S*-nitrosylation was based on the method described by Jaffrey et al. (2001) in which ascorbate reduces R-SNO to R-SH. Quantity of free thiol groups is assayed by DTNB (Riddles et al., 1983). Proteins were extracted from fine powder of barley seeds with the extraction buffer containing 50 mM HEPES (pH 8.0), 1 mM EDTA, 0.1 mM neocuprine, 0.2% (w/v) SDS and 0.5% (w/v) CHAPS. Samples were homogenized for 30 minutes on ice and centrifuged for 10 minutes at 15000 g at 4 ºC. Supernatant was collected as protein solution. Proteins were precipitated by 2 volumes of chilly acetone (- 20 ºC) overnight. After centrifuging at 4 ºC at 15000 g for 10 minutes, protein pellet was washed 4 times by chilly 70% acetone. The protein samples were re-suspended in the same volume of the extraction buffer and centrifuged briefly. Clear supernatant was collected as protein solution to measure

quantity of R-SNO. The collected protein solution of each sample was divided into treatment and control groups separately, and the volume of the protein solution in each group was 0.9 ml. 50 µl of 100 mM ascorbate was added into treatments and the same volume of ddH_2O was added into control. After incubating for 1 h at 25 ºC, 50 µl of 10 mM DTNB in 75 mM phosphate buffer (pH 7.0) was added into both treatment and control groups to react for another 10 min. Absorbance of all the samples at 412 nm was determined. Mixture of ascorbate and DTNB in extraction buffer, and DTNB in the same buffer were set up as blank for treatment and control groups, respectively. The net absorbance between samples and control groups was used to calculate the quantity of R-SH, which was quantified by regressive equation acquired from reaction of L-cysteine (Sigma-Aldrich) with DTNB. The quantity of R-SH corresponded to that of R-SNO.

2.2.14 Determination of pH value in scutellum and endosperm

Fine powder of scutellum and endosperm was homogenized respectively with ddH_2O with proportion of water and tissue FW at 1 ml : 10 mg. Samples were centrifuged at 15000 g for 10 minutes and supernatants were collected to measure pH value which was determined by a pH meter (ORION 3 STAR pH Benchtop, Thermo Scientific).

2.2.15 Determination of organic acids

Extraction of organic acids was referred to the method of Jham et al. (2002). Organic acids were extracted from scutellum and endosperm respectively by homogenizing

fine powder of tissue with 80% methanol at 40 ºC for half hour. The extract was centrifuged at 15000 g for 10 minutes. The supernatant was collected as solution of organic acids. 100 µl of each sample was transferred to a glass vial and dried by nitrogen (Nitrogen evaporator, Pierce Reacti-Vap lll #18826, Thermo Scientific). Sample derivatization was referred to the method of Roessner et al. (2000). Dry residue of organic acids was derivatized by adding 50µl of MOX Reagent (2% methoxyamine hydrochloride in pyridine, Thermo SCIENTIFIC), vortexed shortly and incubated for 2 h at 37 ºC, and then 50 µl of 50% BSTFA (Sigma-Aldrich) in pyridine was added into each vial. Vials were vortexed shortly and incubated for another 40 minutes at 70 ºC.

Organic acids were analyzed by gas chromatography – mass spectrometry (GC-MS) according to the method of Roessner et al. (2000). Briefly, trimethylsilyl (TMS) derivatives of the organic acids were separated in a gas chromatography (GC) (Varian CP-3800, USA) equipped with a flame ionization detector (FID) and an ion trap mass spectrometer (Varian 220-MS, USA). The GC was equipped with a pair of CP-Sil 5 CB low bleed MS columns (WCOT silica 30 m × 0.25 mm), one in line with the FID and the other with the MS. Temperature in the injector oven and FID oven was set at 230 ºC and 300 ºC respectively. Samples, 1 µl, were injected twice (once to each column) in splitless mode and simultaneously eluted with the following oven temperature program: the initial temperature of 70 ºC was held for 5 minutes, followed by a temperature increase (7.5 ºC min^{-1}) to 300 ºC, where the final temperature was

held for 2 minutes. High purity Helium was used as a carrier gas and constant flow rate was 1 ml min^{-1}. Compounds were identified on the basis of their co-elution with authentic standards and their electron ionization - mass spectra (50-650 amu). Quantification of the organic acids in samples was based on FID peak areas and independently derived calibration curves for citric acid, malic acid and succinic acid (Figure A24, A25 and A26, Appendices).

2.2.16 Statistical calculation

R program was used in the statistical calculation. Statistically significant changes of samples between time points and barley cultivars, and the changes between different treatments such as the barley seeds treated by SNP, GA, ABA and KNO_3 were calculated by Two-Way ANOVA and One-Way ANOVA respectively. The significance threshold was $P < 0.01$.

3 Results

3.1 Germination of Harrington and Sundre seeds

A Harrington seeds

B Sundre seeds

C Embryos of Sundre seeds

Figure 6 Germination of barley seeds after twenty-four hours

A: Harrington seeds with imbibition in dark at 23 ºC for 24 h; B: Sundre seeds with imbibition in dark at 23 ºC for 24 h; C: Embryos of Sundre seeds with imbibition in dark at 23 ºC for 3 days

Germination rate of Harrington seeds was about 96% after 24 h at 23 ºC (Figure 6 A), and the seed's germination was much more uniform and faster than that of Sundre

seeds whose germination rate and germination resistance were about 20% after 24 h (Figure 6 B) and 1.2 days respectively. Almost all of Sundre seeds were viable because 94% of the Sundre seeds treated with 0.5 mM GA or 2% sodium hypochlorite germinated after 3 days, indicating that the treatment of GA and sodium hypochlorite on Sundre seeds resulted in alleviation of dormancy and germination of the seeds. Therefore, the non-germinated Sundre seeds in the research represented dormant but viable ones at the particular time of assay. Embryos isolated from Sundre seeds totally lost their dormancy and germinated uniformly under the same conditions (Figure 6 C). From 15 to 48 h, the plumule and radicles of both Harrington and Sundre seeds grew longer but non-germinated Sundre seeds showed no obvious changes except for slight expansion due to water uptake (Figure A10 E and F, Appendices).

3.2 Content of soluble proteins in embryos of barley seeds

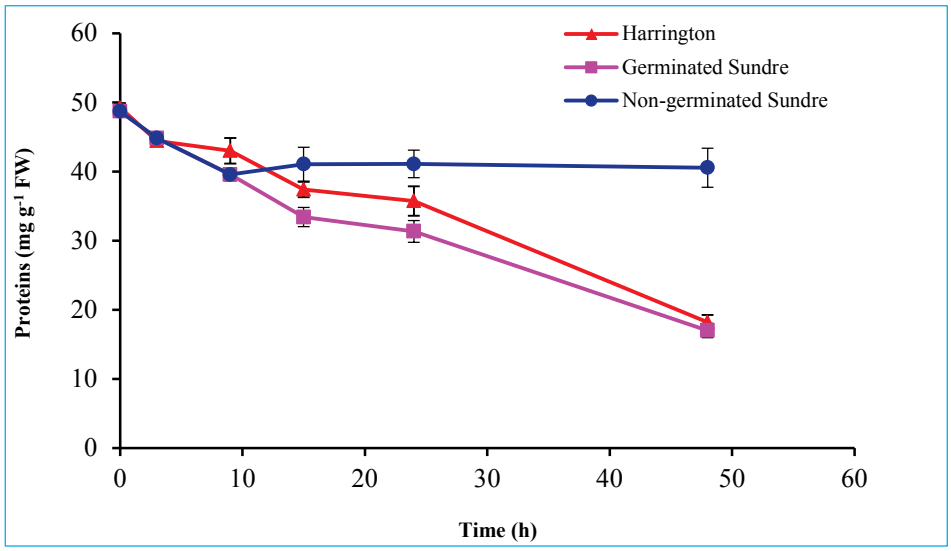

Figure 7 Content of soluble proteins in embryos of barley seeds in the process of seed germination

The content of soluble proteins in embryos decreased from 49.2 mg g^{-1} FW in dry Harrington seeds and 48.7 mg g^{-1} FW in dry Sundre seeds to 18.2 and 17.0 mg g^{-1} FW respectively after imbibition for 48 h. The protein content decreased more than twice after imbibition for 48 h in the process of seed germination whereas the content of soluble proteins in non-germinated Sundre seeds remained unchanged within 48 h (Figure 7). However, content of soluble proteins in whole seeds was about two folds lower than that in embryos, which declined gradually in Harrington seeds and both germinated and non-germinated Sundre seeds in the process of seed germination (Figure A11, Appendices).

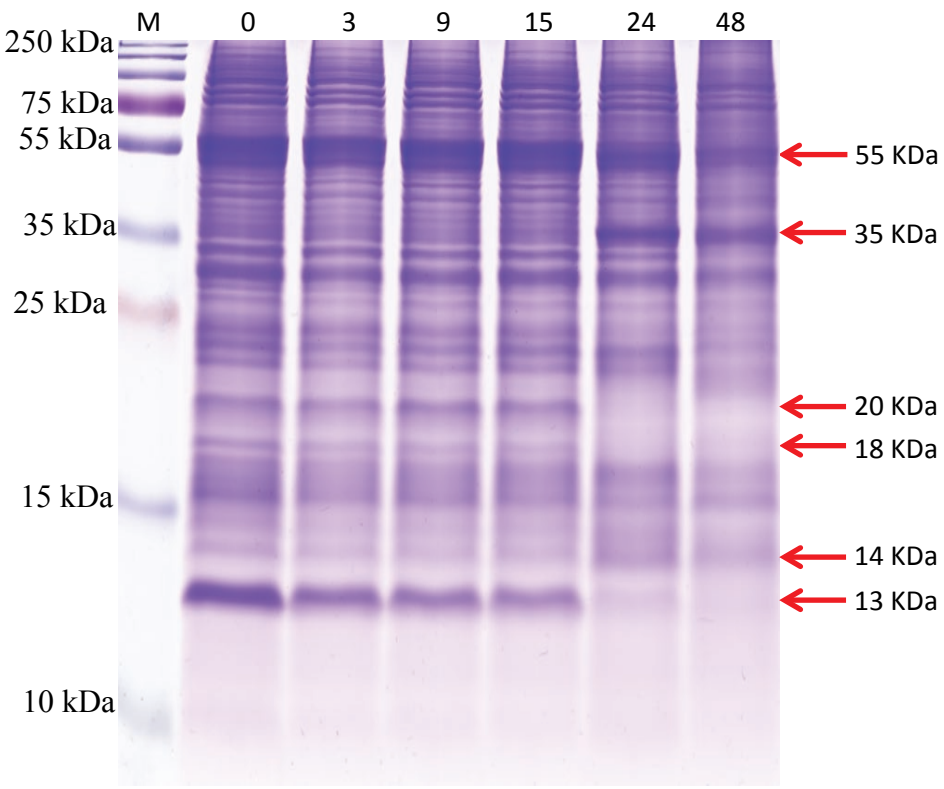

Figure 8A Profile of soluble proteins in embryos of Harrington seeds in the process of germination

M: marker; 0, 3, 9, 15, 24 and 48: Harrington seeds incubated for 0, 3, 9, 15, 24 and 48 h respectively with imbibition of sterile ddH_2O; 25 µg of proteins of each sample was loaded into wells in the polyacrylamide gel consisting of 5% stacking gel and 12.5% separating gel. Protein concentration was measured by Bradford reagent.

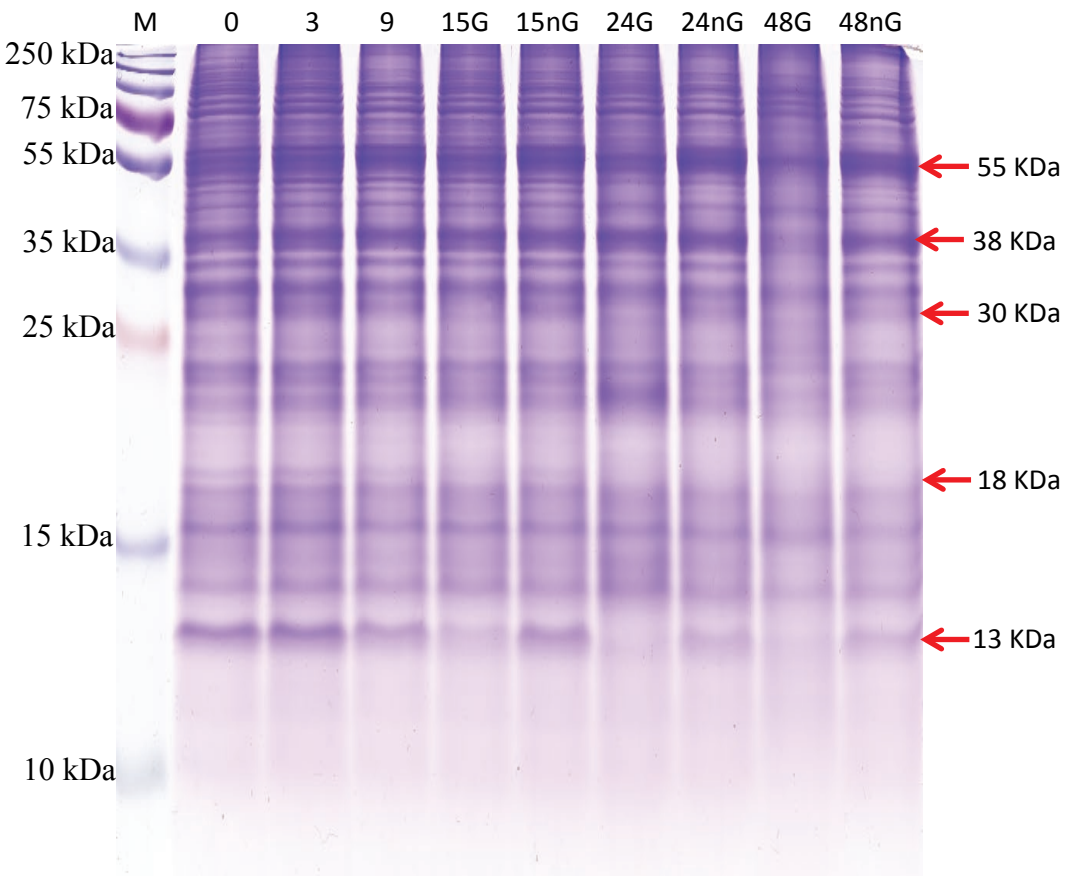

Figure 8B Profile of soluble proteins in embryos of Sundre seeds in the process of germination

M: marker; 0, 3 and 9: Sundre seeds incubated for 0, 3 and 9 h respectively with imbibition of sterile ddH_2O; 15G, 24G and 48G: germinated Sundre barley seeds incubated for 15, 24 and 48 h respectively with imbibition of sterile ddH_2O; 15nG, 24nG and 48 nG: non-germinated Sundre seeds incubated for 15, 24 and 48 h respectively with imbibition of sterile ddH_2O; 25 µg of proteins of each sample was loaded into wells in the polyacrylamide gel consisting of 5% stacking gel and 12.5% separating gel. Protein concentration was measured by Bradford reagent.

SDS-PAGE band pattern of proteins in embryos of Harrington seeds showed that proteins with molecular weight of approximately 20, 18 and 13 kDa disappeared after 24 h and quantity of proteins of 55 kDa became less and less after 15 h (Figure 8 A).

In Sundre seeds, proteins with molecular weight of approximately 55, 38, 30, 13 kDa became less and less after 15 h in germinated ones but not in non-germinated ones. A protein band at about 18 kDa disappeared from 24 to 48 h in both germinated and non-germinated ones (Figure 8 B). In non-germinated Sundre seeds, the density of protein bands decreased slightly even though the pattern of bands did not change significantly (Figure 8 B). From the overall investigation in the profile of protein bands in the process of seed germination, the number of protein bands became less in embryos of barley seeds.

3.3 Accumulation of adenosine triphosphate and adenosine diphosphate in embryos

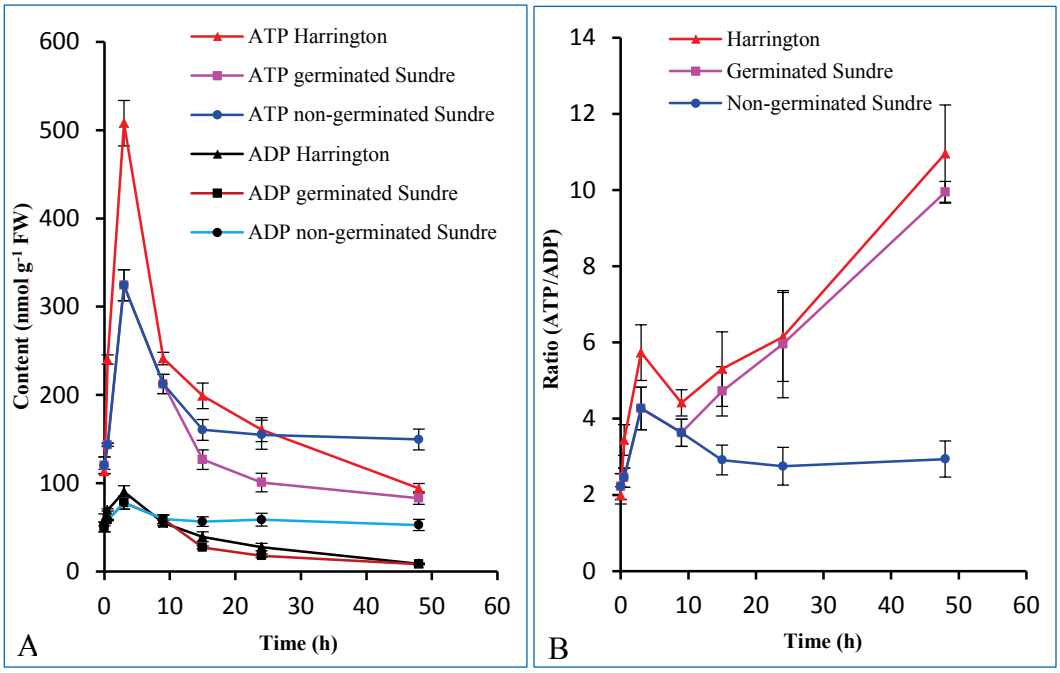

Figure 9 Content of ATP and ADP and their ratio in embryos of barley seeds in the process of germination

Content of ATP in embryos of Harrington and germinated Sundre seeds was elevated quickly to peak value, 507.9 and 324.2 nmol g^{-1} FW within the first three hours and declined to 94.3 and 83.2 nmol g^{-1} FW respectively with imbibition for 48 h. In embryos of germinated Sundre seeds, ATP content was lower than that in Harrington seeds except in dry seeds. In non-germinated Sundre seeds, its content did not change remarkably, which was between about 150 and 160 nmol g^{-1} FW from 15 to 48 h (Figure 9 A). However, ATP content in whole seeds was much lower than that in embryos (Figure A12, Appendices). Content of ADP showed similar tendency to ATP nonetheless its content was much lower than that of ATP. ADP content rose up to its highest value, 90.3 and 77.8 nmol g^{-1} FW with imbibition within the first 3 h and descended to 8.8 and 8.4 nmol g^{-1} FW respectively in Harrington and germinated Sundre seeds with imbibition for 48 h. However, its content in non-germinated Sundre seeds did not change remarkably and fluctuated between 52.7 and 58.7 nmol g^{-1} FW from 15 to 48 h (Figure 9 A). The ATP/ADP ratio in embryos ascent to 10.96 in Harrington seeds and 9.94 in germinated Sundre seeds respectively with imbibition for 48 h but the ratio in non-germinated Sundre seeds did not change obviously from 15 to 48 h (Figure 9 B).

3.4 Levels of H_2O_2 and $O_2^{\bullet-}$ in embryos

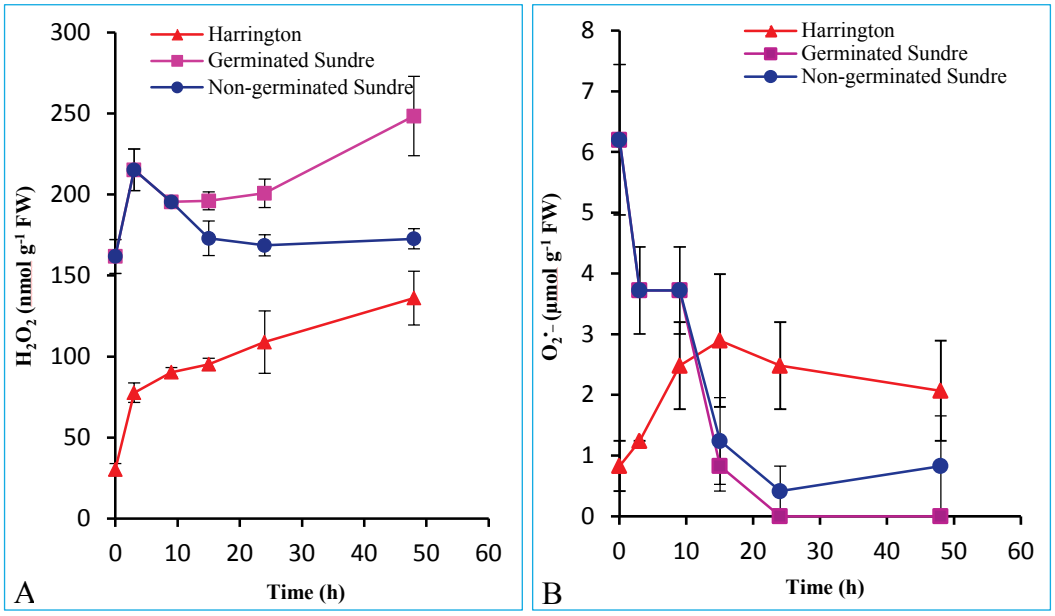

Figure 10 Content of H_2O_2 and $O_2^{\bullet-}$ in embryos of barley seeds in the process of germination

Concentration of H_2O_2 increased from 30.3 and 161.8 nmol g^{-1} FW at 0 h to 136.1 and 248.4 nmol g^{-1} FW in embryos of Harrington and germinated Sundre seeds respectively with imbibition for 48 h, but its content in non-germinated Sundre seeds remained on a stable level, at about 170 nmol g^{-1} FW, which was slightly higher than that in dry Sundre seeds (Figure 10 A). There was a temporary peak of H_2O_2 content in Sundre seeds, reaching 215.3 nmol g^{-1} FW within the first three hours but not in Harrington seeds (Figure 10 A). In whole barley seeds, changes of H_2O_2 were similar to that in embryos but its content was much lower than that in embryos (Figure A13, Appendices). Compared to H_2O_2, the content of $O_2^{\bullet-}$ in tissue of Harrington seeds was much higher, rising up from 0.8 μmol g^{-1} FW in embryos of dry seeds to 2.9 μmol g^{-1}

FW after imbibition for 15 h, and dropping to 2.1 μmol g^{-1} FW after 48 h. Content of $O_2^{\bullet-}$ was the highest, 6.2 μmol g^{-1} FW in embryos of dry Sundre seeds and dropped to an undetectable level later in germinated Sundre seeds whereas its content in embryos of non-germinated Sundre seeds decreased from 15 h to 24 h, increasing to 0.83 μmol g^{-1} FW from 24 to 48 h with imbibition (Figure 10 B).

3.5 Activities of enzymes involved in scavenging reactive oxygen species in embryos

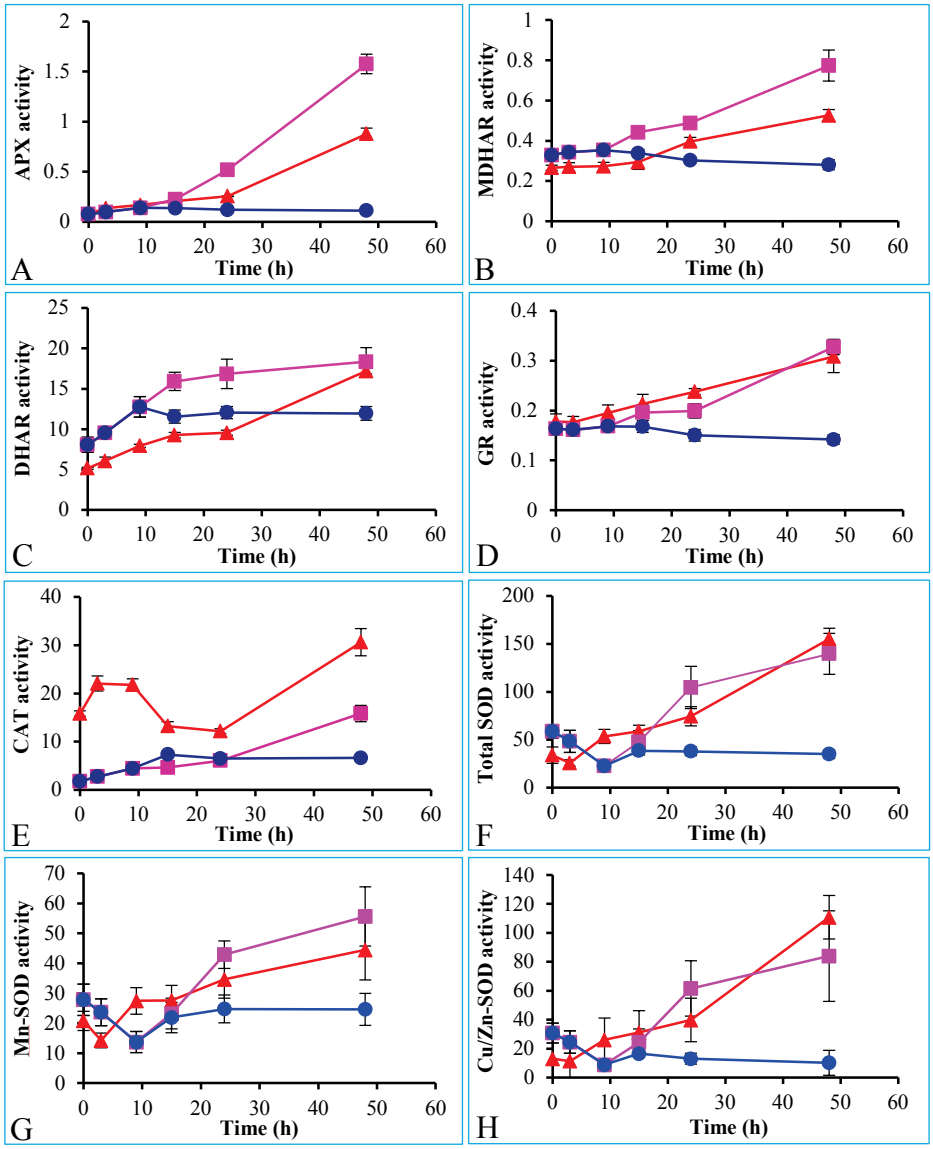

Figure 11 Activities of enzymes involved in scavenging of ROS during germination of barley seeds

A: APX activity, B: MDHAR activity, C: DHAR activity, D: GR activity, E: CAT activity, F: total SOD activity, G: Mn-SOD activity, H: Cu/Zn-SOD activity. Unit of activity of APX, MDHAR, DHAR, Gr and CAT is μmol min^{-1} mg^{-1} protein, and unit of activity of total SOD, Mn-SOD and Cu/Zn-SOD is U mg^{-1} protein. Harrington Germinated Sundre Non-germinated Sundre

Activities of APX, MDHAR, DHAR, GR, CAT, total SOD, Mn-SOD and Cu/Zn-SOD in embryos of Harrington seeds were elevated to 0.87, 0.53, 17.19, 0.31, 30.61 μmol min^{-1} mg^{-1} protein, 155.22, 44.45 and 110.77 U mg^{-1} protein, respectively, after imbibition for 48 h. CAT had a temporary peak of activity in Harrington seeds at the beginning of germination and activity of SOD decreased in the two barley cultivars in the first few hours. In embryos of germinated Sundre seeds, their activities rose up to 1.58, 0.77, 18.35, 0.33, 15.85 μmol min^{-1} mg^{-1} protein, 139.61, 55.64 and 83.96 U mg^{-1} protein after imbibition for 48 h, except for decrease of SOD activity in the first few hours. In the embryos of non-germinated Sundre seeds, activities of these enzymes did not change significantly from 15 to 48 h and were much lower than those in germinated Sundre seeds (Figure 11 A, B, C, D, E, F, G and H). Activities of APX, MDHAR, DHAR and GR in whole barley seeds were much lower than those in embryos (Figure A14, Appendices).

3.6 Content of ascorbate and dehydroascorbate and their ratio in embryos

A:

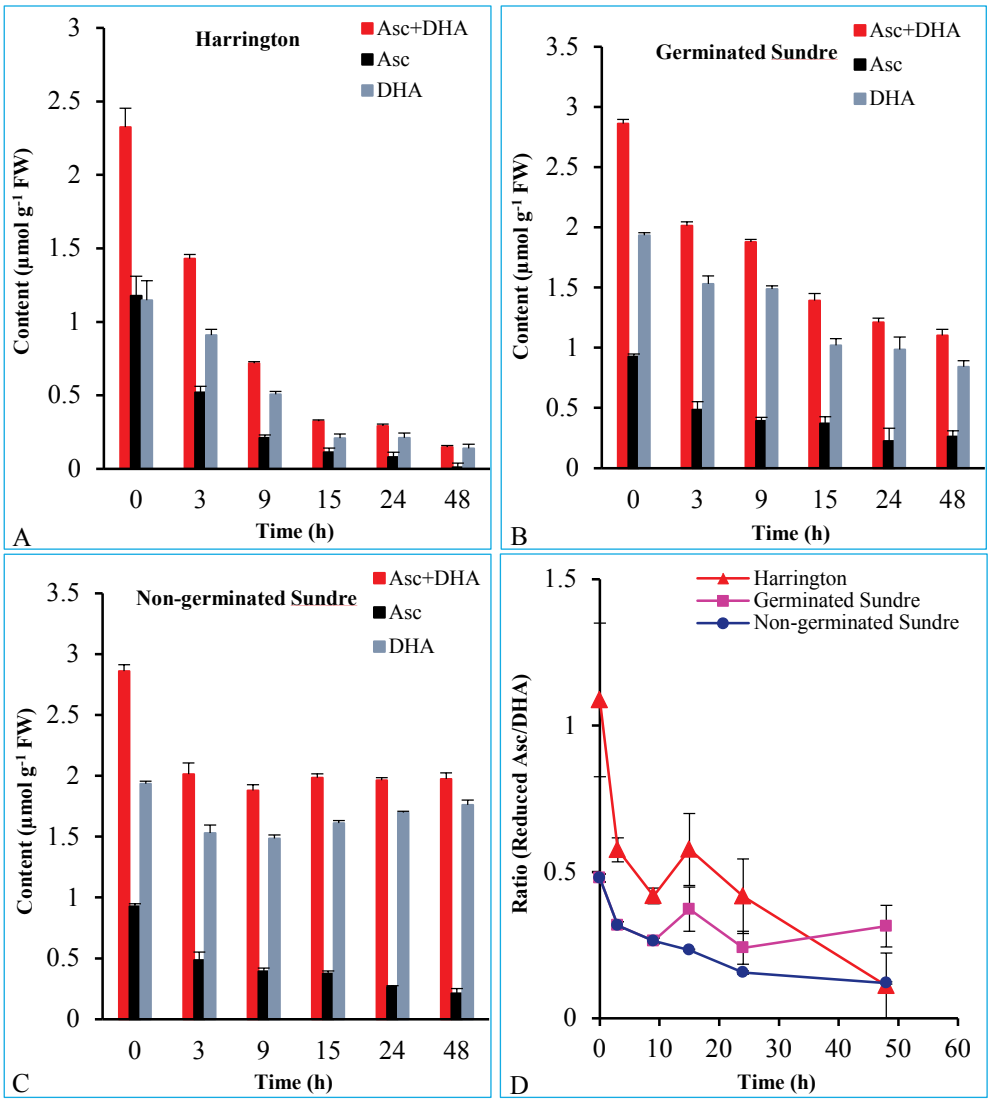

Figure 12 Content of ascorbate and DHA and their ratio in embryos of barley seeds in the process of germination

content of Asc and DHA in embryo of Harrington seeds; B: content of ascorbate and DHA in embryos of germinated Sundre seeds; C: content of ascorbate and DHA in embryos of non-germinated Sundre seeds; D: Asc/DHA ratio in embryos of Harrington and Sundre seeds, respectively; Asc: ascorbate. Asc + DHA: total content of ascorbate including reduced ascorbate and DHA.

In the process of germination, content of total ascorbate including reduced ascorbate and DHA decreased in germinating Harrington and Sundre seeds but in non-

germinated Sundre seeds total content of ascorbate did not change obviously (Figure 12 A, B and C). Content of ascorbate and DHA decreased from 1.18 and 1.15 μmol g^{-1} FW in Harrington seeds at 0 h to 0.01 and 0.14 μmol g^{-1} FW respectively after imbibition for 48 hours (Figure 12 A). In Sundre seeds, the content of ascorbate was much lower than that of DHA. In germinated Sundre seeds, content of ascorbate and DHA dropped from 0.93 and 1.93 μmol g^{-1} FW at 0 h to 0.26 and 0.84 μmol g^{-1} FW respectively after imbibition of 48 hours (Figure 12 B). In embryos of non-germinated Sundre seeds, change of ascorbate levels was similar to that in germinated Sundre seeds but the change of DHA was strikingly different from that in germinated ones, which was that its content increased to 1.76 μmol g^{-1} FW after imbibition for 48 h (Figure 12 C). In whole barley seeds, content of both ascorbate and DHA decreased in the process of germination and content of DHA was much higher than ascorbate (Figure A15 A, B and C, Appendices).

Ascorbate/DHA in embryos of Harrington and non-germinated Sundre seeds declined gradually from 1.09 and 0.48 at 0 h to 0.11 and 0.31 respectively after imbibition for 48 h. Although the content of ascorbate and DHA decreased in germinated Sundre seeds, their ratio had slight increase from 0.24 to 0.37 after imbibition from 24 to 48 h (Figure 12 D). However, the ratio had an insignificant and transient increase at time point of 15 h in both Harrington and germinated Sundre seeds. In whole barley seeds, the value of ascorbate/DHA rose up within the first 9 h but decreased later, which was different from that in embryos of the two barley cultivars (Figure A15 D, Appendices).

3.7 Content of glutathione, glutathione disulfide, glutatione/glutathione disulfide and reduction potential of glutathione disulfide/glutathione couple in embryos

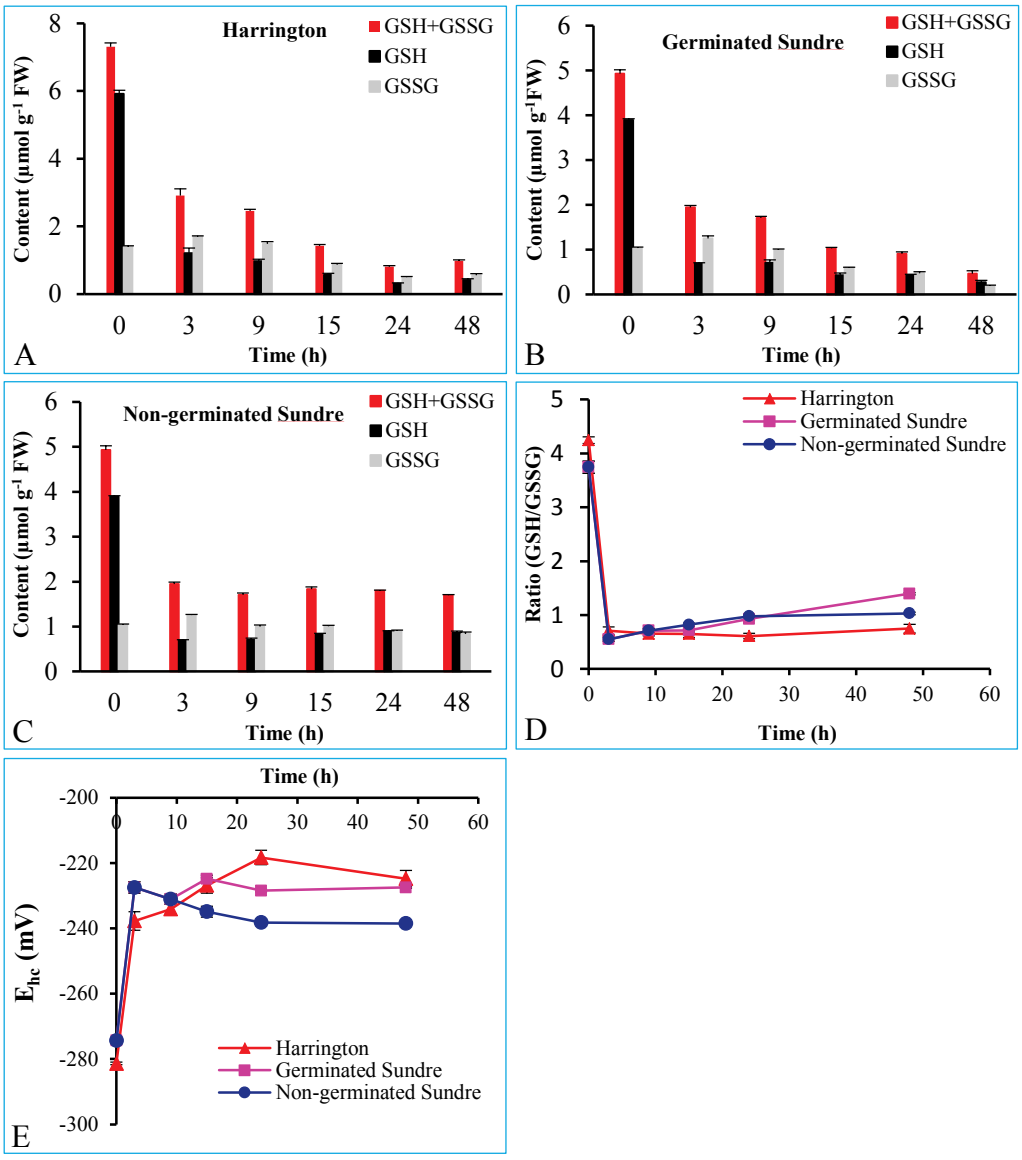

Figure 13 Content of GSH and GSSG, GSH/GSSG and reduction potential of GSSG/2GSH couple in embryos of barley seeds in the process of germination

A: content of GSH and GSSG in embryos of Harrington seeds; B: content of GHS and GSSG in embryos of germinated Sundre seeds; C: content of GSH and GSSG in embryos of non-germinated Sundre seeds; D: value of GSH/GSSG in ebryos of Harrington, germinated and non-germinated Sundre seeds, E: redox potential of GSSG/2GSH couple in embryos of Harrington, germinated and non-germinated Sundre seeds; GSH + GSSG: total content of GSH including GSH and GSSG.

In the process of germination, content of total GSH including GSH and GSSG decreased in germinating Harrington and Sundre seeds except for a increase from 24 to 48 h in Harrington seeds but in non-germinated Sundre seeds the total content did not change remarkably (Figure 13 A, B and C). Content of GSH was much higher than GSSG in embryos of both dry Harrington and Sundre seeds. In embryos of Harrington seeds, GSH content declined dramatically from 5.92 μmol g^{-1} FW at 0 h to 1.21 μmol g^{-1} FW after 3 h, and further decreased to 0.31 μmol g^{-1} FW after imbibtion for 24 h. GSSG content in the Harrington seeds rose up from 1.39 μmol g^{-1} FW at 0 hour to 1.70 μmol g^{-1} FW after 3 hours and then decreased to 0.50 μmol g^{-1} FW after 24 h. Content of both GSH and GSSG increased mildly from 24 to 48 h in the seeds (Figure 13 A). In embryos of Sundre seeds, content of GSH declined dramatically from 3.89 μmol g^{-1} FW at 0 h to 0.69 μmol g^{-1} FW whereas content of GSSG rose up slightly from 1.04 μmol g^{-1} FW at 0 h to 1.25 μmol g^{-1} FW within the first 3 h (Figure 13 B and C). Content of GSH and GSSG in embryos of germinated Sundre seeds decreased to 0.27 and 0.19 μmol g^{-1} FW respectively with imbibition for 48 h, but in embryos of non-germinated Sundre barley seeds, content of GSH fluctuated between 0.83 and 0.90 and so did GSSG content between 0.84 and 1.01 μmol g^{-1} FW from 15 h to 48 h (Figure 13 C), namely without significant change. In the whole barley seeds, their content was much lower than in embryos but the tendancy of their change was similar (Figure A16 A, B and C, Appendices).

The value of GSH/GSSG in embryos of Harrington and Sundre seeds dropped sharply from 4.24 and 3.74 at 0 hour to 0.71 and 0.55, respectively, after imbibition for 3 h. Later the ratio remained constant in Harrington seeds, and it was enhanced to 1.40 and 1.03 respectively in the tissue of germinate and non-germinated Sundre seeds with imbibition for 48 h (Figure 13 D). Reduction potential of the GSSG/2GSH couple in embryos of Harrington seeds was raised up quickly from -281.4 mV at 0 h to -237.7 mV with imbibition for 3 h, and continued to increase to -218.3 mV gradually after 24 h. In embryos of Sundre seeds, the reduction potential was enhanced sharply from -274.4 mV at 0 h to -227.5 mV with imbibition for 3 h but later it increased and remained between -228.5 mV and -224.9 mV in germinated Sundre seeds from 15 to 48 h. The reduction potential in embryos of non-germinated Sundre seeds was lower and fluctuated between -234.9 and -238.5 mV from 15 to 48 h (Figure 13 E). In whole barley seeds, the overall change of GSH/GSSG and reduction potential of GSSG/2GSH couple was similar to that in embryos (Figure A16 D and E, Appendices).

3.8 Activities of enzymes in fermentation and activity of pyruvate-phosphate dikinase in embryos

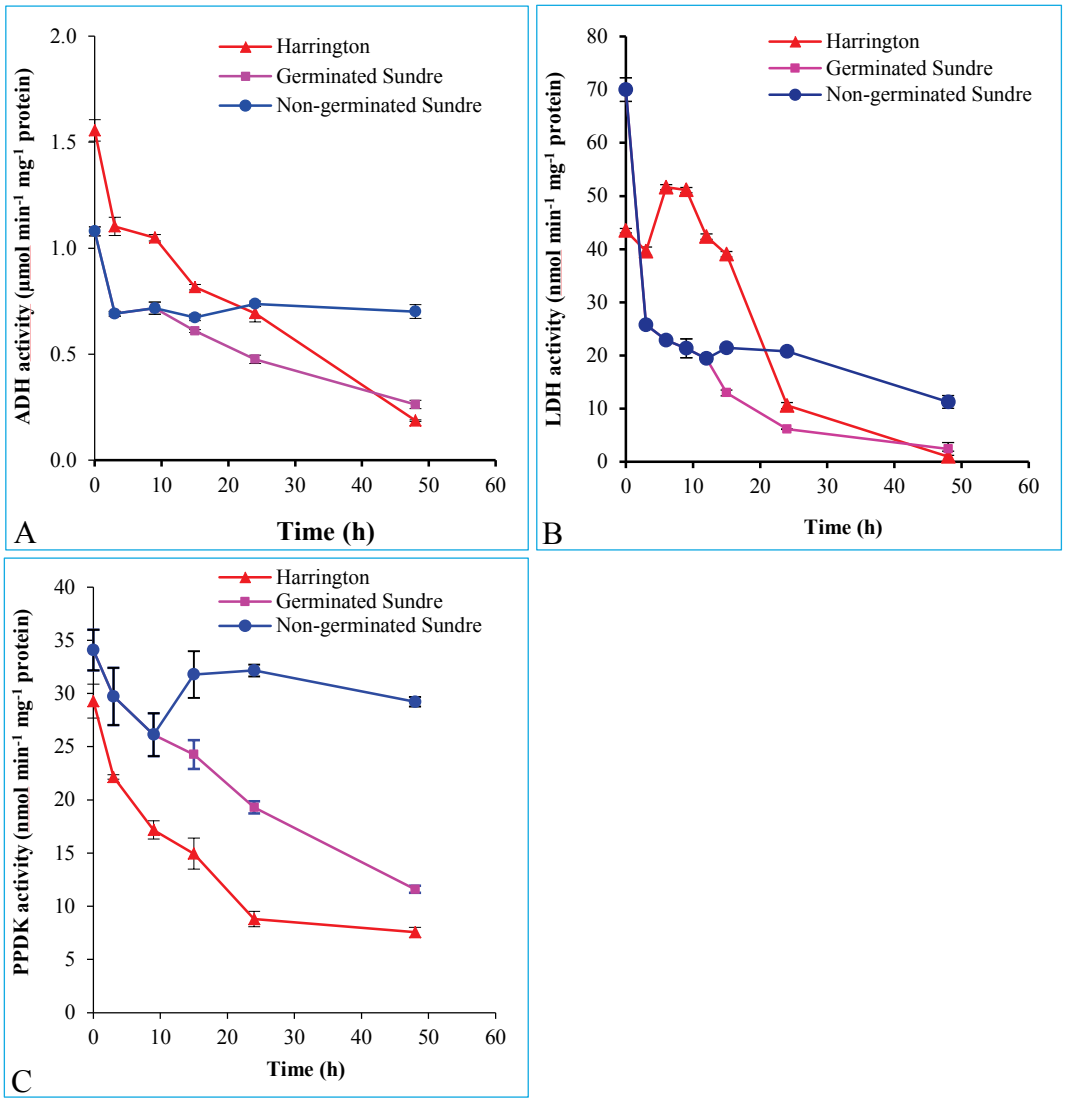

Figure 14 Activities of ADH, LDH and PPDK in embryos of barley seeds in the process of germination

ADH activity in embryos of Harrington and germinated Sundre seeds decreased from 1.56 and 1.08 μmol min^{-1} mg^{-1} protein at 0 h to 0.19 and 0.26 μmol min^{-1} mg^{-1} protein respectively after imbibition for 48 h but its activity in non-germinated Sundre seeds

remained on a stable level, about 0.70 μmol min^{-1} mg^{-1} protein from 15 to 48 h (Figure 14 A). Compared with ADH, activity of LDH in embryos was much lower, decreasing from 43.5 and 69.99 nmol min^{-1} mg^{-1} protein at 0 h to 1.00 nmol min^{-1} mg^{-1} protein in Harrington seeds and 2.40 nmol min^{-1} mg^{-1} protein in germinated Sundre seeds respectively after imbibition for 48 h although its activity in Harrington seeds had a temporary increase from 3 to 15 h. LDH activity went down in both germinated and non-germinated Sundre seeds even though its activity remained on a higher level in non-germinated Sundre seeds after imbibition for 48 h (Figure 14 B). Activity of PPDK decreased gradually in embryos of both Harrington and germinated Sundre seeds from 29.28 and 34.07 nmol min^{-1} mg^{-1} protein at 0 h to 7.55 and 11.59 nmol min^{-1} mg^{-1} protein respectively after imbibition for 48 h. However, its activity remained on a high level, about 30.00 nmol min^{-1} mg^{-1} protein from 15 to 48 h in embryos of non-germinated Sundre seeds (Figure 14 C). Activities of the three enzymes in whole barley seeds were much lower than these of them in embryos (Figure A17 A, B and C, Appendices).

3.9 Expression of *ascorbate peroxidase*, *alcohol dehydrogenase III* and *hemoglobin* in embryos of barley seeds

3.9.1 Extraction of total RNA

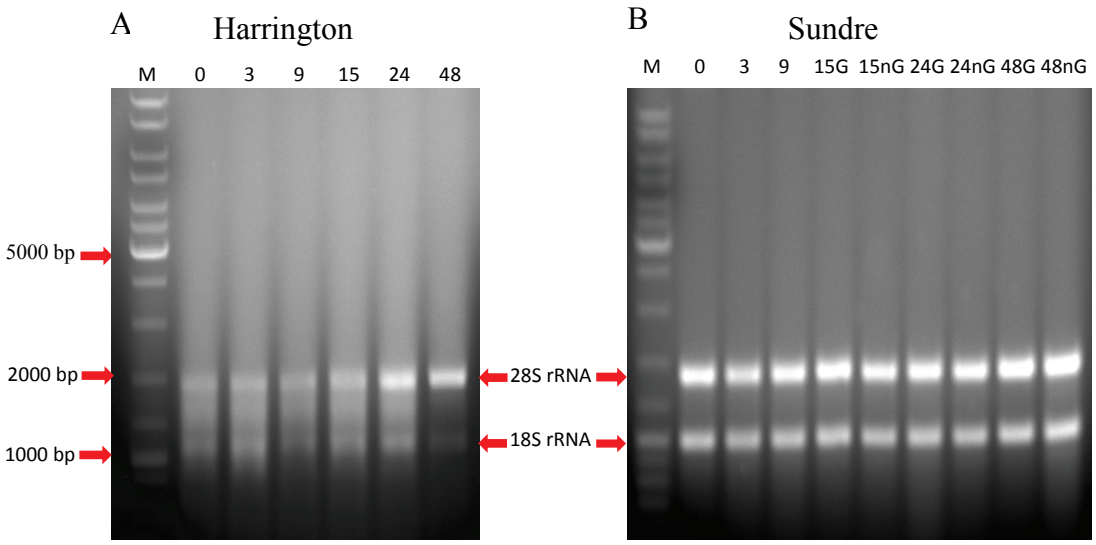

Figure 15 Total RNA in embryos of barley seeds in the process of germination

A: total RNA extracted from embryos of Harrington seeds; 0, 3, 9, 15, 24, 48: total RNA extracted from Harrington seeds incubated for 0, 3, 9 15, 24 and 48 h with imbibition of sterile ddH_2O. B: total RNA extracted from embryos of Sundre seeds; 0, 3 and 9: total RNA extracted from embryos of Sundre seeds incubated for 0, 3 and 9 h with imbibition of sterile ddH_2O; 15G, 24G, 48G: total RNA extracted from germinated Sundre seeds incubated for 15, 24 and 48 h with imbibition of sterile ddH_2O; 15nG, 24nG and 48nG: total RNA extracted from non-germinated Sundre seeds incubated for 15, 24 and 48 h with imbibition of sterile ddH_2O; M: Marker. 1.5 µg of RNA of each sample was loaded into wells in 1% agarose gel.

Total RNA from embryo tissue of barley seeds was extracted with high quality and quantity even though the quality of total RNA from Harrington seeds was worse than that of total RNA from Sundre seeds. The bands of 28S and 18S rRNA on agarose gel for Harrington seeds treated from 0 to 15 h were not as clear as those in Sundre seeds (Figure 15 A and B) indicating the quality of the total RNA from Harrington seeds

was not as good as that from Sundre seeds. The bands of 28S and 18S rRNA on agarose gel for Harrington seeds treated from 24 to 48 h and Sundre seeds treated from 0 to 48 h were clear, indicating their total RNA was intact (Figure 15 A and B). After digestion by DNase, 1 μg RNA was used in reverse transcription. The size of RT PCR product and specificity of the primers of *APX* (181 bp), *ADH3* (177 bp), *Hb* (149 bp) and *mub1* (119 bp) were inspected by electrophoresis in 2% agarose gel, showing that the PCR product of each gene was same in the two cultivars and the primers for the genes were specific (Figure A18 A, B, C and D, Appendices). The shape of their melt curves further confirmed high specificity of the primers for each gene (Figure A19 A, B, C and D, Appendices). Their standard curves showed that efficiency of their primers was almost 100% (Figure A20 A, B, C and D, Appendices).

3.9.2 Expression of ascorbate peroxidase, alcohol dehydrogenase III and hemoglobin in embryos of barley seeds

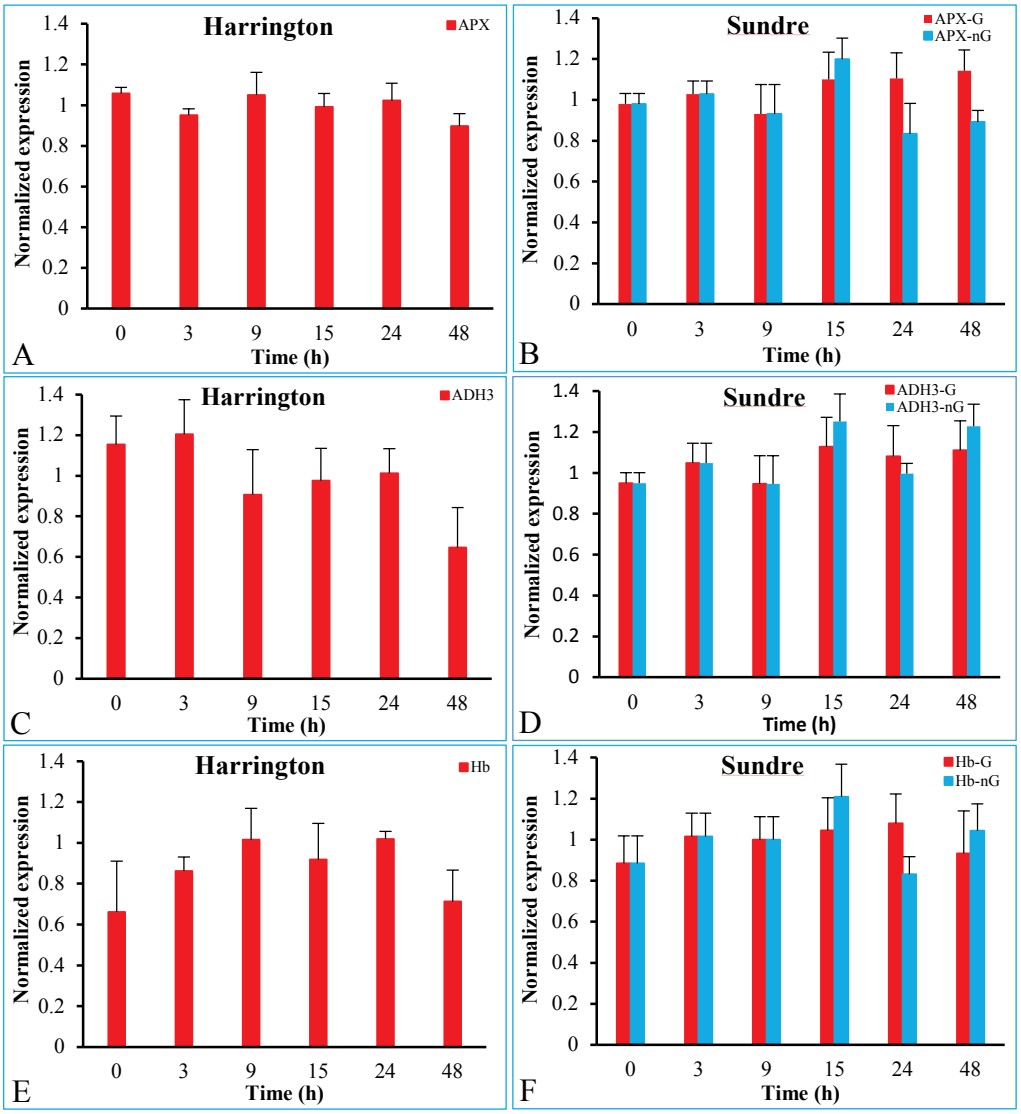

Figure 16 Expression of *APX*, *ADH3* and *Hb* in embryos of barley seeds in the process of germination

A: normalized expression of *APX* in embryos of Harrington seeds, B: normalized expression of *APX* in embryos of germinated and non-germinated Sundre seeds, C: normalized expression of *ADH3* in embryos of Harrington seeds, D: normalized expression of *ADH3* in embryos of germinated and non-germinated Sundre seeds, E: normalized expression of *Hb* in embryos of Harrington seeds, F: normalized expression of *Hb* in embryos of germinated and non-germinated Sundre seeds, G: germinated Sundre seeds, nG: non-germinated Sundre seeds.

Data from RT PCR displayed that expression of *APX* in embryos did not change significantly from 0 to 48 h during germination of Harrington and Sundre seeds. Even though its expression was a little lower in embryos of non-germinated Sundre seeds, the difference was not significant between the germinated and non-germinated Sundre seeds (Figure 16 A and B). Relative expression of *ADH3* decreased from 0 to 48 h in embryos of Harrington seeds in the process of germination. Relative expression of *ADH3* in embryos of Harrington seeds was about 1.20 from 0 to 3 h, decreased to about 0.98 between 9 and 24 h and further declined to about 0.65 after imbibition for 48 h (Figure 16 C). Expression of *ADH3* in embryos of germinated and non-germinated Sundre seeds fluctuated insignificantly from 0 to 48 h even though its relative expression in non-germinated Sundre seeds was a little higher than that in germinated ones (Figure 16 D). Relative expression of *Hb* in embryos of Harrington seeds increased from 0.66 to 1.02 within 9 h, remained on this level between 9 and 24 h and then fell to 0.71 after imbibition for 48 h (Figure 16 E). Relative expression of *Hb* in embryos of germinated Sundre seeds increased from 0.88 at 0 h to 1.08 after 24 h and then decreased to 0.93 after imbibition for 48 h. Its expression in embryos of non-germinated Sundre seeds increased to 1.21 after 15 h but decreased to 1.04 after imbibition for 48 h (Figure 16 F). The results here displayed that the relative expression of *ADH3* and *Hb* was different between the two cultivars but their change in Sundre seeds was similar.

3.10 Effect of sodium nitroprusside on root growth of Harrington seeds

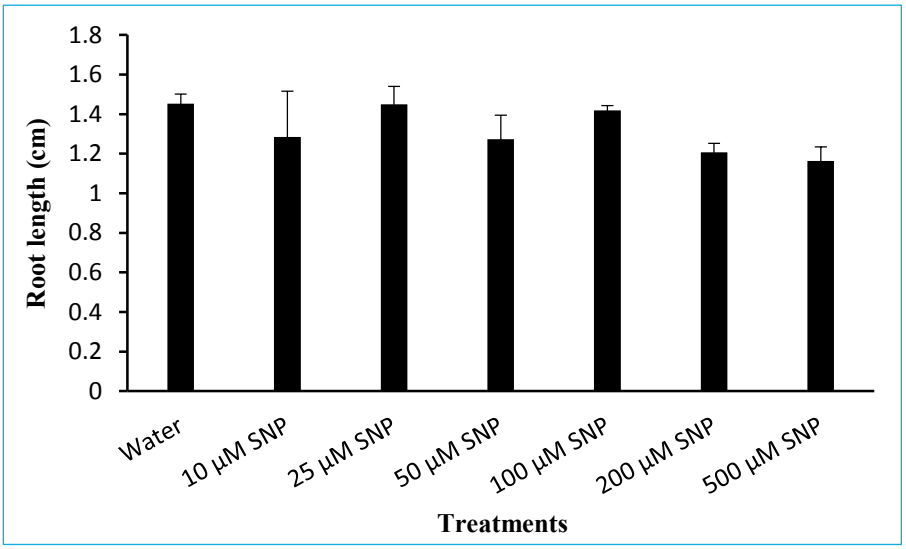

Figure 17 Effect of SNP on root growth of Harrington seeds in the process of germination

Average root length of Harrington seeds in all of the treatments from control to 500 µM SNP was approximately between 1.2 cm and 1.5 cm. Thus, SNP did not stimulate root growth of Harrington seeds, and even the root length of seeds under some treatments of SNP such as 10, 200 and 500 µM was slightly shorter than those of seeds imbibed by water but no significant inhibition of SNP was observed (Figure 17).

3.11 Interaction of sodium nitroprusside and abscisic acid during root growth of Harrington seeds

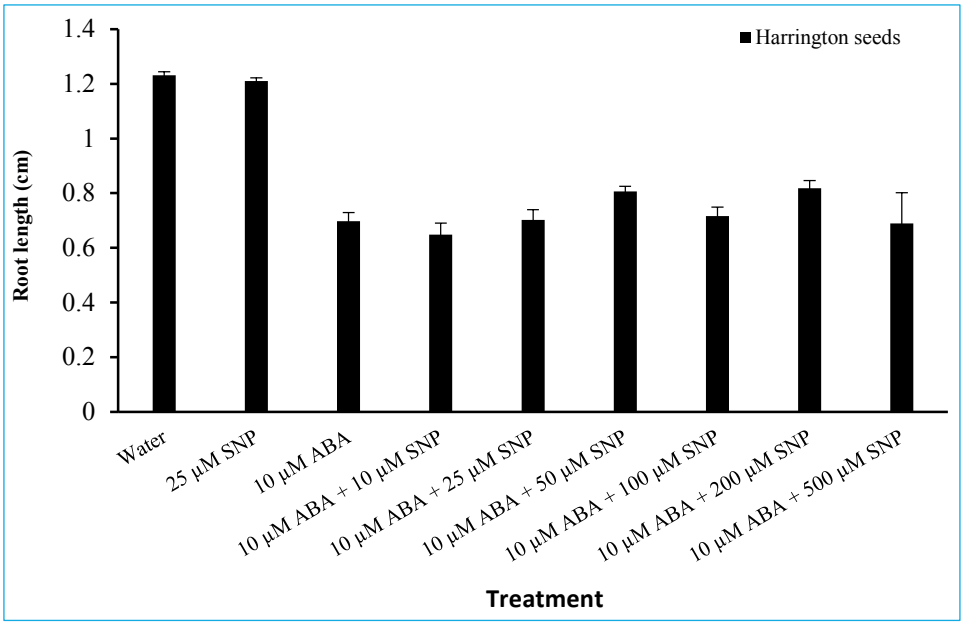

Figure 18 Interaction of SNP and ABA on root growth of Harrington seeds in the process of germination

The average root length of Harrington seeds treated by ddH_2O and 25 μM SNP was similar, about 1.2 cm, which was much longer than that of seeds treated by ABA and mixture of ABA and SNP, about 0.6 to 0.8 cm (Figure 18). The results demonstrated that SNP did not stimulate or inhibit root growth of Harrington seeds but ABA suppressed it substantially. Mixture of ABA and SNP had parallel suppression on root

growth with ABA, indicating that SNP did not counteract inhibition of ABA on root growth.

3.12 Effect of sodium nitroprusside and KNO_3 on germination of Sundre seeds

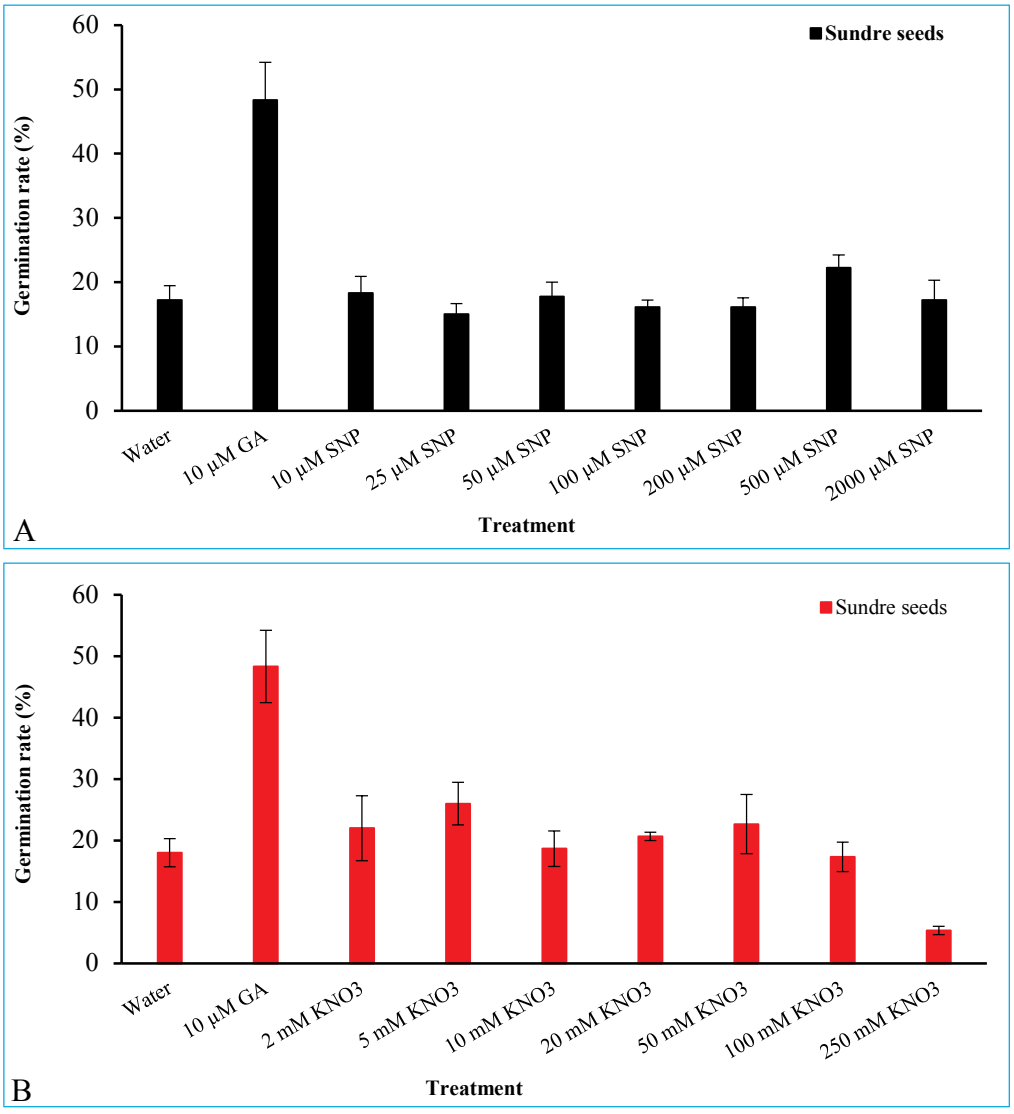

Figure 19 Effect of SNP and KNO_3 on germination of Sundre seeds

The germination rate of Sundre seeds treated by SNP from 10 to 2000 μM was about 18% after 48 hours, which was similar to that of the seeds treated by water (Figure 19 A), displaying that SNP did not stimulate germination of dormant Sundre seeds. Only low concentrations of KNO_3, 2 and 5 mM, promoted germination rate of the seeds to about 22% and 26% respectively. The later one was significantly higher than the water control. When concentration of KNO_3 was between 10 and 100 mM, germination rate of the seeds was similar to that of the Sundre seeds treated by sterile ddH_2O. However, 250 mM KNO_3 suppressed germination of the seeds significantly (Figure 19 B). On the other hand, Sundre seeds treated by 10 μM GA had much higher germination rate which was about 48.3%, showing that GA stimulated germination of Sundre seeds remarkably.

3.13 Effect of sodium nitroprusside and abscisic acid on activity of ascorbate peroxidase and catalase in whole Harrington seeds

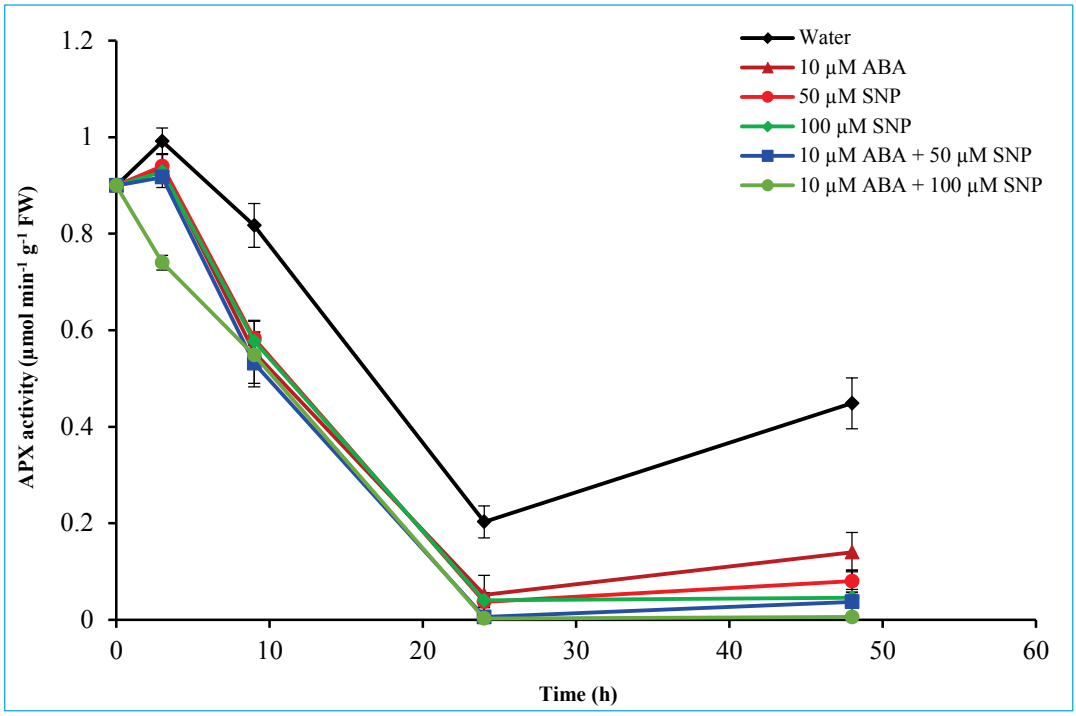

Figure 20 Activities of APX in Harrington seeds treated with SNP and ABA in the process of germination

Activity of APX in whole Harrington barley seeds treated by water rose up to 0.99 μmol min^{-1} g^{-1} FW after 3 h, then decreased to 0.20 μmol min^{-1} g^{-1} FW after 24 h and later increased to 0.45 after imbibition for 48 h, which was higher than that in the seeds treated by ABA, SNP or their combination. In Harrington seeds treated by mixture of 10 μM ABA and 100 μM SNP, activity of APX was supressed most substantially, which dropped to zero after 24 h. Activity of APX in other treatments such as 10 μM ABA, 50 μM SNP, 100 μM SNP and 10 μM ABA + 50 μM SNP was

between that in the seeds treated with ddH_2O and 10 µM ABA + 100 µM SNP (Figure 20). Comparing APX activity in all of the treatments, it indicated that the higher concentration of SNP was, the stronger inhibition effect it had, and addition of ABA imposed more serious inhibition effect on APX activity.

3.14 Activity of catalase in Harrington seeds

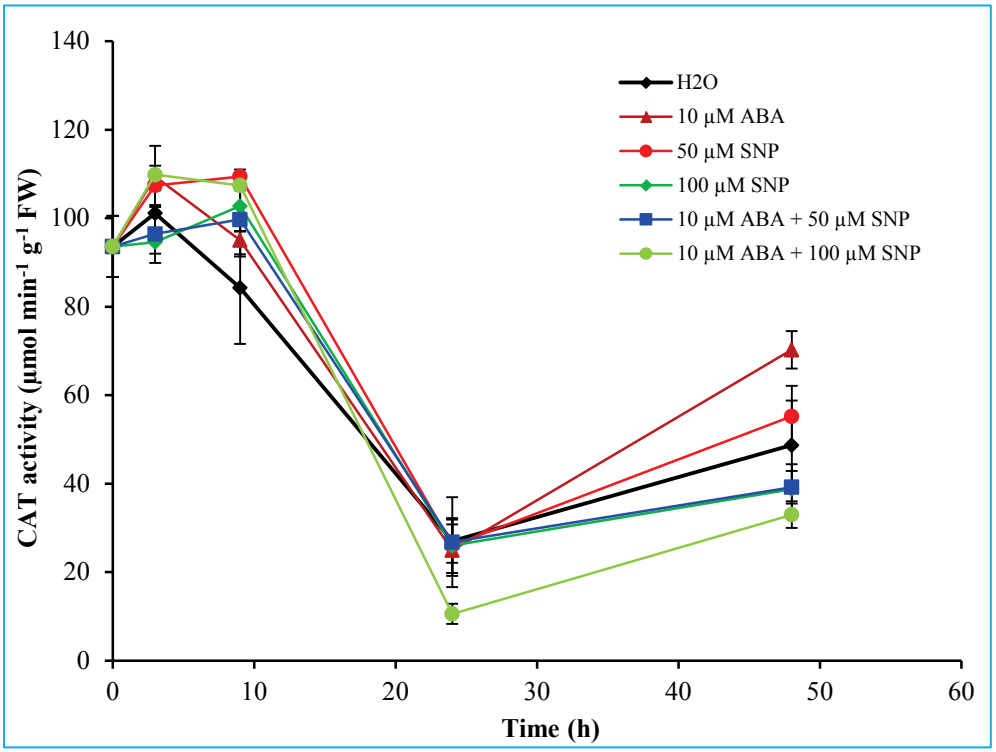

Figure 21 Activity of CAT in Harrington seeds treated with ABA and SNP in the process of germination

CAT activity in whole Harrington seeds increased in the first few hours but declined to 27.00, 24.97, 25.99, 25.94, 26.80 and 10.56 µmol min^{-1} g^{-1} FW after 24 h, which rose up to 48.73, 70.25, 55.23, 38.78, 39.19 and 32.98 µmol min^{-1} g^{-1} FW after imbibition

for 48 h in Harrington seeds treated with ddH_2O, 10 μM ABA, 50 μM SNP, 100 μM SNP, 10 μM ABA + 50 μM SNP and 10 μM ABA + 100 μM SNP, respectively (Figure 21). Change of CAT activity in the first few hours showed that SNP, ABA and their mixture promoted activity of CAT whereas its activity after imbibition for 48 h showed that only 50 μM SNP or 10 μM ABA stimulated its activity. SNP with higher concentrations such as 100 μM prevented activity of CAT and addition of ABA into SNP solution enhanced its prevention effect on the enzyme activity (Figure 21). If CAT activity was compared among all the treatments after imbibition for 48 h, the sequence of enzyme activity from high to low was: 10 μM ABA > 50 μM SNP > ddH_2O > 10 μM ABA + 50 μM SNP > 100 μM SNP > 10 μM ABA + 100 μM SNP (Figure 21), indicating that dosage of SNP was crucial to the outcome of experiments. In addition, mixture of SNP and ABA inhibited activity of CAT and the inhibition became more intense when dosage of SNP increased.

3.15 Change of NO content in embryo tissue during germination

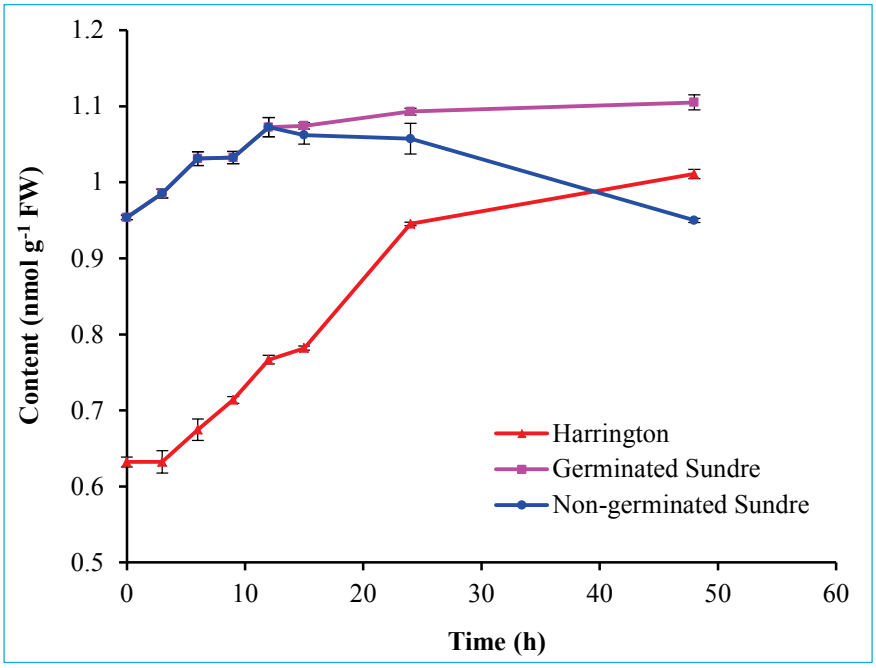

Figure 22 Content of NO in embryos of barley seeds in the process of germination

Content of NO increased from 0.63 and 0.95 nmol g^{-1} FW at 0 h to 1.01 and 1.10 nmol g^{-1} FW after imbibition for 48 h in embryos of Harrington and germinated Sundre seeds respectively but its content in embryos of non-germinated Sundre seeds declined to 0.95 nmol g^{-1} FW from 15 to 48 h with imbibition. Its content in embryos of Sundre seeds was higher than in Harrington seeds (Figure 22), which was similar to that in whole barley seeds (Figure A21, Appendices). However, NO content in the whole barley seeds was much lower than that in embryo tissue of the seeds.

3.16 *S*-Nitrosylation levels of soluble proteins in embryos of barley seeds

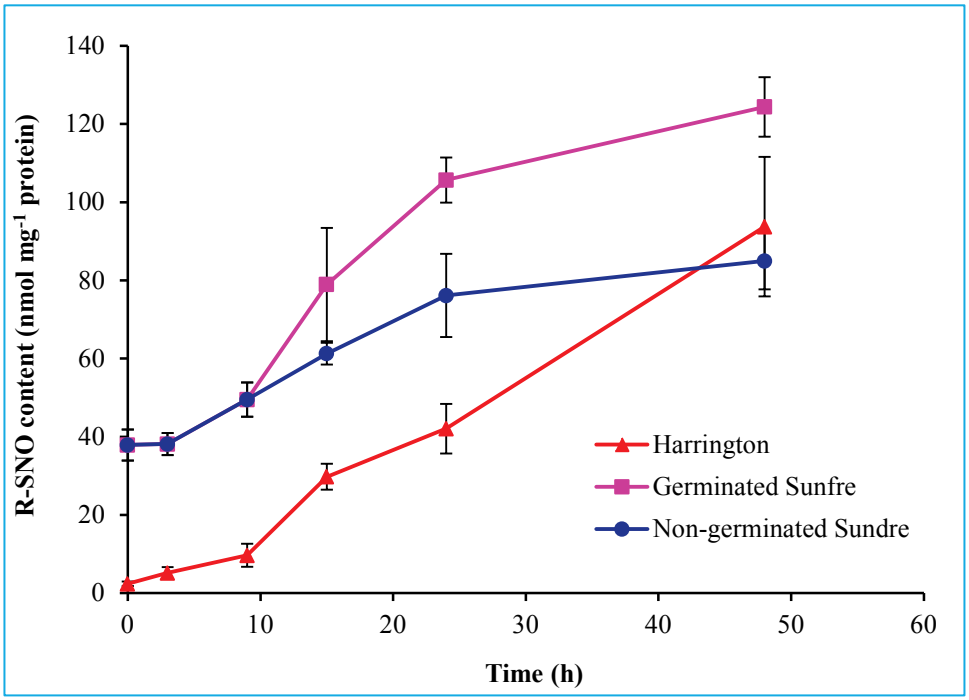

Figure 23 Content of R-SNO in soluble proteins of barley embryos in the process of germination

Content of R-SNO in soluble proteins increased from 2.38 and 37.89 nmol mg^{-1} protein at 0 h to 93.74 and 124.39 nmol mg^{-1} protein in Harrington and germinated Sundre seeds respectively after imbibition for 48 h but its content in non-germinated Sundre barley seeds did not increase as much as that in germinated seeds. The content of R-SNO in embryos of Sundre seeds was much higher than that in Harrington seeds (Figure 23).

3.17 Activity of *S*-nitrosoglutathione reductase in embryos of barley seeds

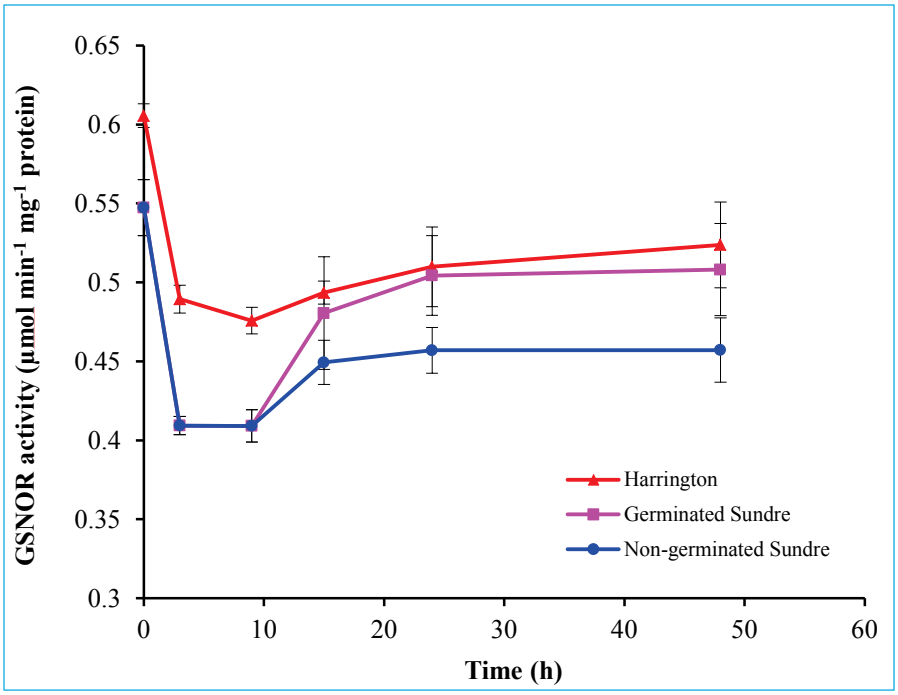

Figure 24 Activity of GSNOR in embryos of barley seeds in the process of germination

Activity of GSNOR decreased from 0.61 and 0.55 µmol min^{-1} mg^{-1} protein at 0 h to 0.48 and 0.41 after 15 h and later rose up to 0.52 and 0.51 µmol min^{-1} mg^{-1} protein after imbibition for 48 h in Harrington and germinated Sundre barley seeds, respectively. However, its activity in non-germinated Sundre seeds remained constant from 15 to 48 h, about 0.46 µmol min^{-1} mg^{-1} protein (Figure 24). Its activity in embryos was much higher than that in whole barley seeds (Figure A22, Appendices)

3.18 Change of protein concentration in scutellum of barley seeds in the process of germination and seedling growth

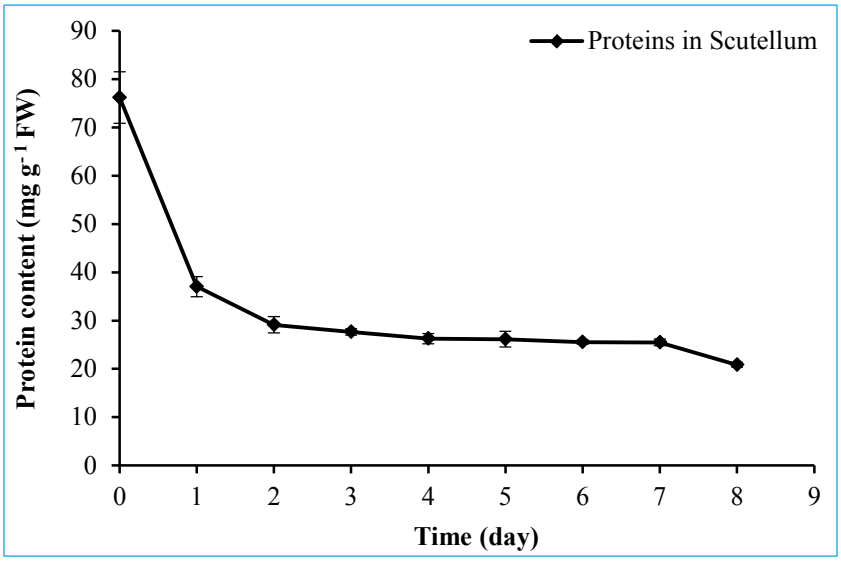

Figure 25 Content of soluble proteins in scutellum of Harrington seeds germinating from 0 to 8 days

The content of total soluble proteins in scutellum decreased quickly from 76.21 mg g^{-1} FW in dry Harrington seeds to 29.14 mg g^{-1} FW within the first two days. After this, content of soluble proteins remained on a similar level from day 2 to day 7 even though it declined on day 8 (Figure 25).

3.19 pH value in scutellum and endosperm of barley seeds in the process of germination and seedling growth

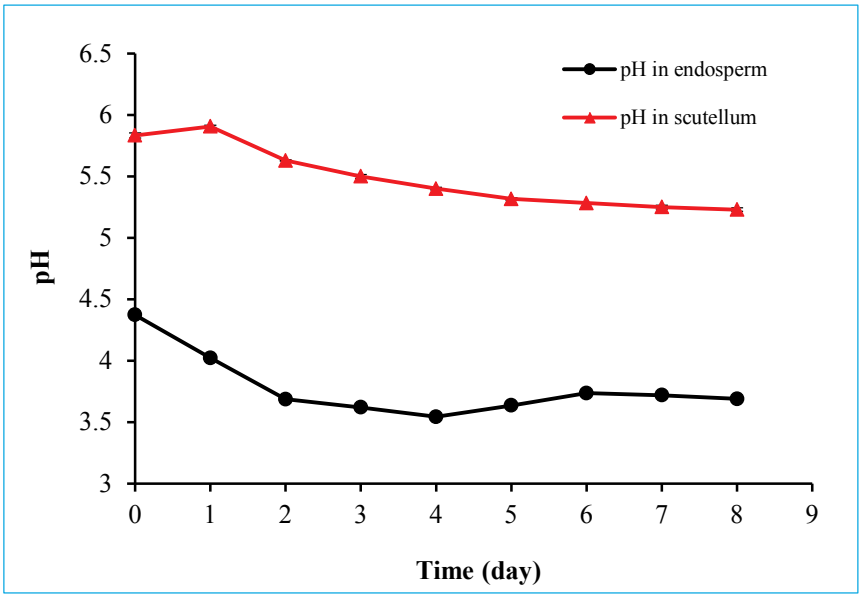

Figure 26 pH value in scutellum and endosperm of Harrington seeds germinating for 8 days

Value of pH in scutellum of Harrington seeds increased from 5.83 to 5.91 within the first day but later it decreased to 5.23 within 8 days gradually. In endosperm of Harrington seeds, pH value decreased from 4.37 on day 0 to 3.54 on day 4 whereas after that it increased slightly to 3.69 on day 8 (Figure 26).

3.20 Content of H_2O_2 in scutellum of barley seeds in the process of germination and seedling growth

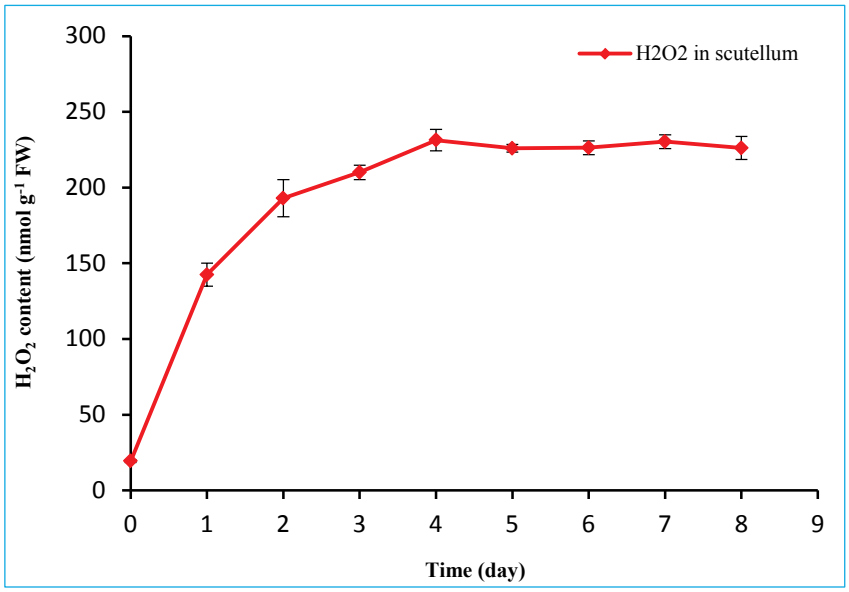

Figure 27 Content of H_2O_2 in scutellum of Harrington seeds germinating from 0 to 8 days

Content of H_2O_2 in scutellum of Harrington seeds increased more than ten times from day 0 to day 4, up to 231.31 nmol g^{-1} FW on day 4 and later it remained stable on the level (Figure 27).

3.21 Content of ascorbate and dehydroascorbate in scutellum of Harrington seeds in the process of germination and seedling growth

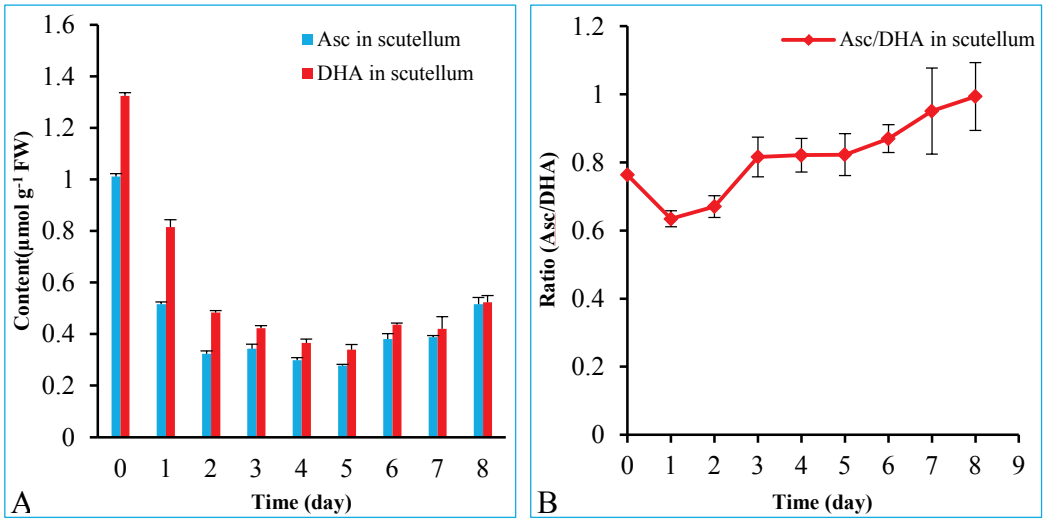

Figure 28 Content of ascrobate and DHA and their ratio in scutellum of Harrington seeds germinating from 0 to 8 days

Asc: ascorbate

Content of ascorbate and DHA decreased from 1.01 and 1.32 μmol g^{-1} FW at 0 day to 0.28 and 0.34 μmol g^{-1} FW in scutellum of Harrington seeds germinating for 5 days respectively but later their content was enhanced to almost the same amount, about 0.52 μmol g^{-1} FW on day 8 (Figure 28 A). Accompanying change of their content, the ascorbate/DHA declined from 0.76 in dry seeds to 0.63 on day 1 and then rose up to 0.99 in scutellum of the barley seeds germinating for 8 days (Figure 28 B).

3.22 Content of glutathione and glutathione disulfide and their ratio in scutellum of barley seeds in the process of germination and seedling growth

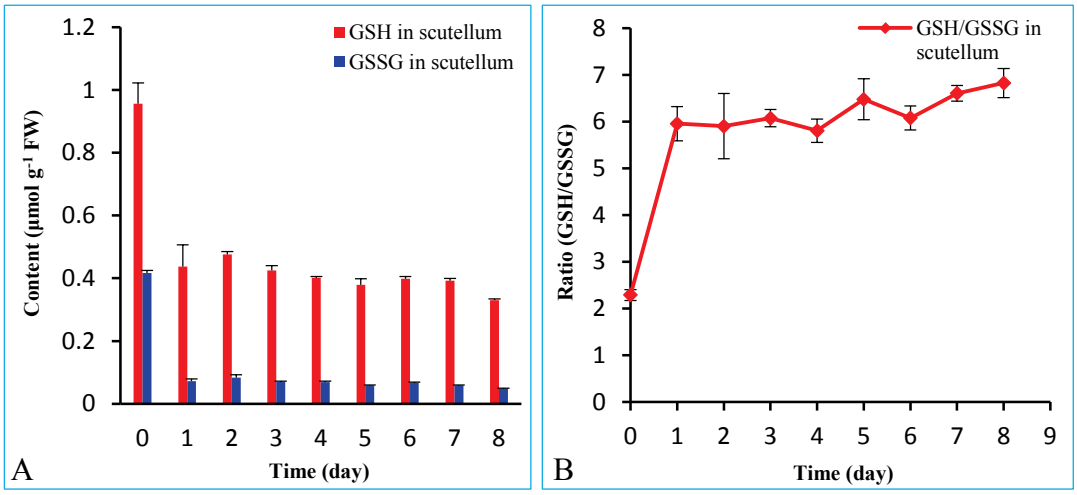

Figure 29 Content of GSH and GSSG and their ratio in scutellum of Harrington seeds germinating from 0 to 8 days

Content of GSH and GSSG dropped sharply from 0.96 and 0.42 μmol g^{-1} FW on day 0 (dry seeds) to 0.44 and 0.07 μmol g^{-1} FW respectively on day 1. From day 2 to day 8, their content decreased slightly and almost remained on a similar level even though their content rose up a little from day 1 to day 2 (Figure 29 A). With the change of their content, GSH/GSSG in scutellum rose up quickly from 2.29 on day 0 to 5.96 on day 1, and then remained on a similar value from day 2 to day 8 (Figure 29 B).

3.23 Content of adenosine triphosphate and adenosine diphosphate and their ratio in scutellum of barley seeds in the process of germination and seedling growth

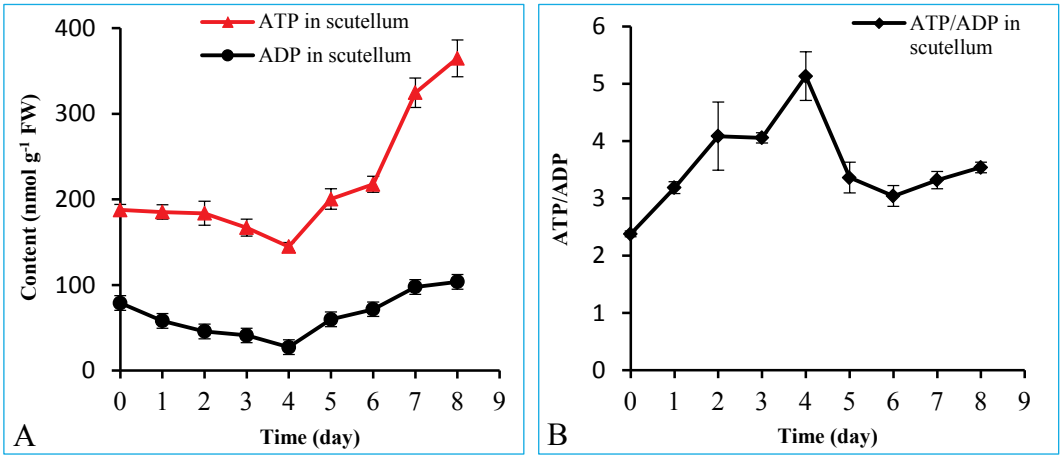

Figure 30 Content of ATP and ADP and their ratio in scutellum of Harrington seeds germinating from 0 to 8 days

Content of ATP and ADP decreased from 188 and 79 nmol g^{-1} FW in dry seeds (at 0 day) to 145 and 27 nmol g^{-1} FW after 4 days respectively but their content increased to 365 and 104 nmol g^{-1} FW respectively in scutellum of Harrington seeds germinating for 8 days (Figure 30 A). Accompanying change of ATP and ADP content, ATP/ADP increased gradually from 2.38 on day 0 to 5.13 on day 4 whereas the ratio went down to 3.04 on day 6. From day 6 to day 8, the ratio increased to 3.54 (Figure 30 B).

3.24 Activity of enzymes specific to glyoxylate cycle in scutellum of barley seeds in the process of germination and seedling growth

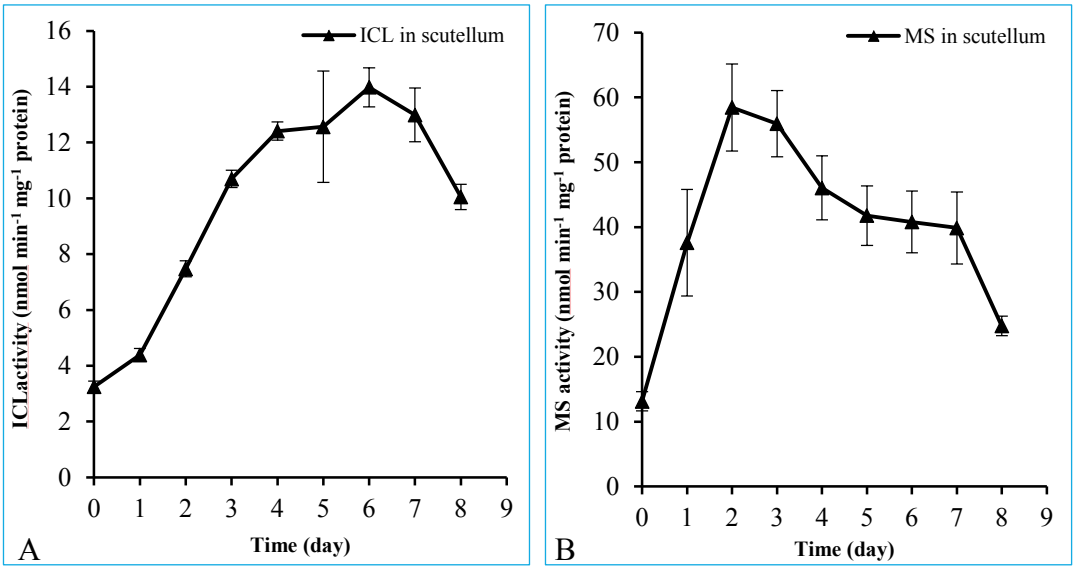

Figure 31 Activities of ICL and MS in scutellum of Harrington seeds germinating from 0 to 8 days

Activity of ICL rose up gradually from 3.24 nmol min^{-1} mg^{-1} protein on day 0 to 13.98 nmol min^{-1} mg^{-1} protein on day 6 and decreased to 10.05 nmol min^{-1} mg^{-1} protein on day 8 (Figure 31 A). Activity of MS was raised up quickly from 13.14 nmol min^{-1} mg^{-1} protein on day 0 to 58.46 nmol min^{-1} mg^{-1} protein on day 2 whereas its activity dropped gradually later (Figure 31 B). Activity of MS was much higher than that of ICL even though both of them were in the glyoxylate cycle.

3.25 Activity of succinate dehydrogenase and fumarase in scutellum of barley seeds in the process of germination and seedling growth

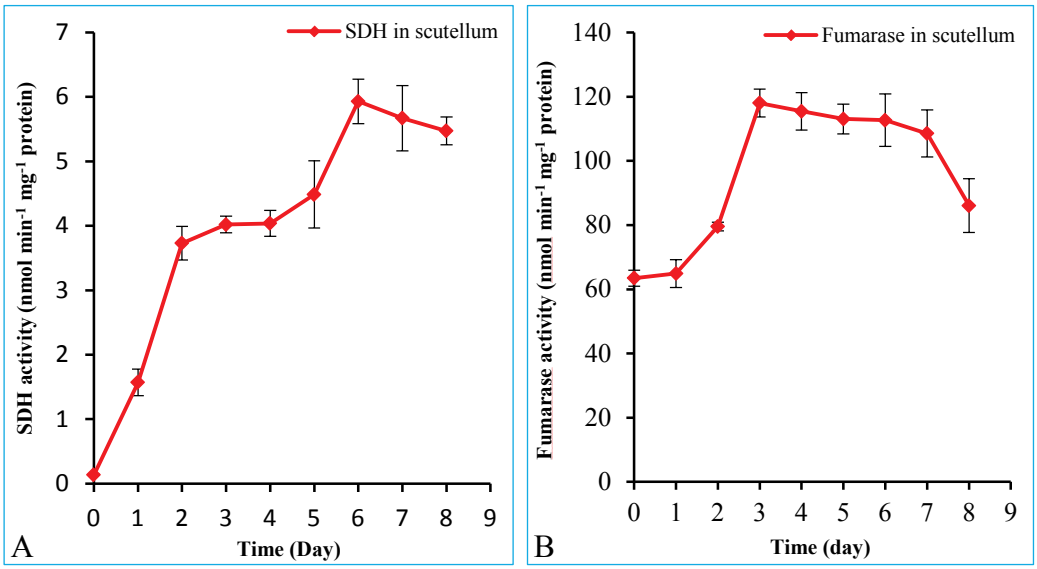

Figure 32 Activities of SDH and fumarase in scutellum of Harrington seeds germinating from 0 to 8 days

Activity of SDH rose up quickly within the first two days and continued to increase gradually to about 5.93 nmol min^{-1} mg^{-1} protein on day 6. From day 6 to day 8, its activity decreased (Figure 32 A). Activity of fumarase was elevated from 63.48 nmol min^{-1} mg^{-1} protein on day 0 to 118.03 nmol min^{-1} mg^{-1} protein in the first 3 days, remained on a similar level from day 3 to day 7, and then decreased to 86.07 nmol min^{-1} mg^{-1} protein on day 8 (Figure 32 B).

3.26 Content of organic acids in scutellum and endosperm of barley seeds in the process of germination and seedling growth

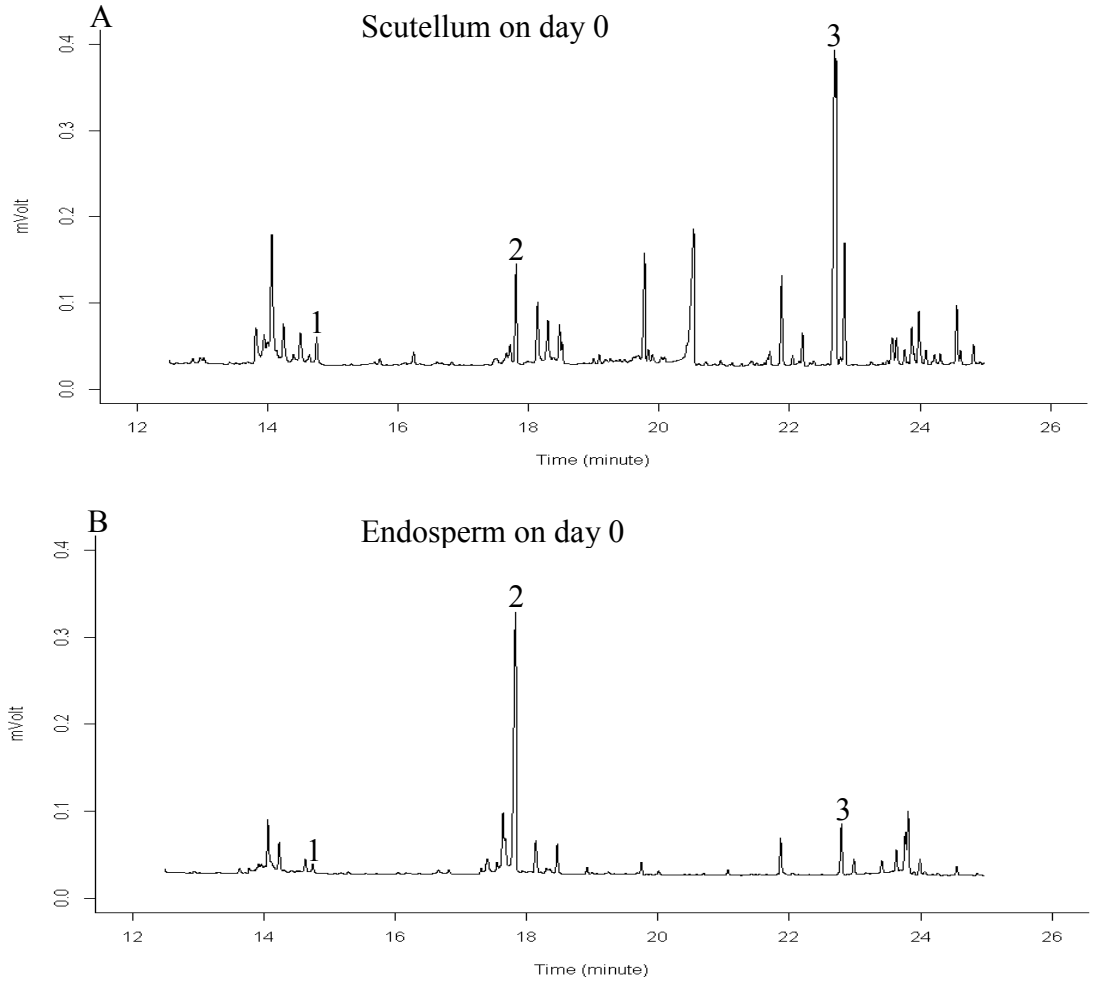

Figure 33 GC-MS chromatograms of trimethylsilyl derivatives of succinic acid, malic acid and citric acid in scutellum and endosperm of Harrington seeds

1: Succinic acid, di(trimethylsilyl) ester 2: Malic acid, O-(trimethylsilyl-, bis(trimethylsilyl) ester
3: Citric acid, tris(trimethylsilyl) ester

In the analysis of organic acids by GC-MS, succinic acid, malic acid and citric acid in scutellum (Figure 33 A) and endosperm (Figure 33 B) of Harrington seeds on day 0 were identified by their retention time (Figure A27, figure A28 and figure A29, Appendices) and mass spectrum (Figure A30, figure A31 and figure A32, Appendices) of standards. These organic acids also were identified in both scutellum (Figure A33 A, B, C, D, E, F, G and H, Appendices) and endosperm (Figure A34 A, B, C, D, E, F, G and H, Appendices) of the barley seeds germinating from day 1 to day 8 with the same method. The retention time of trimethylsilyl derivatives of succinic acid, malic acid and citric acid in scutellum was 14.703, 17.842 and 22.772 minutes, respectively (Figure 33 A), and their retention time of endosperm samples was similar to that in scutellum, which was 14.719, 17.834 and 22.756 minutes, respectively (Figure 33 B).

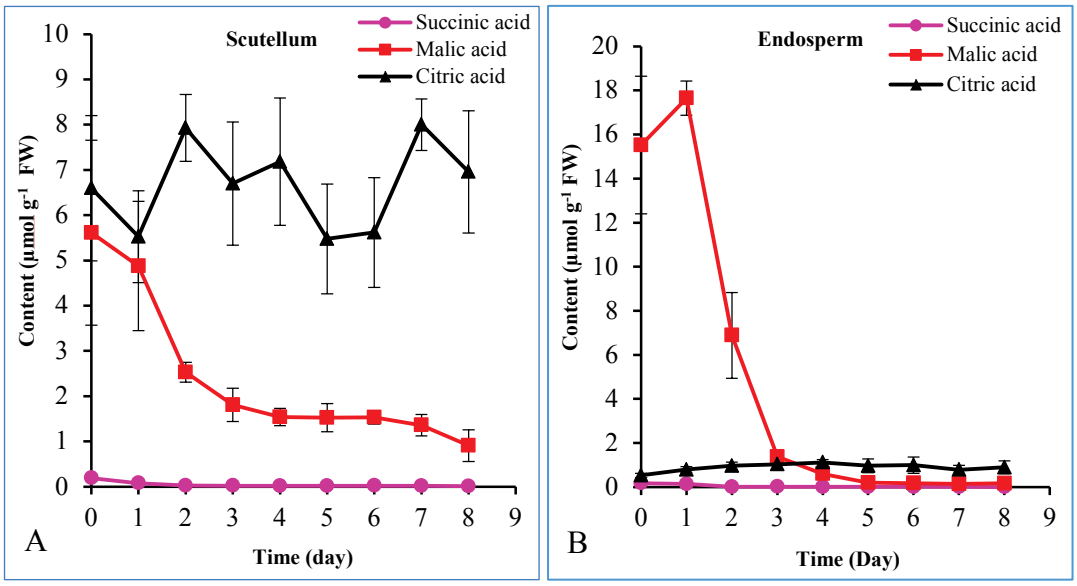

Figure 34 Content of succinic acid, citric acid and malic acid in scutellum and endosperm of Harrington seeds germinating from 0 to 8 days

Content of succinic acid was low in scutellum and even lower in endosperm. Its content in scutellum decreased from 0.19 μmol g^{-1} FW on day 0 to 0.02 μmol g^{-1} FW on day 3 and later remained on the similar level (Figure 34 A). In endosperm, content of succinic acid dropped down quickly from 0.18 μmol g^{-1} FW on day 0 to 0.01 μmol g^{-1} FW on day 2, and later its content was only on a hint level, almost 0 (Figure 34 B). Content of citric acid in scutellum fluctuated between 5.53 and 8.00 μmol g^{-1} FW from 0 to 8 days, which was much higher than that in endosperm where its content increased from 0.53 μmol g^{-1} FW on day 0 to 1.12 μmol g^{-1} FW after 4 days but later decreased to 0.90 μmol g^{-1} FW on day 8 (Figure 34 A and B). Content of malic acid in scutellum dropped quickly from 5.61 μmol g^{-1} FW on day 0 to 1.81 μmol g^{-1} FW in the first three days and continued going down gradually to 0.91 μmol g^{-1} FW on day 8 (Figure 34 A). In endosperm, content of malic acid rose up from 15.52 μmol g^{-1} FW on day 0 to 17.65 μmol g^{-1} FW on day 1 whereas its content dropped sharply to 0.59 μmol g^{-1} FW on day 4. After this, its content remained on a very low level, about 0.15 μmol g^{-1} FW from day 5 to day 8 (Figure 34 B).

3.27 Change of phosphoenopyruvate carboxykinase activity in scutellum of barley seeds

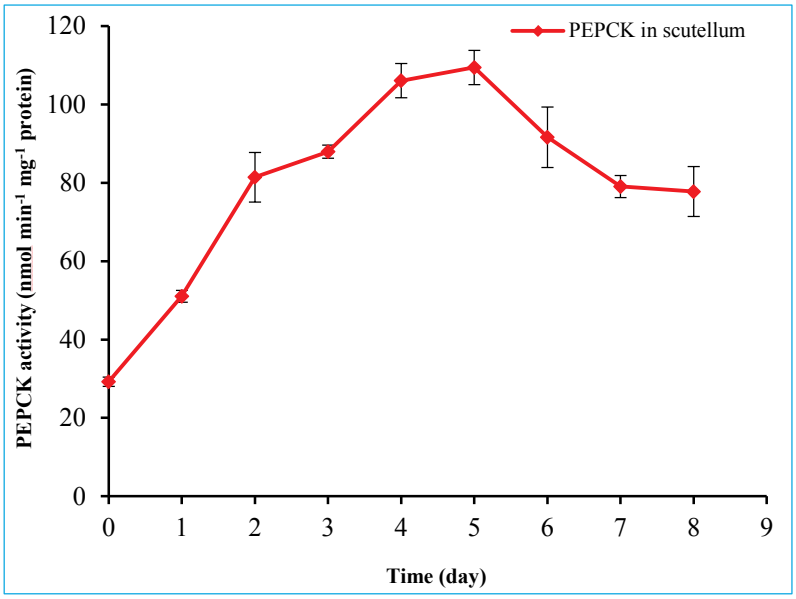

Figure 35 Activity of PEPCK in scutellum of Harrington seeds germinating from 0 to 8 days

Activity of PEPCK in scutellum of Harrington seeds increased gradually from 29.23 nmol min^{-1} mg^{-1} protein on day 0 to its peak value, 109.45 nmol min^{-1} mg^{-1} protein after germinating for 5 days, and then it decreased to 77.76 nmol min^{-1} mg^{-1} protein after seed germination for 8 days (Figure 35).

4 Discussion

4.1 The role of reactive oxygen species during seed germination

Seed germination starts from imbibition and results in radicle protrusion, which corresponds to the first two phases of the process described by Bewley (1997). In this study, the first radicles appeared at 15 h (Figure A10 B and E, Appendices), and by 24 h almost all non-dormant seeds developed radicles. The separation between the early and later period of seed germination was assumed by 10 h from imbibition in the research (Figure 1). The activation of respiration with imbibition triggers more active production of ROS and RNS. Accumulation of H_2O_2 stimulates seed germination (Oracz et al., 2007; Bailly et al., 2008) and germination of Arabidopsis seeds is mediated by accumulation of $O_2^{\bullet-}$ and H_2O_2 in radicles (Leymarie et al., 2012). In sunflower (*Helianthus annuus* L.) seeds, germination is shown to be associated with a marked increase in generation of H_2O_2 and $O_2^{\bullet-}$ in the embryonic axes resulting from an inhibition of CAT and SOD and from activation of NADPH oxidase (Oracz et al., 2009). The previous results are consistent with the change of $O_2^{\bullet-}$ in the non-dormant Harrington seeds but contrary to the data in the dormant Sundre seeds (Figure 8 B). Taking effects of sodium hypochlorite on breaking seed dormancy into account, it was concluded that oxidation could break dormancy of the Sundre seeds. Which was more essential to break seed dormancy, H_2O_2, $O_2^{\bullet-}$ or other kinds of ROS was still controversial. In this research, the content of H_2O_2 and $O_2^{\bullet-}$ was higher in the dry dormant Sundre seeds than in non-dormant Harrington seeds (Figure 10 A and B), showing that dormancy of seeds was linked to high content of ROS. Because of

temporary peak of H_2O_2 at beginning of germination of dormant Sundre seeds and high amount of $O_2^{\bullet-}$ in dry dormant Sundre seeds, (Figure 10 A and B), probably H_2O_2 played a more significant role in breaking dormancy and $O_2^{\bullet-}$ was more crucial to keep seed dormancy.

4.2 The role of antioxidants and activity of enzymes scavenging reactive oxygen species

The ascorbate-glutathione cycle plays a crucial role during seed germination and seedling growth as it is required not only for scavenging H_2O_2 but also for adjusting redox potentials of ascorbate and glutathione, both of which are good indicators of the overall cellular redox status (Mitrović et al., 2012). When content of H_2O_2 was increasing in scutellum within the first 4 days, content of ascorbate and DHA was decreasing. When content of H_2O_2 reached to the highest level and remained there, content of ascorbate and DHA increased. This demonstrated two aspects: ascorbate and DHA played a dominant role in scavenging ROS and production of ROS in tissue reached to peak value after 4 days. In addition, in most of the seed samples except dry barley seeds, [GSSG] was higher than [GSH], and [DHA] was higher than [ascorbate], demonstrating that the internal environment of seeds became more oxidized after seeds absorbed water. Total amount of GSH and GSSG was more than that of ascorbate and DHA (Figure 12 A, B and C; Figure 13 A, B and C). Therefore, GSH and GSSG would possibly play a more essential role in adjusting the redox status of cells than ascorbate and DHA. However, perhaps only a part of GSH and GSSG

joined the ascorbate-glutathione cycle as activity of GR was very low (Figure 11 D). The reduction potential of GSSG/2GSH couple is determined by [GSH] and [GSH]/[GSSG] (Schafer and Buettner, 2001). Therefore, the change of one of both [GSH] and [GSH]/[GSSG] will affect redox status of cells. However, in this research, no data showed that [GSH], [GSSG] and their reduction potential influenced seed germination or dormancy directly. Taking into consideration the content of H_2O_2, ascorbate, DHA, GSH and GSSG in tissue, it could be proposed that change of antioxidant metabolism in seed germination and early period of seedling growth was intense, and the antioxidant metabolism became smooth and no apparent turn point appeared when barley seedlings went to vegetative growth.

Summarizing the data about enzymes scavenging ROS in the research, except for SOD, if the activities of these enzymes were ranked from high to low, it was CAT and DHAR > APX > MDHAR > GR. Even though DHAR, APX, MDAHR and GR take part in the ascorbate-glutathione cycle, their activities are apparently different, displaying that re-generation of ascorbate through DHAR is dominant and DHAR plays a main role in maintaining the ascorbate pool. The high activity of CAT and SODs demonstrated that they contributed very much to scavenge ROS. Compared activity of Cu/Zn-SOD to that of Mn-SOD, it demonstrated that in dry barley seeds and early period of seed germination, Mn-SOD located in mitochondria plays a more important role in scavenging $O_2^{\bullet-}$ but after 15 h Cu/Zn SOD located in cytosol became more dominant, which suggested that the composition of SOD isoforms before

germination was different from that after seed germination. Activity of APX increased apparently (Figure 11 A) but its gene expression did not increase in the process of seed germination (Figure 16 A), displaying that the increase of its activity was caused by outcome after transcription such as modification of the protein or higher amount of translation.

4.3 NO generation and scavenging

Except for ROS, RNS are another factor that should not be ignored, which play a key role in regulating seed germination and dormancy. In the anaerobic stage of seed germination besides fermentation, it is also related to turnover of NO which might be important for regulating redox state and energy (Igamberdiev et al., 2010). In this research, NO content in embryo tissue increased gradually in germinating seeds within 48 h (Figure 22). After radicle protrudes seed coat in the process, the internal environment of seeds will be aerobic instead of anaerobic. Therefore, NO production in later phase of the seed germination has no direct relationship with anaerobic conditions and fermentation. In addition, nitrosylaton/denitrosylation of APX adjusts its function in Arabidopsis (Correa-Aragunde et al., 2013), displaying that NO, as a signal molecule or product of metabolism, is essential to specific modification of proteins, and even it may join plant development.

SNP as a NO donor could reduce seed dormancy (Bethke et al., 2004) but it could not break dormancy of Sundre seeds in this research. KNO_3 only increased germination

rate of Sundre seeds on the first day but no stimulation in the later days. In addition, KNO_2 almost had no stimulation effect on the seed germination (Figure A23, Appendices). All of the data obtained showed that NO could not break dormancy of the Sundre seeds, which was different from conclusions of Bethke et al. (2004), by which it could be assumed that NO could break some types of seed dormancy but not all.

NO could be scavenged not only via hemoglobin-mediated mechanism (Igamberdiev and Hill, 2004) but also via denitrosylation of RSNO, one of which is denitrosylation of *S*-nitrosoglutathione catalyzed by GSNOR holding high activity in dry barley seeds (Figure 24). Activity of GSNOR in non-dormant Harrington seeds was higher than that in more dormant Sundre cultivar (Figure 24). If activity of GSNOR, content of RSNO in proteins and content of NO in tissue were taken into consideration together, it could be deduced that lower GSNOR activity and higher content of free NO in tissue would lead to higher levels of protein nitrosylation (Figure 22, 23 and 24). Another point was that expression of *ADH3* was not consistent with the change of GSNOR activity (Figure 16 C and D; Figure 24). Expression of *ADH3* and *Hb* in the two barley cultivars was different but their expression in germinated and non-germinated Sundre barley seeds was similar, indicating difference of enzyme activity in the different cultivars was caused by genetics and difference of their enzyme activity in one cultivar was caused by translation of the gene or post translational modification of the proteins.

Levels of NO and nitrosylated proteins increased in the process of seed germination during imbibition for 48 h (Figure 22 and 23). However, which nitrosylated protein(s) play(s) a vital role in regulating seed germination and dormancy and what causes NO release are still unknown. Even what is the main pathway to generate NO in plants is still controversial. Therefore, there are many unknown questions about metabolism of RNS and their role in in regulating seed germination and dormancy, and more research should be imposed on this field in the future.

4.4 Accumulation of adenosine triphosphate and adenosine diphosphate in tissue during seed germination and seedling growth

The first stage of germination was accompanied by a drastic and immediate increase in ATP level even with imbibition for only half hour, reaching peak value after imbibition for 3 h (Figure 9 A), which probably corresponded to the first peak of oxygen consumption in aerobic metabolism to drive ATP synthesis, indicating that except for ROS, RNS and plant hormones, ATP was another essential factor to initiate seed germination. Except the transient peak of ATP content in embryo within the first three hours, ATP and ADP accumulation in scutellum of barley seeds (Figure 30 A) was similar to that in embryo within the first two days. Change of ATP and ADP accumulation in embryo (Figure 9 A) and scutellum (Figure 30 A) of barley seeds had similar tendency to the change of ascorbate (Figure 28 A) except the transient peak of ATP and ADP at the beginning of germination (Figure 9 A), which is consistent with the possible mechanism of mitochondria to adjust redox homeostasis that biosynthesis

of ascorbate is coupled to ETC (Bartoli et al., 2000). However, the sharp elevation of ATP within the first three hours was more similar to the dramatic decrease of GSH even though GHS coupled to ATP synthesis has not been described.

Activities of TCA cycle and glyoxylate increased within the first few days (Figure 31 and 32) but ATP and ADP accumulation in tissue decreased (Figure 9 and 30), which is perhaps caused by quick consumption of ATP and ADP. The sharp increase of ATP content in issue is caused by a sharp elevation of oxygen uptake with imbibition at beginning (Botha et al., 1992). When more oxygen are available and penetrate into tissue, more ATP should be accumulated. However, the results in the research showed that in later period of seed germination and early period of seedling growth, ATP and ADP accumulation did not rise up but decreased (Figure 9 and 30) even though enough oxygen is available and oxygen is much easier to penetrate into tissue of seedlings than that in seeds. After imbibition of seeds, metabolism of seeds is activated and even become more active with development of seed germination. Thus, more ATP and ADP will be consumed to support growth of cells and organs. So, consumption of ATP and ADP plays an important role in keeping balance of ATP and ADP accumulation in tissue.

4.5 The role of glyoxylate cycle

Barley seeds with starch as storage are different from Arabidopsis oily seeds (Baud et al., 2008). Therefore, glyoxylate cycle plays a crucial role in taking advantage of CoA-

acetyl from digestion of lipid in oil seeds (Kornberg and Beevers, 1957; Eastmond and Graham, 2001), but it might have less importance in barley seeds. The low content of succinic acid produced by glyoxylate cycle in barley seeds (Figure 34) supported this assumption. If glyoxylate cycle plays an anaplerotic role to TCA cycle, this should occur in the first few days. When content of succinic acid is very low in tissue (Figure 34), its anaplerotic role will not be remarkable. Comparing activities of ICL and MS in glyoxylate cycle (Figure 31) with SDH and fumarase in TCA cycle (Figure 32), activity of fumarase was higher than MS in glyoxylate cycle. However, from this point, it was difficult to conclude that TCA cycle had stronger activities than glyoxylate cycle as enzyme activities or content of intermediates such as organic acids in TCA cycle were not always higher than those in glyoxylate cycle. In the glyoxylate cycle, activity of MS was about 5 times higher than ICL (Figure 31) and in the TCA cycle fumarase was more than 20 folds higher than SDH (Figure 32), displaying that malic acid production in the metabolism is of huge importance and TCA cycle plays a more dominant role in production of it. Oxygen inhibits activity of ICL apparently (Dilworth and Kennedy, 1963). With development of seed germination and seedling growth, aerobic metabolism will become more intense. Thus, the activity of the glyoxylate cycle will be prevented and its anaplerotic role to TCA cycle will become relatively weaker.

4.6 Effect of succinic acid, malic acid and citric acid on pH value in endosperm and scutellum

The content of intermediates such as succinic acid, malic acid and citric acid had huge difference in scutellum and endosperm. Succinic acid is the output of glyoxylate cycle and an intermediate in TCA cycle but its content in the two kinds of tissue is very low. In addition, content of succinic acid decreased in both scutellum and endosperm (Figure 34) when pH value in the two tissue decreased (Figure 26). Content of isocitric acid was undetectable in both scutellum and endosperm (data were not shown). Therefore, both succinic acid and isocitric acid did not have much influence on pH value in the two tissue, and they did not play an important role in acidification of starch either. Furthermore, the change of succinic acid, malic acid and citric acid in scutellum did not support decrease of pH value in scutellum. Thus, all of them did not affect pH value in scutellum remarkably. The increase of malic acid content in endosperm on the first day was probably used to acidify starch in endosperm, which is favorable to movement and digestion of starch. Citric acid also contributed to acidification of starch since its content increased within the first four days (Figure 34 B) although its increase was not striking. Content of malic acid and citric acid became lower in endosperm in the later period of seedling growth, which could be one cause leading to the slight increase of pH value in endosperm. Low pH value in endosperm is favorable to movement of reserves (Hamabata et al., 1988). However, the low pH value affects activity of many enzymes in metabolism. For example, optimal pH value for APX in barley is 7.0 (Xu et al., 2008). The overall pH value in tissue was not the

value in each compartment in cells. Enzymes or metabolisms sensitive to pH value are protected by membranes of compartments, where optimal pH will be kept for them. Therefore, the overall low pH value in both scutellum and endosperm (Figure 26) will not affect biological reactions in them.

4.7 Interaction between reactive oxygen species, reactive nitrogen species and plant hormones

A crosslink between ROS, RNS and plant hormones is complex and much research has been done on it. The changing oxygen levels and activation of respiration in seeds from imbibition to seedling development trigger the formation of ROS and RNS (Igamberdiev et al., 2014). NO is generated quickly after imbibition of seeds, which stimulates seed germination by inducing expression of inactivating ABA gene and elevating ethylene generation (Arc et al., 2013). Germination of switchgrass seeds is inhibited by ABA and stimulated by NO or ROS, and ROS treatment stimulated production of NO in the seeds. External application of ROS instead of NO can overcome ABA inhibition on germination of the seeds (Sarath et al., 2007a). Furthermore, scavengers of NO such as diphenyleneiodonium (DPI) can counteract with the partial promotion of ROS on seed germination (Sarath et al., 2007b), indicating that NO is essential for seed germination (Sarath et al., 2007a). H_2O_2 treatment improves germination of dormant Arabidopsis seeds, coupled with up-regulation of ABA catabolism genes and GA biosynthesis genes. The whole process is mediated by NO signal transduction because NO scavenger, cPTIO, eliminates the

stimulation effect of H_2O_2. Therefore, the dormancy and germination of seeds are jointly regulated by them (Liu et al., 2010). Content of ROS (Figure 10 A and B) and RNS (Figure 22 and figure 23) remained higher in the more dormant Sundre barley seeds than in non-dormant Harrington seeds, indicating higher content of ROS and RNS was linked to the dormancy of seeds.

However, the interaction between different ROS and NO is not always the same. $^{\bullet}NO$ and H_2O_2 reciprocally raise generation of each other but $^{\bullet}NO$ and $O_2^{\bullet-}$ display reciprocal inhibition on each other's production (Zhao, 2007). While ROS production is aerobic, the production of NO in the reductive pathway is facilitated by transition to anaerobic conditions (Dordas et al., 2003). All in all, the cross-talk between ROS, RNS and plant hormones was particularly important for triggering seed germination, and dosage of ROS, RNS and plant hormones would be crucial in their physiological function. In addition, it is very important to understand the physiological characteristics of dormant and non-dormant barley seeds in the germination process, which is helpful to screen cultivars in barley breeding.

5. Conclusions

5.1 In the process of seed germination from 0 to 48 h (in embryo tissue mainly)

Ascorbate-glutathione cycle became more active in embryos of barley seeds. Content of H_2O_2 and $O_2^{\bullet-}$ in the tissue rose up while activities of enzymes scavenging ROS such as APX, MDHAR, DHAR, GR, CAT and SOD, having certain activities in dry

seeds, were elevated in germinating barley seeds instead of non-germinated Sundre seeds except for decrease of $O_2^{\bullet-}$ content in Sundre seeds in the germination process and SOD activity at beginning of seed germination. Accompanying intense change of ROS metabolism in germinating barley seeds, levels of NO and nitrosothiols in the tissue rose up gradually in the process of seed germination but activity of GSNOR declined in the first few hours, followed by later increase.

Expression of *APX* did not change significantly within the 48 h in both Harrington and Sundre seeds although its expression was little lower in dormant barley seeds. In Harrington seeds, expression of *ADH3* decreased in the germination process but expression of *Hb* increased in the first few hours, remained on a high level and later decreased. In germinated or non-germinated Sundre seeds, expression of *ADH3* and *Hb* did not change significantly. However, the change of APX and GSNOR activities was not consistent with that of their gene expression in the germination process.

Contents of ascorbate, DHA, GSH and GSSG decreased while reduction potential of GSSG/2GSH couple, NO and R-SNO in proteins increased in germinating barley seeds. Their change in non-germinated Sundre seeds was not as intense as in germinated ones. ATP highly accumulated to a very high level at the beginning of seed germination while content of ADP holding similar tendency of change was much lower than ATP. Activities of ADH, LDH and PPDK decreased gradually in

germinating seeds whereas their activities were kept higher in non-germinated Sundre seeds.

KNO_3 with low concentration instead of SNP and KNO_2 stimulated germination of the dormant Sundre seeds but its stimulation was weaker than GA. SNP did not stimulate root growth of Harrington seeds and it did not counteract prevention effect of ABA on this. SNP and mixture of SNP and ABA seriously inhibited activity of APX but not CAT in Harrington seeds. SNP with low dosage stimulated activity of CAT but SNP with high dosage and mixture of SNP and ABA inhibited its activity.

Enzyme activities about scavenging ROS and RNS, content of antioxidants, ATP, ADP, H_2O_2, NO and R-SNO in proteins, and reduction potential of GSG/2GSH couple in germinated barley seeds displayed that metabolisms in germinating barley seeds were much more active than in dormant seeds with imbibition where they remained on a stable level and were similar to or a little higher than those in dry seeds.

5.2 In the process of seed germination and seedling establishment from 0 to 8 days (in scutellum and endosperm tissue)

In scutellum, activities of ICL and MS in glyoxylate cycle, and SDH and fumarase in TCA cycle increased within the first few days and then decreased, displaying the similar change of activities of the two cycles. Meanwhile, accumulation of ATP and ADP in scutellum deceased in the tissue accompanying increase of ATP/ADP within

the first few days but later their content in the tissue increased with decrease of ATP/ADP. Content of malic acid and citric acid was much higher than succinic acid in both scutellum and endosperm. Content of succinic acid and malic acid in endosperm decreased except for instantaneous increase of malic acid on the first day. Content of citric acid in scutellum was stable and much higher than that in endosperm where its content increased in the first few days and then decreased.

In scutellum, content of H_2O_2 reached to the top level while content of ascorbate dropped to the lowest almost at same time, within 4 or 5 days, reflecting the dominant role of ascorbate in scavenging H_2O_2. Ascorbate/DHA in the tissue increased from day 1 to day 8 but it declined from day 0 to day 1. Content of GSH and GSSG in the tissue decreased significantly and GSH/GSSG sharply increased on the first day, but later they remained on a stable level.

Summarizing change of content of ascorbate, GSH, ATP, ADP, H_2O_2, succinic acid, malic acid, citric acid and activities of relative enzymes such as MS and fumarase in embryos from 0 to 48 h and in scutellum from day 0 to day 8, day 4 was the turning point, demonstrating that the change of their metabolism in the process of seed germination and early period of seedlings was intense. Later when plants went into vegetative growth, the change of their metabolism was smooth relatively.

References

Alscher RG (2002) Role of superoxide dismutases (SODs) in controlling oxidative stress in plants. J Exp Bot **53**: 1331–1341

Aoyagi K, Bassham JA (1983) Pyruvate Orthophosphate Dikinase in Wheat Leaves. PLANT Physiol **73**: 853–854

Arc E, Galland M, Cueff G, Godin B, Lounifi I, Job D, Rajjou L (2011) Reboot the system thanks to protein post-translational modifications and proteome diversity: How quiescent seeds restart their metabolism to prepare seedling establishment. Proteomics **11**: 1606–1618

Arc E, Sechet J, Corbineau F, Rajjou L, Marion-Poll A (2013) ABA crosstalk with ethylene and nitric oxide in seed dormancy and germination. Front Plant Sci. doi: 10.3389/fpls.2013.00063

Armstrong JM (1964) The molar extinction coefficient of 2,6-dichlorophenol indophenol. Biochim Biophys Acta **86**: 194–197

Arnelle DR, Stamler JS (1995) NO+, NO, and NO- donation by S-nitrosothiols: implications for regulation of physiological functions by S-nitrosylation and acceleration of disulfide formation. Arch Biochem Biophys **318**: 279–285

Arnold WP, Longnecker DE, Epstein RM (1984) Photodegradation of sodium nitroprusside: biologic activity and cyanide release. Anesthesiology **61**: 254–260

Bailly C, El-Maarouf-Bouteau H, Corbineau F (2008) From intracellular signaling networks to cell death: the dual role of reactive oxygen species in seed physiology. C R Biol **331**: 806–814

Bao X, Pollard M, Ohlrogge J (1998) The biosynthesis of erucic acid in developing embryos of *Brassica rapa*. Plant Physiol **118**: 183–190

Bartoli CG, Pastori GM, Foyer CH (2000) Ascorbate biosynthesis in mitochondria is linked to the electron transport chain between complexes III and IV. Plant Physiol **123**: 335–344

Baskin JM, Baskin CC (2004) A classification system for seed dormancy. Seed Sci Res. doi: 10.1079/SSR2003150

Baud S, Dubreucq B, Miquel M, Rochat C, Lepiniec L (2008) Storage Reserve Accumulation in Arabidopsis: Metabolic and Developmental Control of Seed Filling. Arab Book **6**: e0113

Beeckmans S, Khan AS, Kanarek L, Van Driessche E (1994) Ligand binding on to maize (*Zea mays*) malate synthase: a structural study. Biochem J **303 (Pt 2)**: 413–421

Bethke PC, Gubler F, Jacobsen JV, Jones RL (2004) Dormancy of Arabidopsis seeds and barley grains can be broken by nitric oxide. Planta **219**: 847–855

Bewley JD (1997) Seed Germination and Dormancy. PLANT CELL ONLINE **9**: 1055–1066

Bewley JD (2001) Seed Germination and Reserve Mobilization. Encycl. Life Sci. 1–7

Bortman SJ, Trelease RN, Miernyk JA (1981) Enzyme development and glyoxysome characterization in cotyledons of cotton seeds. Plant Physiol **68**: 82–87

Botha FC, Potgieter GP, Botha A-M (1992) Respiratory metabolism and gene expression during seed germination. Plant Growth Regul **11**: 211–224

Brzezinski R, Talbot BG, Brown D, Klimuszko D, Blakeley SD, Thirion J-P (1986) Characterization of alcohol dehydrogenase in young soybean seedlings. Biochem Genet **24**: 643–656

Buchanan BB, Arnon DI (1969) [30] The reductive carboxylic acid cycle. Methods Enzymol. Elsevier, pp 170–181

Bush DS, Sticher L, van Huystee R, Wagner D, Jones RL (1989) The calcium requirement for stability and enzymatic activity of two isoforms of barley aleurone alpha-amylase. J Biol Chem **264**: 19392–19398

Chelikani P, Fita I, Loewen PC (2004) Diversity of structures and properties among catalases. Cell Mol Life Sci CMLS **61**: 192–208

Cohn MA, Castle L (1984) Dormancy in red rice. IV. Response of unimbibed and imbibing seeds to nitrogen dioxide. Physiol Plant **60**: 552–556

Correa-Aragunde N, Foresi N, Delledonne M, Lamattina L (2013) Auxin induces redox regulation of ascorbate peroxidase 1 activity by *S*-nitrosylation/denitrosylation balance resulting in changes of root growth pattern in Arabidopsis. J Exp Bot **64**: 3339–3349

Crawford NM (2006) Mechanisms for nitric oxide synthesis in plants. J Exp Bot **57**: 471–478

D'Alessandro S, Posocco B, Costa A, Zahariou G, Schiavo FL, Carbonera D, Zottini M (2013) Limits in the use of cPTIO as nitric oxide scavenger and EPR probe in plant cells and seedlings. Front Plant Sci. doi: 10.3389/fpls.2013.00340

Delgado-Alvarado A, Walker RP, Leegood RC (2007) Phosphoenolpyruvate carboxykinase in developing pea seeds is associated with tissues involved in solute transport and is nitrogen-responsive. Plant Cell Environ **30**: 225–235

De los Reyes BG, Myers SJ, McGrath JM (2003) Differential induction of glyoxylate cycle enzymes by stress as a marker for seedling vigor in sugar beet (*Beta vulgaris*). Mol Genet Genomics MGG **269**: 692–698

Del Río LA, Corpas FJ, Barroso JB (2004) Nitric oxide and nitric oxide synthase activity in plants. Phytochemistry **65**: 783–792

De Pinto MC, Locato V, Sgobba A, Romero-Puertas MDC, Gadaleta C, Delledonne M, De Gara L (2013) *S*-nitrosylation of ascorbate peroxidase is part of programmed cell death signaling in tobacco Bright Yellow-2 cells. Plant Physiol **163**: 1766–1775

Dilworth MJ, Kennedy IR (1963) Oxygen inhibition in *Azotobacter vinelandii*. Some enzymes concerned in acetate metabolism. Biochim Biophys Acta **67**: 240–253

Donaldson RP, Assadi M, Karyotou K, Olcum T, Qiu T (2001) Plant Peroxisomes and Glyoxysomes. Encycl. Life Sci.

Dordas C, Hasinoff BB, Igamberdiev AU, Manac'h N, Rivoal J, Hill RD (2003) Expression of a stress-induced hemoglobin affects NO levels produced by alfalfa root cultures under hypoxic stress. Plant J Cell Mol Biol **35**: 763–770

Eastmond PJ, Germain V, Lange PR, Bryce JH, Smith SM, Graham IA (2000) Postgerminative growth and lipid catabolism in oilseeds lacking the glyoxylate cycle. Proc Natl Acad Sci U S A **97**: 5669–5674

Eastmond PJ, Graham IA (2001) Re-examining the role of the glyoxylate cycle in oilseeds. Trends Plant Sci **6**: 72–78

Eckardt NA (2005) Peroxisomal Citrate Synthase Provides Exit Route from Fatty Acid Metabolism in Oilseeds. PLANT CELL ONLINE **17**: 1863–1865

El-Maarouf-Bouteau H, Bailly C (2008) Oxidative signaling in seed germination and dormancy. Plant Signal Behav **3**: 175–182

Farge G, Touraille S, Debise R, Alziari S (2002) The respiratory chain complex thresholds in mitochondria of a *Drosophila subobscura* mutant strain. Biochimie **84**: 1189–1197

Fernie AR, Carrari F, Sweetlove LJ (2004) Respiratory metabolism: glycolysis, the TCA cycle and mitochondrial electron transport. Curr Opin Plant Biol **7**: 254–261

Foresi N, Correa-Aragunde N, Parisi G, Caló G, Salerno G, Lamattina L (2010) Characterization of a nitric oxide synthase from the plant kingdom: NO generation from the green alga *Ostreococcus tauri* is light irradiance and growth phase dependent. Plant Cell **22**: 3816–3830

Foyer CH, Halliwell B (1976) The presence of glutathione and glutathione reductase in chloroplasts: A proposed role in ascorbic acid metabolism. Planta **133**: 21–25

Gibon Y (2004) A Robot-Based Platform to Measure Multiple Enzyme Activities in Arabidopsis Using a Set of Cycling Assays: Comparison of Changes of Enzyme Activities and Transcript Levels during Diurnal Cycles and in Prolonged Darkness. PLANT CELL ONLINE **16**: 3304–3325

Gillespie KM, Ainsworth EA (2007) Measurement of reduced, oxidized and total ascorbate content in plants. Nat Protoc **2**: 871–874

Goldstein S, Russo A, Samuni A (2003) Reactions of PTIO and Carboxy-PTIO with $^{\bullet}NO$, $^{\bullet}NO2$, and $O_2^{\bullet-}$. J Biol Chem **278**: 50949–50955

Good AG, Muench DG (1992) Purification and characterization of an anaerobically induced alanine aminotransferase from barley roots. Plant Physiol **99**: 1520–1525

Gordon AG (1971) THE GERMINATION RESISTANCE TEST — A NEW TEST FOR MEASURING GERMINATION QUALITY OF CEREALS. Can J Plant Sci **51**: 181–183

Graham IA, Denby KJ, Leaver CJ (1994) Carbon Catabolite Repression Regulates Glyoxylate Cycle Gene Expression in Cucumber. Plant Cell **6**: 761–772

Gupta AS, Webb RP, Holaday AS, Allen RD (1993) Overexpression of Superoxide Dismutase Protects Plants from Oxidative Stress (Induction of Ascorbate Peroxidase in Superoxide Dismutase-Overexpressing Plants). Plant Physiol **103**: 1067–1073

Gupta KJ, Igamberdiev AU (2011) The anoxic plant mitochondrion as a nitrite: NO reductase. Mitochondrion **11**: 537–543

Hamabata A, García-Maya M, Romero T, Bernal-Lugo I (1988) Kinetics of the Acidification Capacity of Aleurone Layer and Its Effect upon Solubilization of Reserve Substances from Starchy Endosperm of Wheat. Plant Physiol **86**: 643–644

Hendricks SB, Taylorson RB (1974) Promotion of seed germination by nitrate, nitrite, hydroxylamine, and ammonium salts. Plant Physiol **54**: 304–309

Higgins CF, Payne JW (1977) Characterization of active dipeptide transport by germinating barley embryos: Effects of pH and metabolic inhibitors. Planta **136**: 71–76

Hoffman NE, Bent AF, Hanson AD (1986) Induction of lactate dehydrogenase isozymes by oxygen deficit in barley root tissue. Plant Physiol **82**: 658–663

Holzmeister C, Fröhlich A, Sarioglu H, Bauer N, Durner J, Lindermayr C (2011) Proteomic analysis of defense response of wildtype *Arabidopsis thaliana* and plants with impaired NO- homeostasis. Proteomics **11**: 1664–1683

Igamberdiev AU, Baron K, Manac'h-Little N, Stoimenova M, Hill RD (2005) The haemoglobin/nitric oxide cycle: involvement in flooding stress and effects on hormone signalling. Ann Bot **96**: 557–564

Igamberdiev AU, Bykova NV, Shah JK, Hill RD (2010) Anoxic nitric oxide cycling in plants: participating reactions and possible mechanisms. Physiol Plant **138**: 393–404

Igamberdiev AU, Hill RD (2004) Nitrate, NO and haemoglobin in plant adaptation to hypoxia: an alternative to classic fermentation pathways. J Exp Bot **55**: 2473–2482

Igamberdiev AU, Popov VN, Falaleeva MI (1995) Alternative system of succinate oxidation in glyoxysomes of higher plants. FEBS Lett **367**: 287–290

Igamberdiev AU, Ratcliffe RG, Gupta KJ (2014) Plant mitochondria: Source and target for nitric oxide. Mitochondrion. doi: 10.1016/j.mito.2014.02.003

Jaffrey SR, Erdjument-Bromage H, Ferris CD, Tempst P, Snyder SH (2001) Protein S-nitrosylation: a physiological signal for neuronal nitric oxide. Nat Cell Biol **3**: 193–197

Jensen DE, Belka GK, Du Bois GC (1998) S-Nitrosoglutathione is a substrate for rat alcohol dehydrogenase class III isoenzyme. Biochem J **331 (Pt 2)**: 659–668

Jham GN, Fernandes SA, Garcia CF, da Silva AA (2002) Comparison of GC and HPLC for the quantification of organic acids in coffee. Phytochem Anal PCA **13**: 99–104

Jones RL (1980) The isolation of endoplasmic reticulum from barley aleurone layers. Planta **150**: 58–69

Ke J, Behal RH, Back SL, Nikolau BJ, Wurtele ES, Oliver DJ (2000) The role of pyruvate dehydrogenase and acetyl-coenzyme A synthetase in fatty acid synthesis in developing Arabidopsis seeds. Plant Physiol **123**: 497–508

Kondrashov FA, Koonin EV, Morgunov IG, Finogenova TV, Kondrashova MN (2006) Evolution of glyoxylate cycle enzymes in Metazoa: evidence of multiple horizontal transfer events and pseudogene formation. Biol Direct **1**: 31

Koornneef M, Bentsink L, Hilhorst H (2002) Seed dormancy and germination. Curr Opin Plant Biol **5**: 33–36

Kornberg HL, Beevers H (1957) A mechanism of conversion of fat to carbohydrate in castor beans. Nature **180**: 35–36

Kwon E, Feechan A, Yun B-W, Hwang B-H, Pallas JA, Kang J-G, Loake GJ (2012) AtGSNOR1 function is required for multiple developmental programs in Arabidopsis. Planta **236**: 887–900

Leitner M, Vandelle E, Gaupels F, Bellin D, Delledonne M (2009) NO signals in the hazeNitric oxide signalling in plant defence. Curr Opin Plant Biol **12**: 451–458

Leymarie J, Vitkauskaité G, Hoang HH, Gendreau E, Chazoule V, Meimoun P, Corbineau F, El-Maarouf-Bouteau H, Bailly C (2012) Role of reactive oxygen species in the regulation of Arabidopsis seed dormancy. Plant Cell Physiol **53**: 96–106

Lin M, Oliver DJ (2008) The Role of Acetyl-Coenzyme A Synthetase in Arabidopsis. PLANT Physiol **147**: 1822–1829

Liu Y, Ye N, Liu R, Chen M, Zhang J (2010) H_2O_2 mediates the regulation of ABA catabolism and GA biosynthesis in Arabidopsis seed dormancy and germination. J Exp Bot **61**: 2979–2990

Lorenz MC, Fink GR (2002) Life and death in a macrophage: role of the glyoxylate cycle in virulence. Eukaryot Cell **1**: 657–662

Lu S, Song J, Campbell-Palmer L (2009) A modified chemiluminescence method for hydrogen peroxide determination in apple fruit tissues. Sci Hortic **120**: 336–341

Macnicol PK, Jacobsen JV (1992) Endosperm acidification and related metabolic changes in the developing barley grain. Plant Physiol **98**: 1098–1104

Martínez-Camacho JL, la Vara LG, Hamabata A, Mora-Escobedo R, Calderón-Salinas V (2004) A pH-stating mechanism in isolated wheat (Triticum aestivum) aleurone layers involves malic acid transport. J Plant Physiol **161**: 1289–1298

Martínez-Ruiz A, Lamas S (2004) S-nitrosylation: a potential new paradigm in signal transduction. Cardiovasc Res **62**: 43–52

Matsumuraa T, Tabayashib N, Kamagata Y, Souma C, Saruyama H (2002) Wheat Catalase Expressed in Transgenic Rice Plants Can Improve Tolerance Against Low Temperature Injury. *In* PH Li, ET Palva, eds, Plant Cold Hardiness. Springer US, Boston, MA, pp 277–287

Mitrović A, Janošević D, Budimir S, Bogdanović Pristov J (2012) Changes in antioxidative enzymes activities during *Tacitus bellus* direct shoot organogenesis. Biol Plant **56**: 357–361

Moller IM (2001) PLANT MITOCHONDRIA AND OXIDATIVE STRESS: Electron Transport, NADPH Turnover, and Metabolism of Reactive Oxygen Species. Annu Rev Plant Physiol Plant Mol Biol **52**: 561–591

Moreau M, Lindermayr C, Durner J, Klessig DF (2010) NO synthesis and signaling in plants--where do we stand? Physiol Plant **138**: 372–383

Murphy ME, Noack E (1994) Nitric oxide assay using hemoglobin method. Methods Enzymol **233**: 240–250

Murshed R, Lopez-Lauri F, Sallanon H (2008) Microplate quantification of enzymes of the plant ascorbate-glutathione cycle. Anal Biochem **383**: 320–322

Nathan C (2004) The moving frontier in nitric oxide-dependent signaling. Sci STKE Signal Transduct Knowl Environ **2004**: pe52

Oracz K, El-Maarouf Bouteau H, Farrant JM, Cooper K, Belghazi M, Job C, Job D, Corbineau F, Bailly C (2007) ROS production and protein oxidation as a novel mechanism for seed dormancy alleviation. Plant J Cell Mol Biol **50**: 452–465

Oracz K, El-Maarouf-Bouteau H, Kranner I, Bogatek R, Corbineau F, Bailly C (2009) The mechanisms involved in seed dormancy alleviation by hydrogen cyanide unravel the role of reactive oxygen species as key factors of cellular signaling during germination. Plant Physiol **150**: 494–505

Oyedotun KS, Lemire BD (2004) The quaternary structure of the *Saccharomyces cerevisiae* succinate dehydrogenase. Homology modeling, cofactor docking, and molecular dynamics simulation studies. J Biol Chem **279**: 9424–9431

Palma JM (2006) Antioxidative enzymes from chloroplasts, mitochondria, and peroxisomes during leaf senescence of nodulated pea plants. J Exp Bot **57**: 1747–1758

Pérez FJ, Rubio S (2006) An Improved Chemiluminescence Method for Hydrogen Peroxide Determination in Plant Tissues. Plant Growth Regul **48**: 89–95

Perl M (1986) ATP synthesis and utilization in the early stage of seed germination in relation to seed dormancy and quality. Physiol Plant **66**: 177–182

Poole RK (2005) Nitric oxide and nitrosative stress tolerance in bacteria. Biochem Soc Trans **33**: 176–180

Popov VN, Moskalev EA, Shevchenko MU, Eprintsev AT (2005) Comparative Analysis of Glyoxylate Cycle Key Enzyme Isocitrate Lyase from Organisms of Different Systematic Groups. J Evol Biochem Physiol **41**: 631–639

Pritchard SL, Charlton WL, Baker A, Graham IA (2002) Germination and storage reserve mobilization are regulated independently in Arabidopsis. Plant J Cell Mol Biol **31**: 639–647

Queval G, Noctor G (2007) A plate reader method for the measurement of NAD, NADP, glutathione, and ascorbate in tissue extracts: Application to redox profiling during Arabidopsis rosette development. Anal Biochem **363**: 58–69

Rabinowitch HD, Fridovich I (1983) SUPEROXIDE RADICALS, SUPEROXIDE DISMUTASES and OXYGEN TOXICITY IN PLANTS. Photochem Photobiol **37**: 679–690

Riddles PW, Blakeley RL, Zerner B (1983) Reassessment of Ellman's reagent. Methods Enzymol **91**: 49–60

Rayle DL, Cleland RE (1992) The Acid Growth Theory of auxin-induced cell elongation is alive and well. Plant Physiol **99**: 1271–1274

Rocha M, Sodek L, Licausi F, Hameed MW, Dornelas MC, van Dongen JT (2010) Analysis of alanine aminotransferase in various organs of soybean (Glycine max) and in dependence of different nitrogen fertilisers during hypoxic stress. Amino Acids **39**: 1043–1053

Rockel P, Strube F, Rockel A, Wildt J, Kaiser WM (2002) Regulation of nitric oxide (NO) production by plant nitrate reductase *in vivo* and *in vitro*. J Exp Bot **53**: 103–110

Roessner U, Wagner C, Kopka J, Trethewey RN, Willmitzer L (2000) Technical advance: simultaneous analysis of metabolites in potato tuber by gas chromatography-mass spectrometry. Plant J Cell Mol Biol **23**: 131–142

Sakamoto A, Ueda M, Morikawa H (2002) Arabidopsis glutathione-dependent formaldehyde dehydrogenase is an *S*-nitrosoglutathione reductase. FEBS Lett **515**: 20–24

Sandalio LM, Palma JM, Del Rio LA (1987) Localization of manganese superoxide dismutase in peroxisomes isolated from *Pisum sativum* L. Plant Sci **51**: 1–8

Sarath G, Bethke PC, Jones R, Baird LM, Hou G, Mitchell RB (2006) Nitric oxide accelerates seed germination in warm-season grasses. Planta **223**: 1154–1164

Sarath G, Hou G, Baird LM, Mitchell RB (2007a) Reactive oxygen species, ABA and nitric oxide interactions on the germination of warm-season C4-grasses. Planta **226**: 697–708

Sarath G, Hou G, Baird LM, Mitchell RB (2007b) ABA, ROS and NO are Key Players During Switchgrass Seed Germination. Plant Signal Behav **2**: 492–493

Schafer FQ, Buettner GR (2001) Redox environment of the cell as viewed through the redox state of the glutathione disulfide/glutathione couple. Free Radic Biol Med **30**: 1191–1212

Schmidt G, Stahmann K-P, Sahm H (1996) Inhibition of purified isocitrate lyase identified itaconate and oxalate as potential antimetabolites for the riboflavin overproducer *Ashbya gossypii*. Microbiology **142**: 411–417

Sen S (2010) *S*-Nitrosylation Process Acts as a Regulatory Switch for Seed Germination in Wheat. Am J Plant Physiol **5**: 122–132

Sheoran IS, Olson DJH, Ross ARS, Sawhney VK (2005) Proteome analysis of embryo and endosperm from germinating tomato seeds. Proteomics **5**: 3752–3764

Siddiqui MH, Al-Whaibi MH, Basalah MO (2011) Role of nitric oxide in tolerance of plants to abiotic stress. Protoplasma **248**: 447–455

Singh SP, Wishnok JS, Keshive M, Deen WM, Tannenbaum SR (1996) The chemistry of the *S*-nitrosoglutathione/glutathione system. Proc Natl Acad Sci U S A **93**: 14428–14433

Šírová J, Sedlářová M, Piterková J, Luhová L, Petřivalský M (2011) The role of nitric oxide in the germination of plant seeds and pollen. Plant Sci Int J Exp Plant Biol **181**: 560–572

Sowa AW, Duff SM, Guy PA, Hill RD (1998) Altering hemoglobin levels changes energy status in maize cells under hypoxia. Proc Natl Acad Sci U S A **95**: 10317–10321

Stamler JS, Simon DI, Osborne JA, Mullins ME, Jaraki O, Michel T, Singel DJ, Loscalzo J (1992) *S*-nitrosylation of proteins with nitric oxide: synthesis and characterization of biologically active compounds. Proc Natl Acad Sci U S A **89**: 444–448

Stamler JS, Toone EJ, Lipton SA, Sucher NJ (1997) (S)NO signals: translocation, regulation, and a consensus motif. Neuron **18**: 691–696

Stöhr C, Strube F, Marx G, Ullrich WR, Rockel P (2001) A plasma membrane-bound enzyme of tobacco roots catalyses the formation of nitric oxide from nitrite. Planta **212**: 835–841

Sundquist AR (1995) Kinetics of Nitrosation of Thiols by Nitric Oxide in the Presence of Oxygen. J Biol Chem **270**: 28158–28164

Sun J, Trumpower BL (2003) Superoxide anion generation by the cytochrome bc_1 complex. Arch Biochem Biophys **419**: 198–206

Teixeira FK, Menezes-Benavente L, Galvão VC, Margis-Pinheiro M (2005) Multigene families encode the major enzymes of antioxidant metabolism in *Eucalyptus grandis* L. Genet Mol Biol. doi: 10.1590/S1415-47572005000400007

Valderrama R, Corpas FJ, Carreras A, Fernández-Ocaña A, Chaki M, Luque F, Gómez-Rodríguez MV, Colmenero-Varea P, Del Río LA, Barroso JB (2007) Nitrosative stress in plants. FEBS Lett **581**: 453–461

Van Breusegem F, Slooten L, Stassart JM, Moens T, Botterman J, Van Montagu M, Inzé D (1999) Overproduction of *Arabidopsis thaliana* FeSOD confers oxidative stress tolerance to transgenic maize. Plant Cell Physiol **40**: 515–523

Walker RP, Chen ZH, Tecsi LI, Famiani F, Lea PJ, Leegood RC (1999) Phosphoenolpyruvate carboxykinase plays a role in interactions of carbon and nitrogen metabolism during grape seed development. Planta **210**: 9–18

Wang PG, Xian M, Tang X, Wu X, Wen Z, Cai T, Janczuk AJ (2002) Nitric oxide donors: chemical activities and biological applications. Chem Rev **102**: 1091–1134

Weitbrecht K, Muller K, Leubner-Metzger G (2011) First off the mark: early seed germination. J Exp Bot **62**: 3289–3309

Wunsche H, Baldwin IT, Wu J (2011) S-Nitrosoglutathione reductase (GSNOR) mediates the biosynthesis of jasmonic acid and ethylene induced by feeding of the insect herbivore Manduca sexta and is important for jasmonate-elicited responses in *Nicotiana attenuata*. J Exp Bot **62**: 4605–4616

Xu W, Shi W, Liu F, Ueda A, Takabe T (2008) Enhanced zinc and cadmium tolerance and accumulation in transgenic *Arabidopsis* plants constitutively overexpressing a barley gene (*HvAPX1*) that encodes a peroxisomal ascorbate peroxidase. Botany **86**: 567–575

Yamasaki H (2000) Nitrite-dependent nitric oxide production pathway: implications for involvement of active nitrogen species in photoinhibition in vivo. Philos Trans R Soc Lond B Biol Sci **355**: 1477–1488

Yu Y, Guo G, Lv D, Hu Y, Li J, Li X, Yan Y (2014) Transcriptome analysis during seed germination of elite Chinese bread wheat cultivar Jimai 20. BMC Plant Biol **14**: 20

Yuroff AS, Sabat G, Hickey WJ (2003) Transporter-mediated uptake of 2-chloro- and 2-hydroxybenzoate by *Pseudomonas huttiensis* strain D1. Appl Environ Microbiol **69**: 7401–7408

Zhang X, Wang X, Shanmugam KT, Ingram LO (2011) L-malate production by metabolically engineered *Escherichia coli*. Appl Environ Microbiol **77**: 427–434

Zhao J (2007) Interplay among nitric oxide and reactive oxygen species: a complex network determining cell survival or death. Plant Signal Behav **2**: 544–547

Appendices

1 Standard curve for determining protein concentration

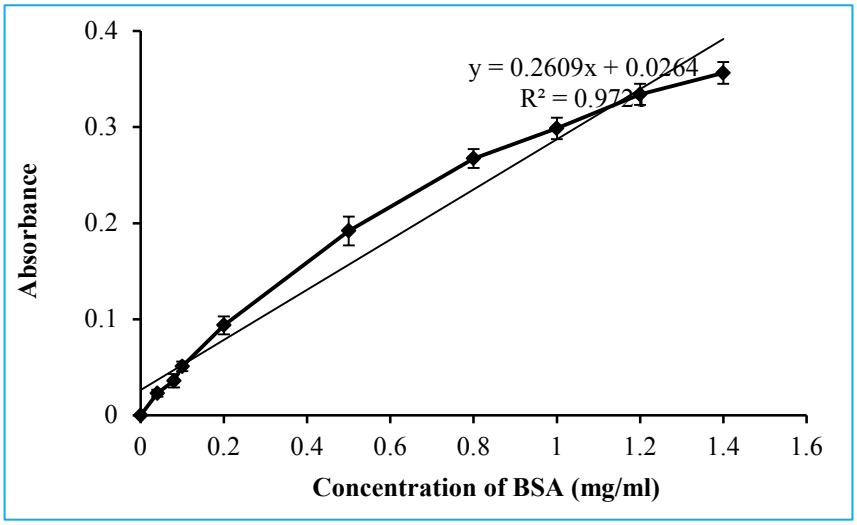

Figure A1 Standard curve for Bovine Serum Albumin (BSA) from assay of Bradford reagent

2 Standard curve for measuring content of ATP and ADP

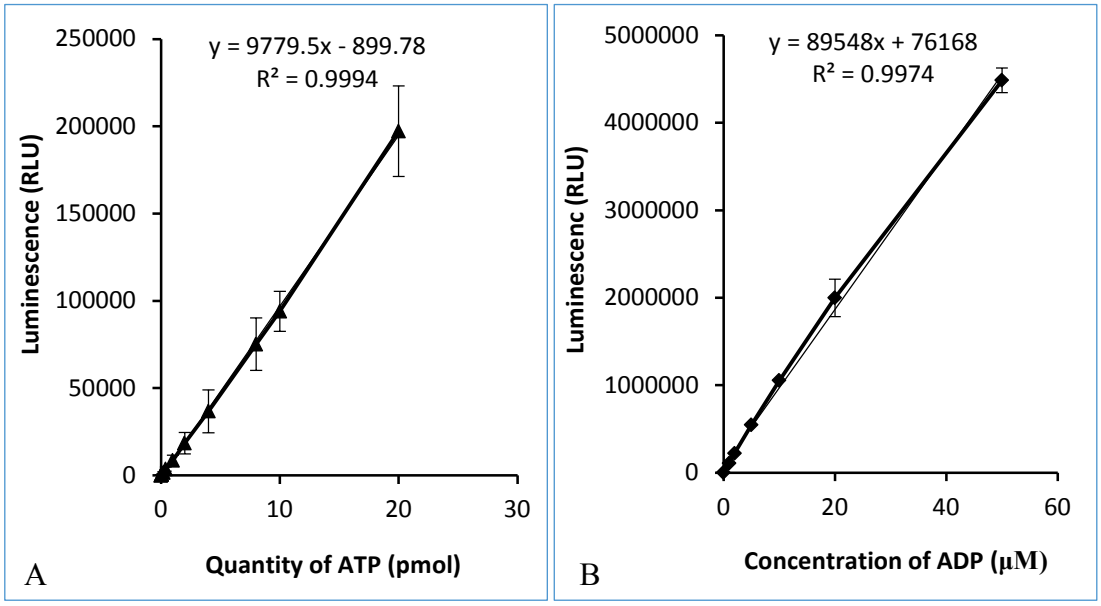

Figure A2 Standard curves for measuring ATP and ADP

3 Standard curve for measuring quantity of H_2O_2

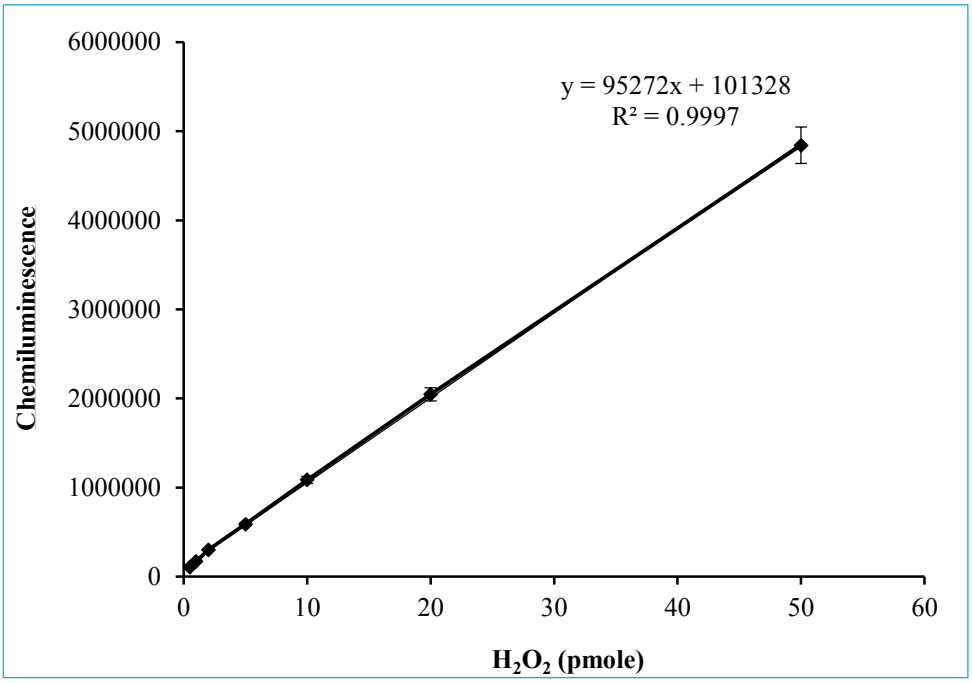

Figure A3 Standard curve for measuring quantity of H_2O_2

4 Standard curve for measuring activity of SOD

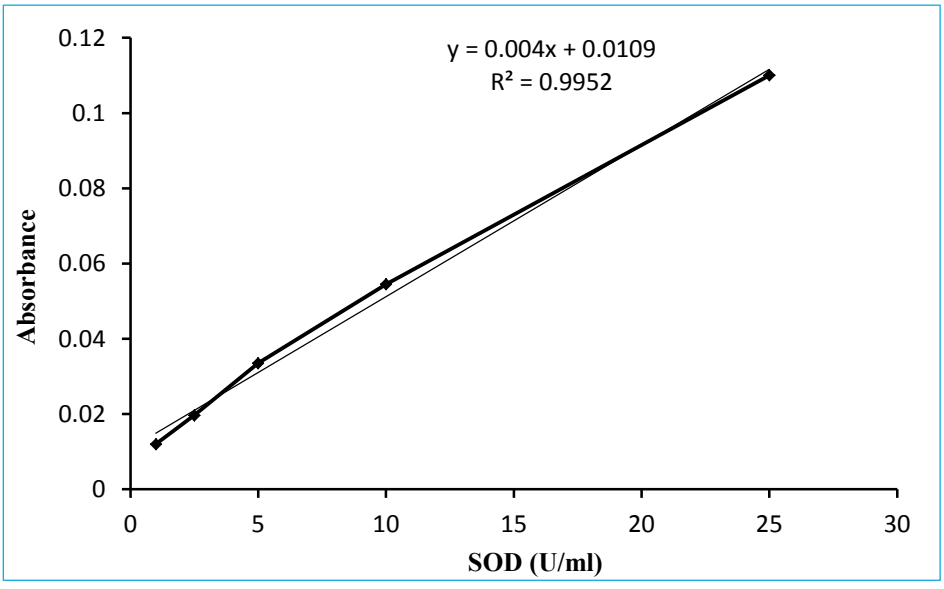

Figure A4 Standard curve for measuring activity of SOD

5 Standard curve for measuring ascorbate and GSH

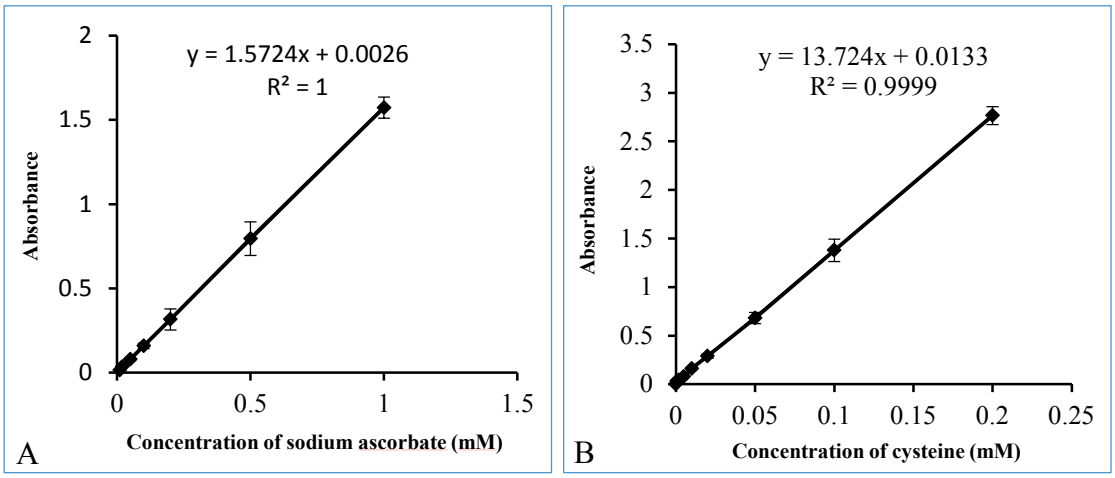

Figure A5 Standard curves for measuring ascorbate and GSH

A: standard curve for measuring ascorbate; B: standard curve for measuring GSH

6. Sequences of cDNA of *APX*, *ADH3*, Hb and *mub1*

Hordeum vulgare ascorbate peroxidase mRNA, complete cds

>gi|15808778|gb|AF411228.1| *Hordeum vulgare* ascorbate peroxidase mRNA, complete cds 1138 bp

GGCACGAGGTCCGTCCCCACACACACGCACGCGTTTGACATTTCCTCCCCACCGCCGCCGGCGCCGCTG

CTCCAGCCATGGCCGCCAAGTGCTACCCAACGGTCAGCGACGAGTACCTGGCCGCCGTCGCCAAGGCCA

GGCGCAAGCTCCGTGGCCTCATCGCCGAGAAGAACTGCGCGCCCCTCATGCTCCGCCTCGCGTGGCACT

CGGCCGGGACCTTCGACGTGGCCACCAAGACCGGCGGGCCCTTCGGCACCATGAAGTGCCCCGCGGAGC

TCGCCCACGGCGCCAACGCCGGCCTCGACATCGCCGTCAGGCTGCTCGAGCCCATCAAGGAGCAGTTCC

CCATCCTCTCCTACGCCGACTTCTACCAGCTCGCTGGAGTCGTCGCCGTCGAGGTGACCGGCGGGCCTG

AGGTTCCCTTCCACCCCGGGAGACAGGACAAGCCCGAGCCTCCTCCAGAAGGCCGTCTTCCTGATGCCA

CCCAAGGCTCTGACCACCTCAGGCAGGTGTTTTCCACTCAGATGGGTTTGAGTGACCAGGACATTGTTG

CTCTTTCTGGTGGTCACACCCTGGGAAGATGCCACAAGGAGAGATCTGGGTTTGAGGGAGCCTGGACCG

CCAACCCTTTGATCTTCGACAACTCTTACTTCACTGAGCTCCTGAGTGGGGAGAAGGAAGGTCTTCTTC

AGTTGCCGACCGACAAGGTCCTGCTGACTGACCCGGCCTTCCGCCCACTTGTGGACAAATATGCTGCGG

ATGAGGATGCGTTCTTTGCTGACTACGCCGAGGCACACCTCAAGCTCTCTGAACTTGGATTCGGCGAGG

CGTCTGAGGGCTGCTGCTGATTCAAGATCGGCGCCTGAGGGTCGGTAATGAAGAAGAAGATCATGAAGA

AGAAGAAGATCATGAAGAAGAAGAGCAATAAGAATCTGTCGTCGGCCCAGTGGCCATGTCATGTGTTTG

TCTGGATTTGGATTAGATCGGTCGGTCGATGGGGTGTTGCATTGTTTTGCTTTTGACGCCTCGTATCTT

GTGATGGACCTGCTTGTAGTGTGAACCGCTAAGTGTTATGTAGTTCCTTTCCGGTTGTTTTTCCCTGTC

GAGAACGAAATGAAATTTTTTTTGGTTCCCCCCA

Figure A6 cDNA sequence of *APX* in barley

Note: the bases in red colour were the forward and reverse primers respectively.

Barley alcohol dehydrogenase III gene, *ADH3* (EC 1.1.1.1) GenBank: X12734.1

>(gi|18885:100-133, 232-368, 463-509, 887-1212, 1309-1391, 1484-1559, 1648-1709, 1795-1890, 1986-2264) 1140 bp

ATGGCGACCGCTGGGAAGGTGATCAAGTGCAAAGCGGCGGTGGCGTGGGAGGCCGGGAAGCCGCTGTCG
ATCGAGGAGGTGGAGGTGGCGCCGCCGCAGGCCATGGAGGTGCGCGTCAAGATCCTCTACACTGCCCTC
TGCCACACCGACGTCTACTTCTGGGAAGCCAAGGGGCAAACTCCGGTTTTCCCTAGGATCTTAGGCCAT
GAAGCTGGAGGCATTGTCGAGAGCGTCGGAGAGGGCGTGACTGAGCTTGTGCCGGGTGACCATGTCCTC
CCGGTGTTCACCGGCGAGTGCAAGGACTGTGCCCACTGCAAGTCAGAGGAGAGCAACCTTTGTGATCTC
CTTAGGATCAATGTGGATCGTGGCGTGATGATCGGCGATGGGCAGTCTCGCTTCACCATCAACGGAAAA
CCGATCTTCCACTTCGTCGGGACCTCCACCTTCAGTGAGTACACCGTCATCCATGTCGGTTGCCTCGCA
AAGATCAACCCCGAGGCTCCCCTCGACAAAGTTTGTGTCCTCAGCTGTGGTCTCTCAACTGGACTTGGT
GCTACGCTCAATGTCGCAAAACCAAAAAAGGGTTCCACGGTGGCCATTTTCGGTCTTGGAGCTGTAGGA
CTGGCTGCCATGGAAGGGGCCAGGATGGCTGGGGCATCAAGGATCATTGGTGTGGATTTGAACCCTGCA
AAATACGAACAAGCTAAGAAATTTGGATGCACAGACTTTGTGAACCCGAAGGACCACACTAAGCCCGTG
CAGGAGGTGCTCGTCGAGATGACCAATGGCGGAGTCGACCGGGCAGTCGAGTGCACTGGCCACATCGAC
GCCATGATCGCCACCTTCGAATGCGTCCATGATGGGTGGGGCGTGGCTGTGCTGGTGGGTGTGCCGCAC
AAGGAGGCGGTGTTCAAGACCCACCCAATGAACTTCCTCAACGAGAAGACCCTGAAAGGCACCTTCTTC
GGTAACTACAAGCCGCGCACCGACCTGCCGGAAGTGGTCGAGATGTACATGAGGAAGGAGCTCGACCTG
GAGAAGTTCATCACACATAGCGTGCCCTTCTCGCAGATCAACACGGCGTTCGACCTCATGCTCAAGGGG
GAGGGCCTGCGCTGCATCACGAGGACGGACCAGTAG

Figure A7 cDNA sequence of *ADH3* in barley

Note: the bases in red colour were the forward and reverse primers respectively.

Hordeum vulgare hemoglobin gene, complete cds GenBank: U94968.1

>gi|2071975|gb|U94968.1|HVU94968 *Hordeum vulgare* hemoglobin gene, complete cds 1173 bp

GAGAACCAAATTAAGCGGGAAGGAAGCCATGTCTGCCGCGGAGGGGGCCGTCGTCTTCAGCGAGGAGAA

GGAGGCGCTGGTGCTCAAGTCATGGGCCATCATGAAGAAGGATTCCGCCAACCTTGGGCTCCGCTTCTT

CCTCAAGTACGTACCCTGCCATTTCTTATTCTATGTGGAAGCAGCGCAATGAAGCCCCCGATGCATCTC

CTTGACATGCATGCTGCTGCGTGCGTGCCTCCAGGATCTTCGAGATCGCGCCGTCGGCGAGGCAGATGT

TCCCGTTCCTGCGCGACTCCGACGTGCCGCTGGAGACCAACCCCAAGCTCAAGACCCACGCCGTGTCCG

TCTTCGTCATGGTAATACACCATGCATCTCCCAACGATCTGCTGCTATGCATTACATATATATGCTTCC

ATGGCTTATCAATGTGTATGGTGTTGCGATGAATGGTGCAGACCTGCGAGGCGGCTGCGCAGTTGCGGA

AAGCCGGCAAGATCACCGTCAGGGAGACCACCCTGAAGAGGCTGGGCGGCACGCACTTGAAATACGGCG

TGGCAGATGGCCACTTCGAGGTATGCCCACTTGCCCATTAGCCTTGTGAATTGTACTAGCATGGGGTGC

GTGTTTGATTTTGCATTGCATTCAAAGTTGTCCCCTCACACGCTGTTGCTTCTTCTTCTTCGTCTTGTC

ACAGGTGACGCGGTTCGCTCTGCTCGAGACGATCAAGGAGGCGCTTCCGGCTGACATGTGGGGGCCCGA

GATGAGGAACGCGTGGGGCGAGGCATACGATCAACTGGTCGCGGCCATCAAGCAAGAGATGAAGCCAGC

TGAGTAGCTCCACCGCACTCATATACCACGCCATTTTCGCCGATTGTCCGTTCAACCTTCCTTGCTTCA

CCAATTCACTCATTTCACCGTTGTGTTTGTATTGTGTGTTTATGTGCACTAAAGTCTATTGTAACACTC

AATAAAAGTACAAATTATGCACGATATTCACCCCGCTCTACTTTACAGTTTTTTTTTTCTGTTAGAGGA

ACTCTGATTTAGAGGTTATGCCTCGTACTAGTACATTGCAATACGCTTAGAAAAGATGCTTAAATAAAT

AAATCAATGTTTTTTAGGCACGCGTGCTTATATGTATCGAGTAAACGTTTAGCCTGTATAAATGAACAC

Figure A8 cDNA sequence of *Hb* in barley

Note: the bases in red colour were the forward and reverse primers respectively.

Hordeum vulgare ubiquitin (mub1) gene cDNA

>gi|167072|gb|M60175.1|BLYMUB1 Barley ubiquitin (mub1) gene, complete cds 1815 bp

GAATTCATGAGCATGTATACATCTCACTAACCTGTTAACTTCGATGCTACCTCGGAAAAAGAAACGAAG

CGATGCTGTGACAGTCGTAACCAATGTTTTTTTTTTTTTGCGAAAGTAACCAATTTTCGAATCTGTAG

TCTTCCTAGTTTATGTATATCTTATTAATTGCGAGGCCAATTCTTTTGCTGGACAAAATGTAGAACTTA

CACATTTACTCTTATATAAAAATAATTTCCACCACTAAATTGAATTTACATATTTCTAGGGCTAAATGA

ATGGAATTTACACGTTTCTTGACTGGAACGAGTTCCTCAGGAGGCATGGGCCCGAAGCAAAATCCAGCC

CAGCCCAAAATAGCGTCCACGAAAGCCAGCCGTCCGATCTGGAACCCCTAGATCCAACAGCTAATATGT

CCCGCCTACTTGTACTTATAAGAAGGCAGACCCTTTCTGCACCCTAGCCTCCGTTCCATCCCGCCGCCC

CCGCCCAAACCCCAGCGCGCCGCCGCCACCGTCGCCGCCGCAGCGCGCGGAGGCGACCACCCCACCGCC

GCCAAGATGCAGATCTTCGTGAAGACCCTGACGGGCAAGACCATCACGCTGGAGGTGGAGTCGTCGGAC

ACCATCGACAACGTCAAGGCCAAGATCCAGGACAAGGAGGGCATCCCGCCGGACCAGCAGCGCCTCATC

TTCGCCGGCAAGCAGCTCGAGGACGGCCGCACCCTCGCCGACTACAACATCCAGAAGGAGTCCACCCTC

CACCTGGTGCTCCGACTCCGCGGTGGCGCCAAGAAGCGCAAGAAGAAGACGTACACCAAGCCCAAGAAG

CAAAAGCACAAGCACAAGAAGGTGAAGCTCGCCGTCCTCCAGTTCTACAAGGTCGACGACGCCACCGGC

AAGGTAACCAGGCTCAGGAAGGAGTGCCCCAACGCCGACTGCGGTGCCGGGACCTTCATGGCCAACCAC

TTCGACCGCCACTACTGCGGCAAGTGCGGACTCACCTATGTCTACAACCAGAAGGCTTAGAACTGGCCT

GTGTTTGCTCTGCTCTTTTACCTATCGCGAATAGAACTCATTTATGTGTCCAGTTTGTCTTTGAAAACT

GAAACCTTGGAGTAATATGTTGTGTTTCCTGGATATTTGATCGCCTATTGCTGAGATGTGATGCGAGCT

TTAAGTTTTGTTCCGTATGCTATGCTATCATTGCTCTGATTGATGCCATCATGGGATATATCTTGTTGA

TACAAGTGTTCTTGAGCTTAACCCTTTATTGCAGGTGTTAGTAGCCAATAGCTATGCATGGCTTGATAT

GTGGATGAATATTTTGCTACTGCTGGTTTATGATATGTTGATTGTTGATGTGTGTGATCTTTGTCACTT

GCAATTATAATTCAGTTCATCCCAAGTGATTGCGTGGTTGGTTTGTTTTAGATACATGTGTTATTTCAT

CCCTAGATGTGTCTGAAACTGTGGCTGTAGACAGTTGCAGTGTGATGATTGCTAGTGTGGAGCATATTG

GTGCCCTGTGGTTTATCCACCATTCACCATTGCCTACCCTGTGGTGCTAAATTTGGTTGGGTCTATCAT

ACCATATGTGACATGTCTATTGGTTTACAGTTGTAGATGTAGTTGAGTTTTGCTGTTCTCTTTTCATTT

TGTTCTTGGGTTGTGATAAAGTCATTTCACATACGCCGATGATATGTAATTTACAACTAATACATAAGA

TGGCTCAAATGCATTGTATGTGAATGCAAACTTGTCACAAATACTACGAGAATTATCTAAACTGCAACA

TCACTTCATGCATTTGAATTC

Figure A9 cDNA sequence of *ubiquitin* (*mub1*) in barley

Note: the bases in red colour were the forward and reverse primers respectively.

7 Morphological characteristics of barley seeds in the process of germination

Figure A10 Morphological characteristics of barley seeds at different germination phases

8 Content of soluble proteins in whole barley seeds in the process of germination

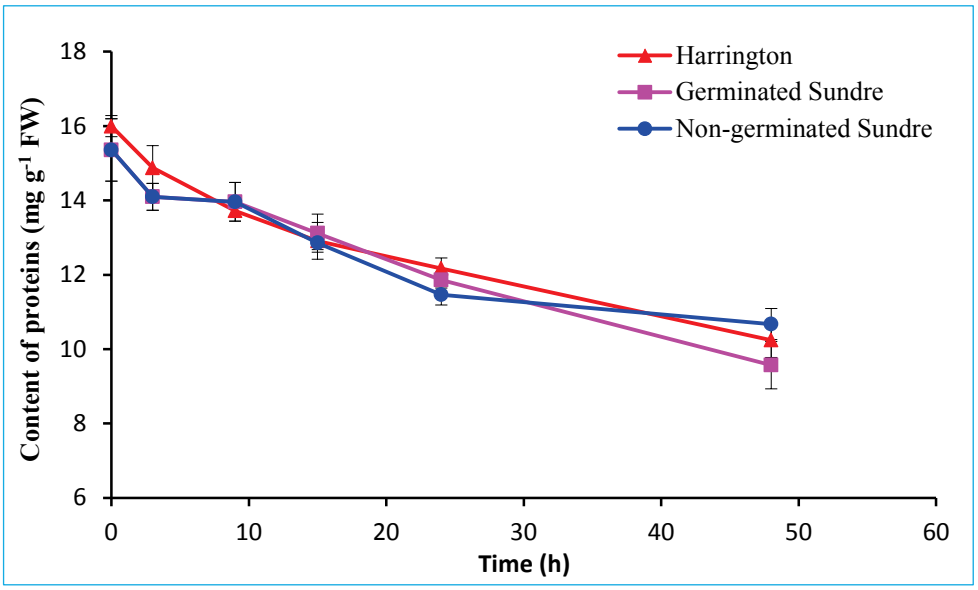

Figure A11 Content of soluble proteins in whole barley seeds in the process of germination

9 Content of ATP in whole barley seeds in the process of germination

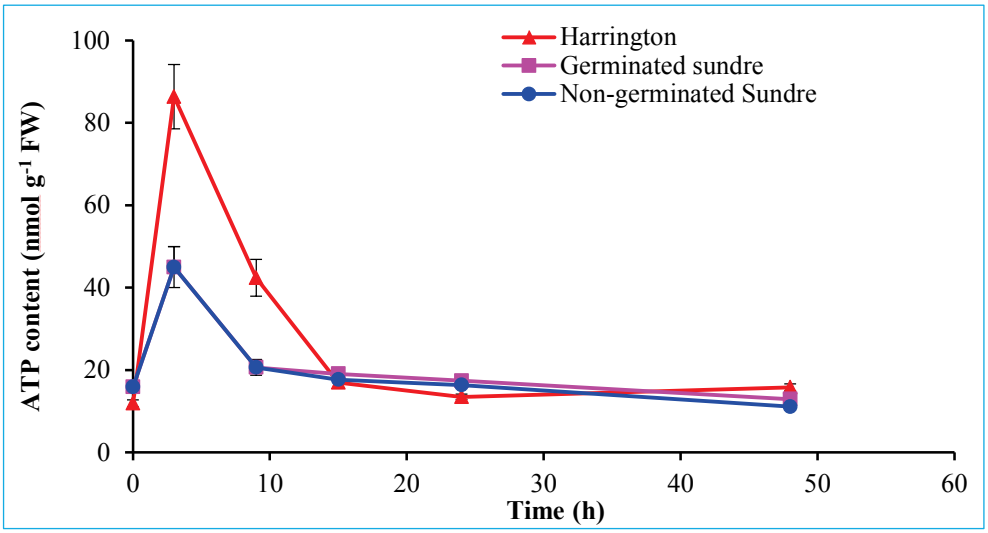

Figure A12 Content of ATP in whole barley seeds in the process of germination

10 Content of H_2O_2 in whole barley seeds in the process of germination

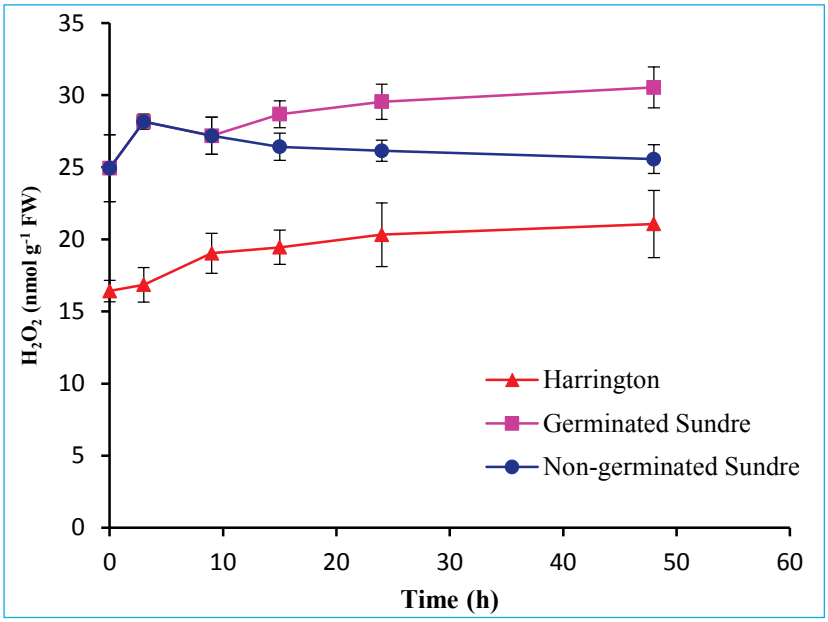

Figure A13 Content of H_2O_2 in whole barley seeds in the process of germination

11 Activity of enzymes scavenging ROS in whole barley seeds in the process of germination

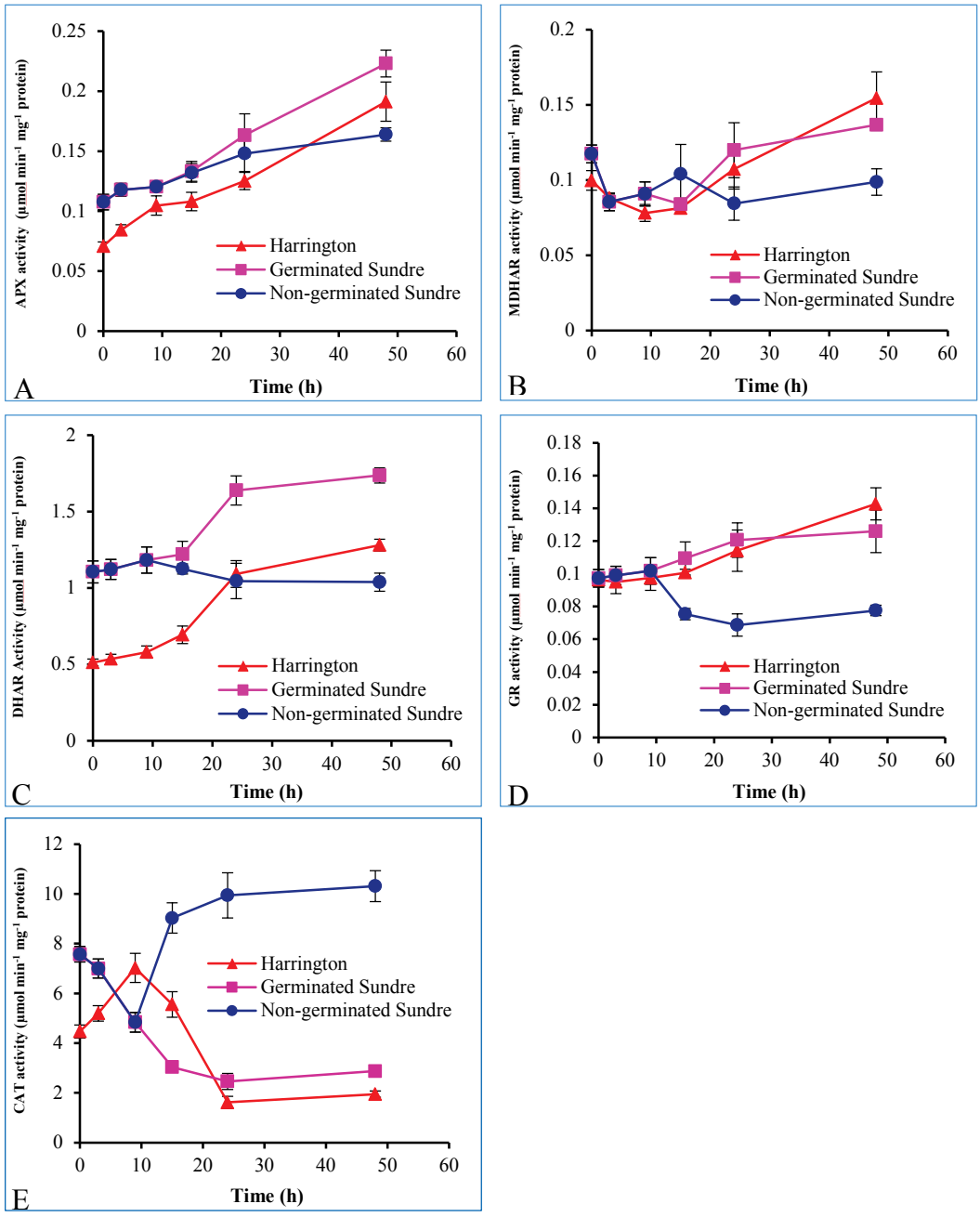

Figure A14 Activity of enzymes scavenging ROS in whole barley seeds in the process of germination

12 Content of ascorbate and DHA and ascorbate/DHA in whole barley seeds in the process of germination

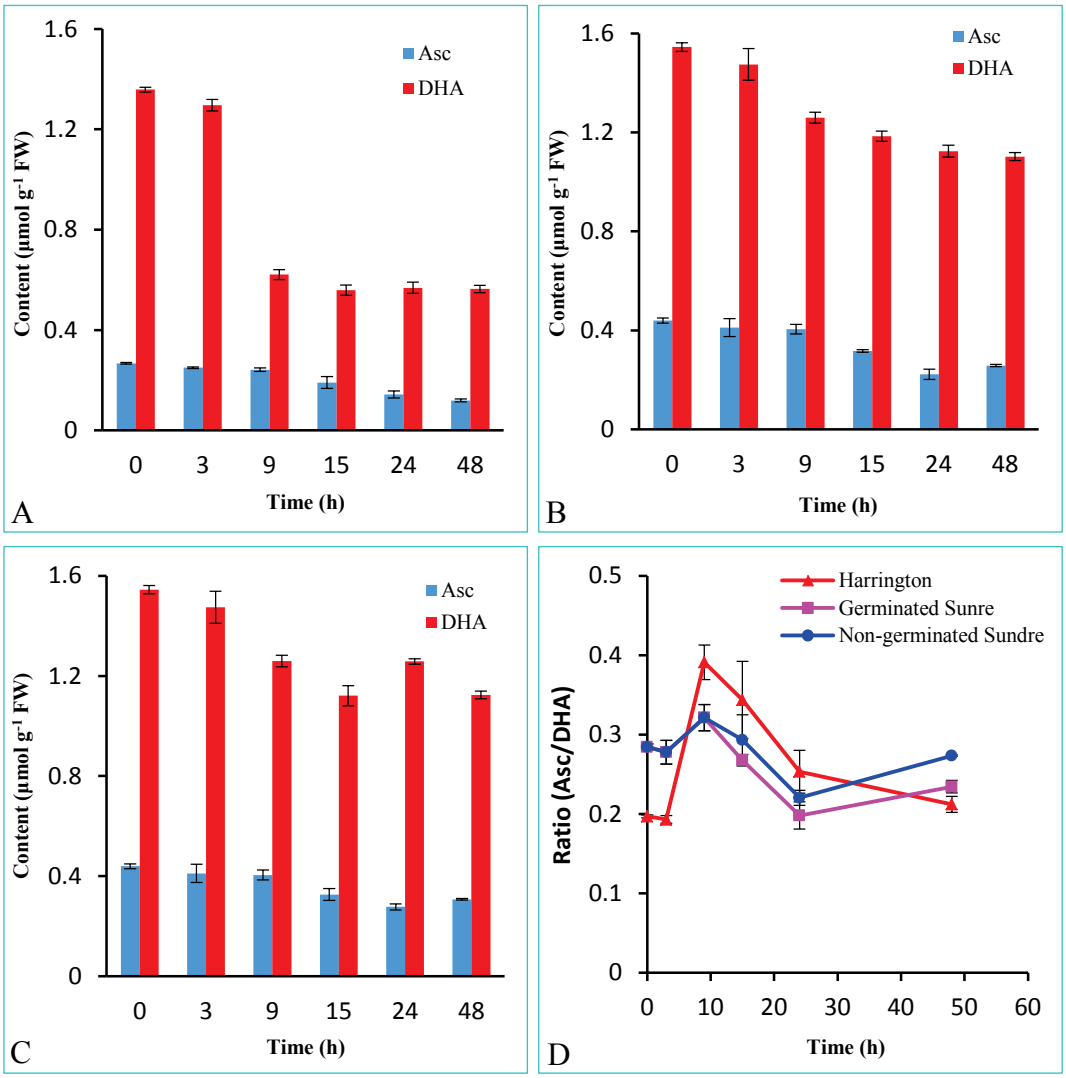

Figure A15 Content of ascorbate and DHA and ascorbate/DHA in whole barley seeds in the process of germination

Asc: ascorbate, DHA: dehydroascorbate

13 Content of GSH and GSSG, GSH/GSSG and redution potential of GSSG/2GSH couple in whole barley seeds in the process of germination

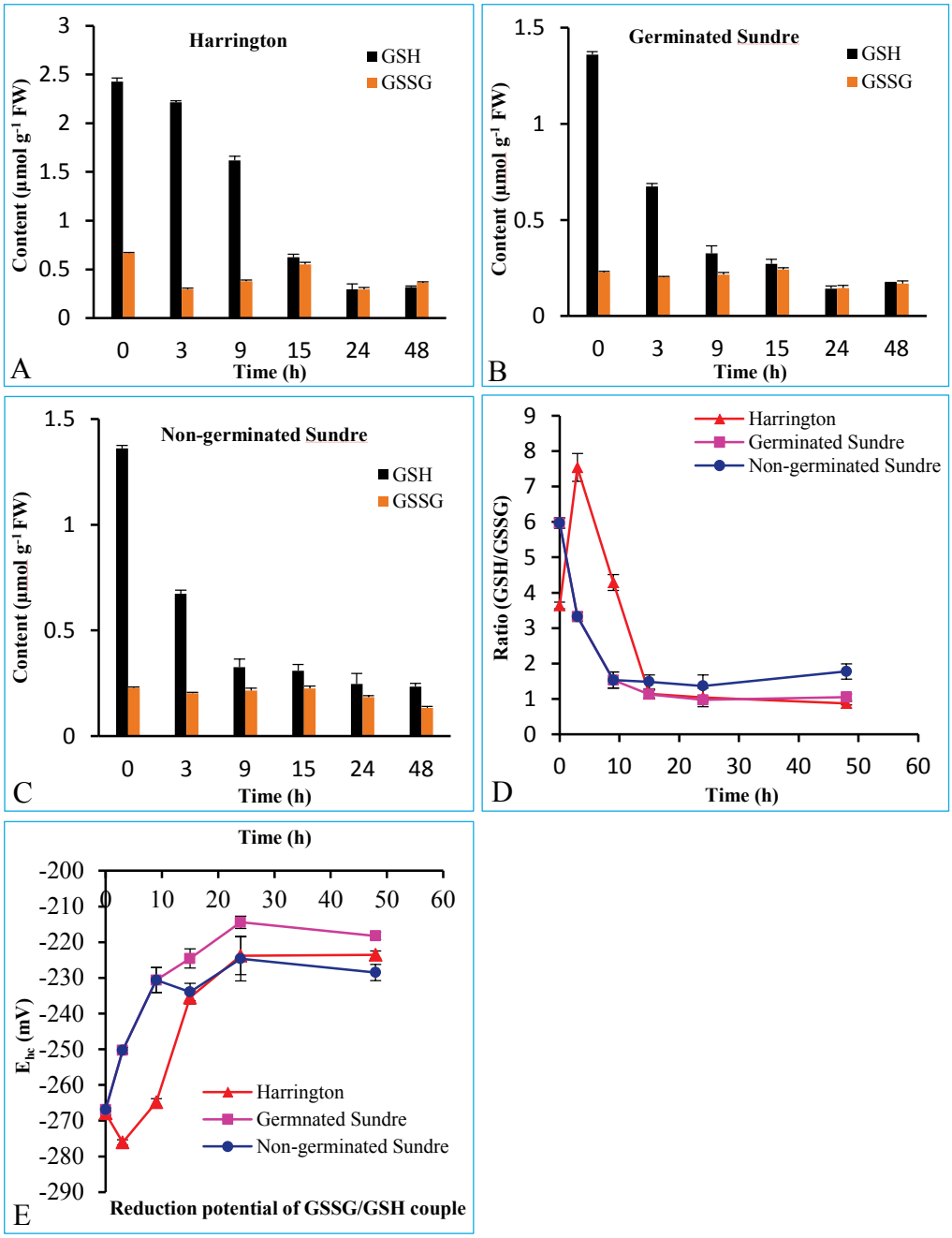

Figure A16 Content of GSH and GSSG, GSH/GSSG and redution potential of GSSG/2GSH couple in whole barley seeds in the process of germination

14 Activity of ADH, LDH and PPDK in whole barley seeds in the process of germination

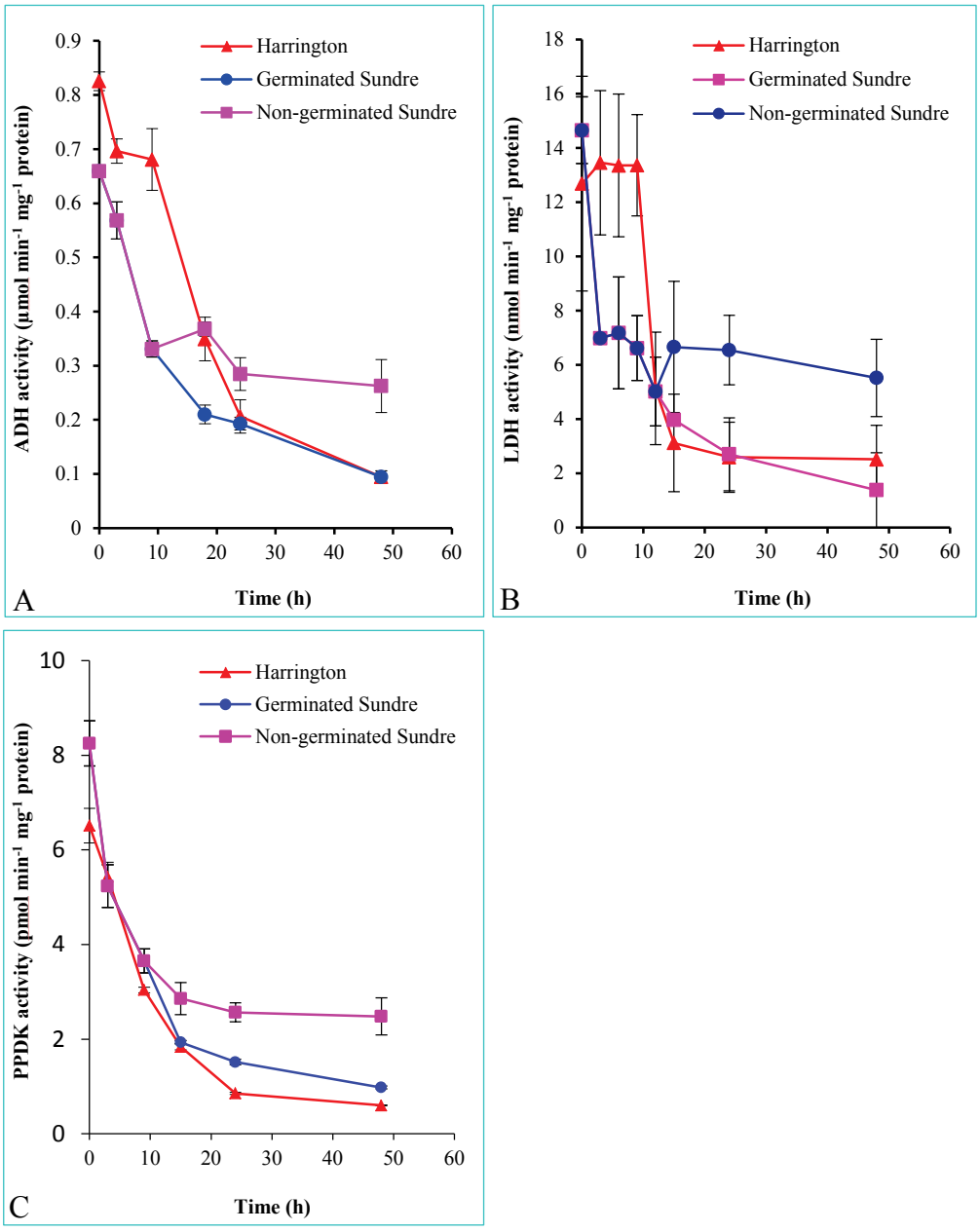

Figure A17 Activity of ADH, LDH and PPDK in whole barley seeds in the process of germination

15 RT PCR products of *Hb*, *APX*, *ADH3*, *TubA* and *mub1*

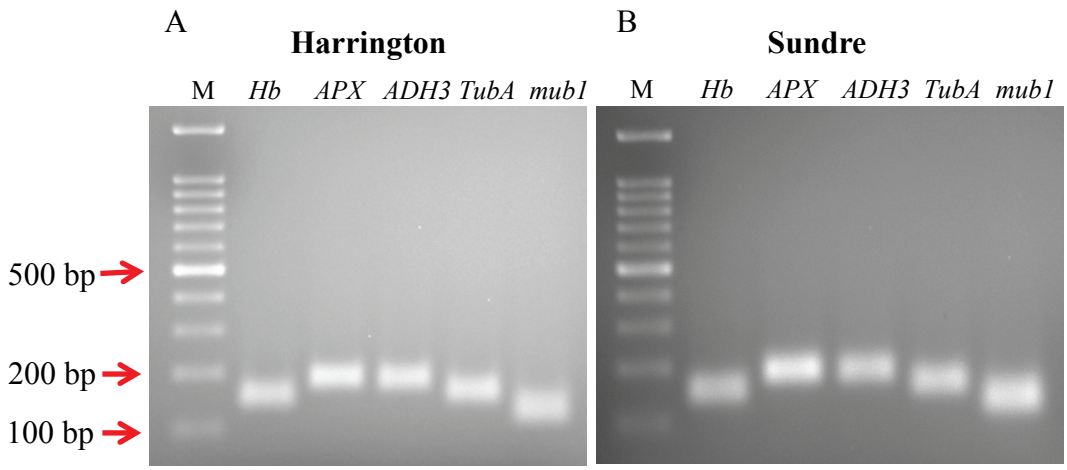

Figure A18 Size of RT PCR products of *Hb*, *APX*, *ADH3*, *TubA* and *mub1* in barley seeds

M: DNA marker, *Hb*: *hemoglobin* 149 bp, *APX*: *ascorbate peroxidase* 181 bp, *ADH3*: *alcohol dehydrogenase III* 177 bp, *TubA*: *alpha tubulin* 151 bp, *mub1*: *Ubiquitin* 119 bp

16 Melt curves of *APX*, *ADH3*, *Hb*, *TubA* and *mub1*

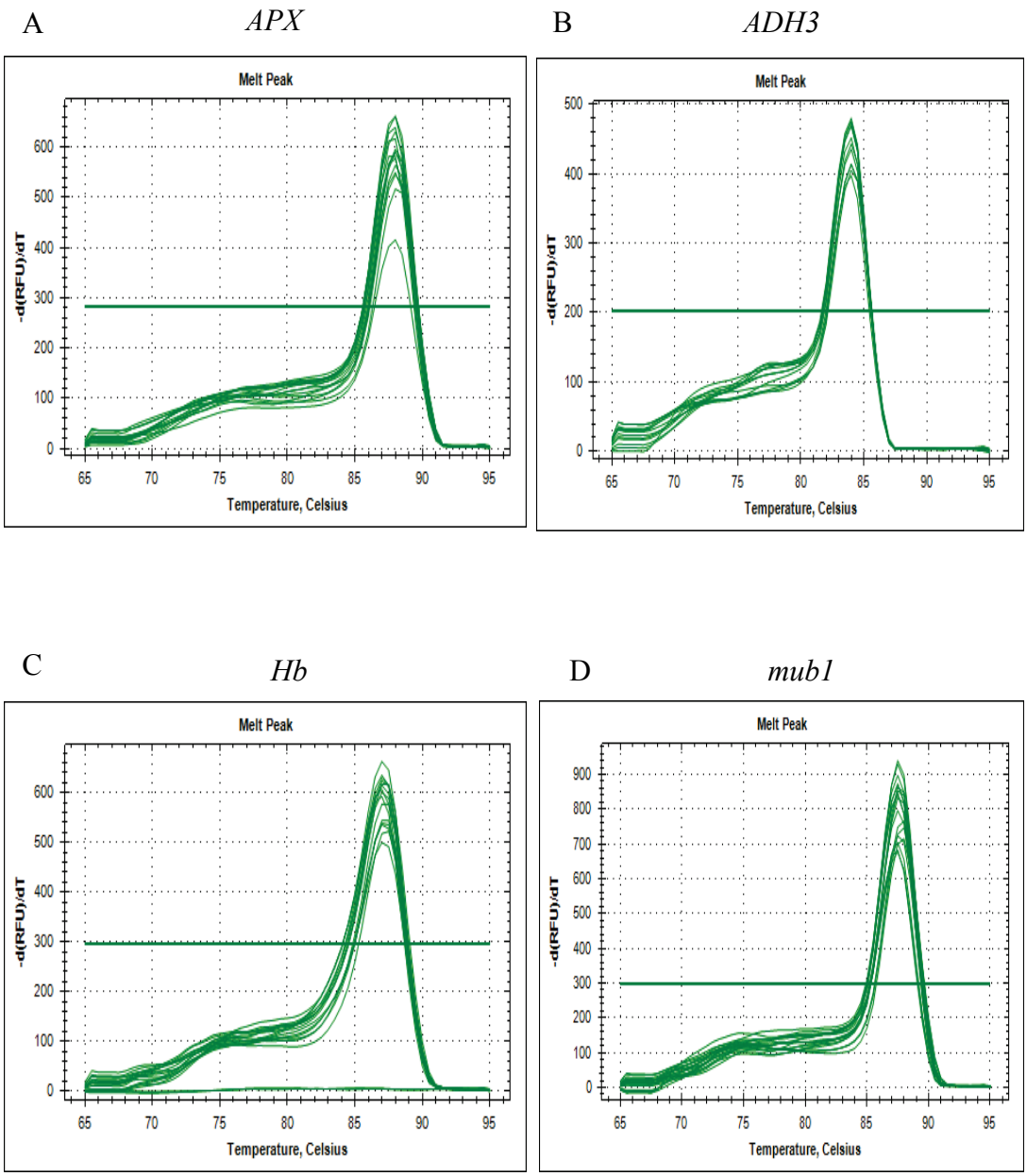

Figure A19 Melt curves of *Hb*, *APX*, *ADH3* and *mub1* in RT PCR

A: *APX* 88.0 ºC, B: *Hb* 87.0 ºC, C: *ADH3* 84.0 ºC, D: *mub1* 82.0 ºC

17 Primer efficiency of *Hb*, *APX*, *ADH3* and *mub1* in RT PCR

A *APX* B *ADH3*

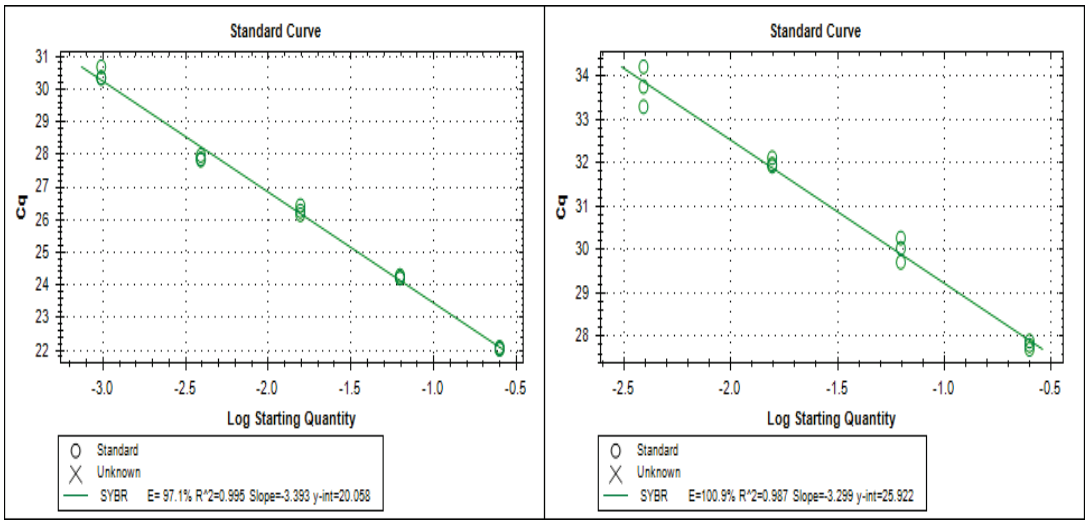

C *Hb* D *mub1*

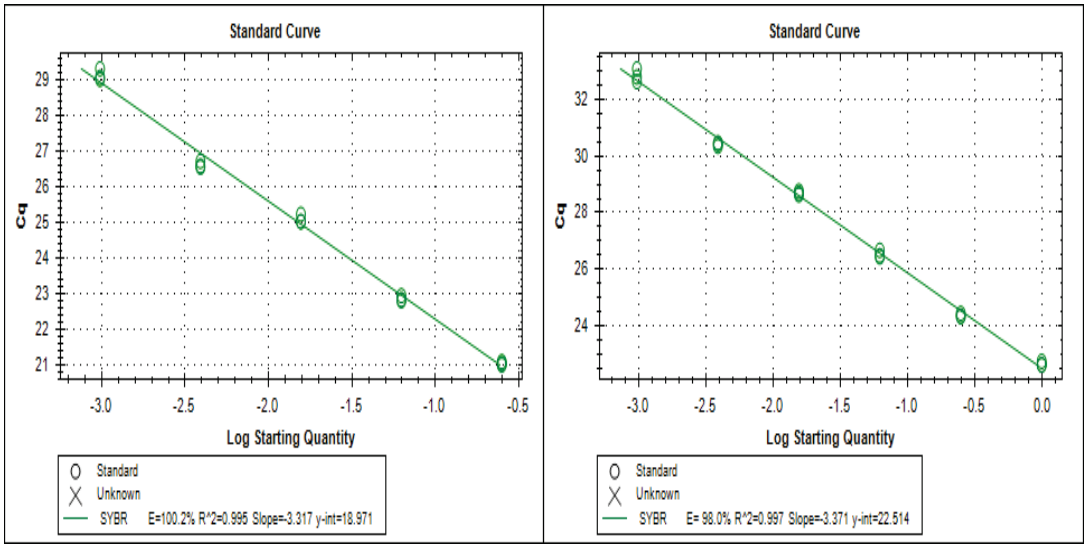

Figure A20 Primer efficiency of *Hb*, *APX*, *ADH3* and *mub1* in RT PCR

A: *APX* 97.1%, B: *Hb* 100.2%, C: *ADH3* 100.9%, D: *mub1* 98.0%

18 NO content in whole barley seeds in the process of germination

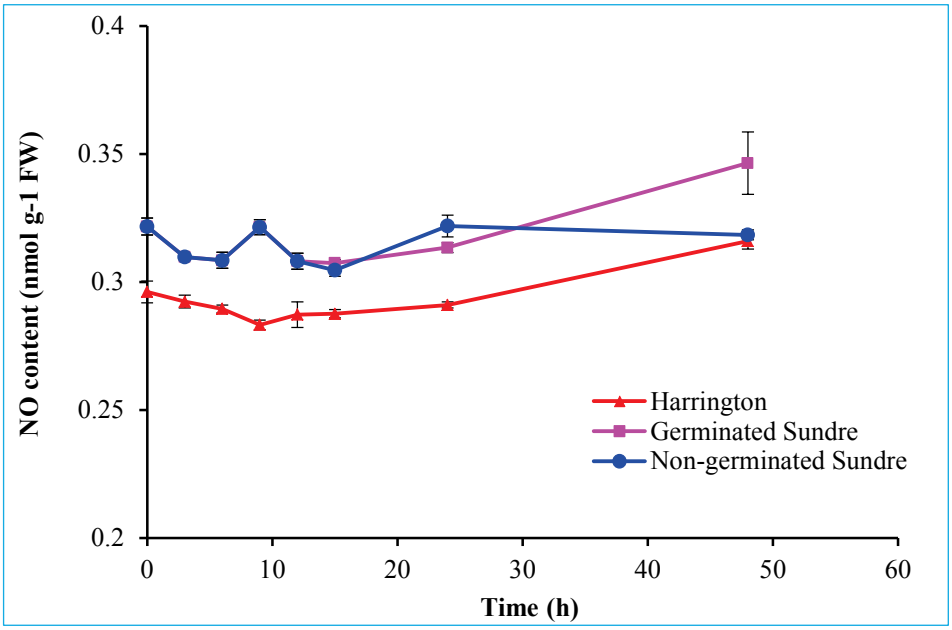

Figure A21 NO content in whole barley seeds in the process of germination

19 Activity of GSNOR in whole barley seeds in the process of germination

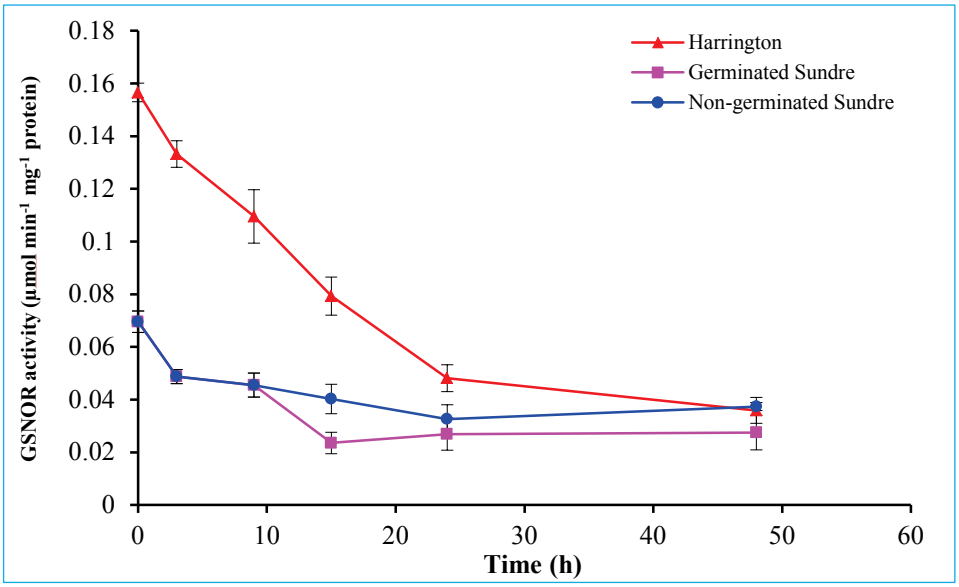

Figure A22 Activity of GSNOR in whole barley seeds in the process of germination

20 Effect of KNO_2 on germination of Sundre seeds

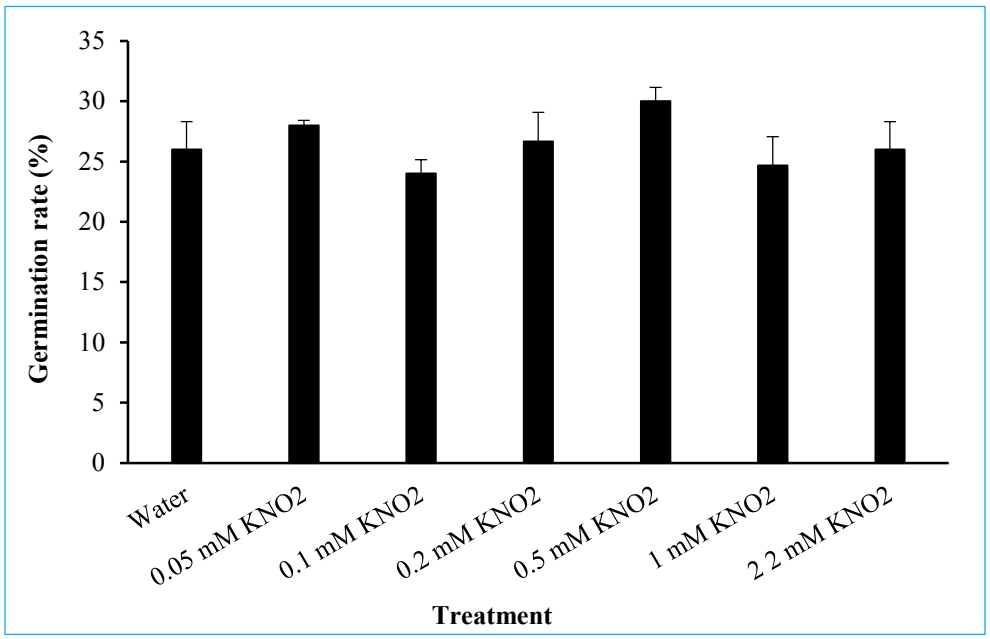

Figure A23 Effect of KNO_2 on germination of Sundre seeds

21 Standard cure for sodium succinate analyzed by GC-MS

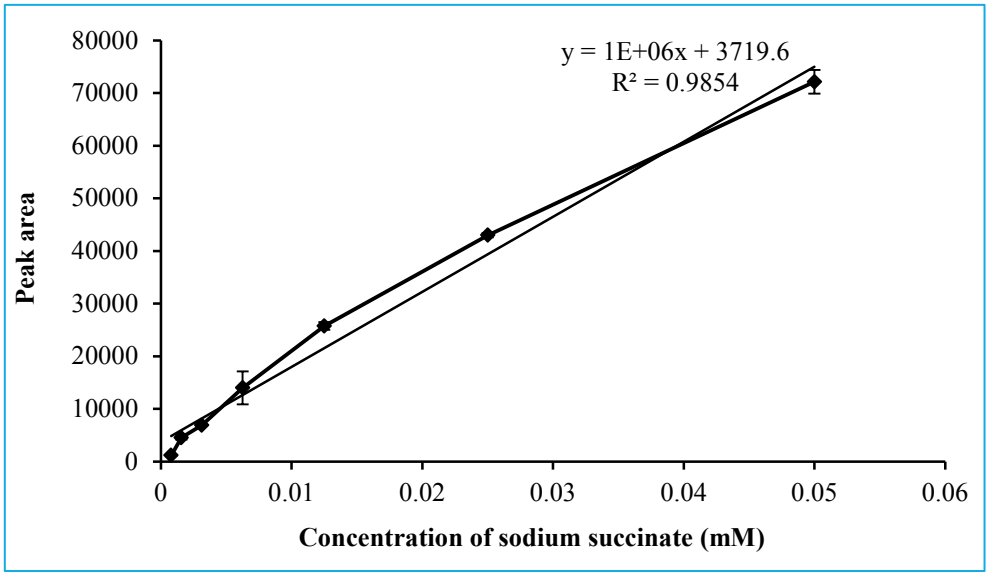

Figure A24 Standard cure for sodium succinate analyzed by GC-MS

22 Standard curve for sodium malate analyzed by GC-MS

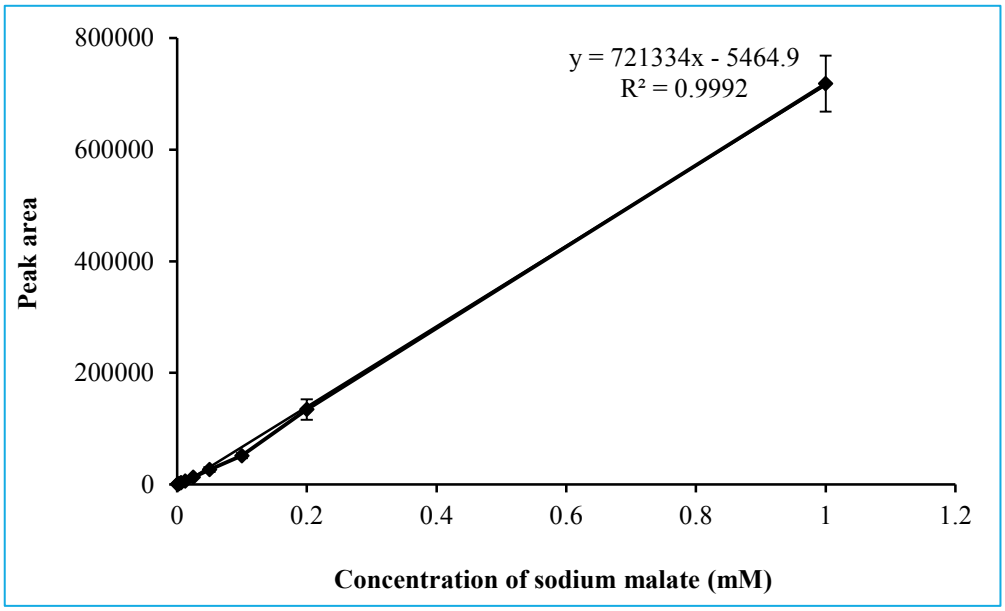

Figure A25 Standard curve for sodium malate analyzed by GC-MS

23 GC chromatogram of trimethylsily of standard sodium citrate

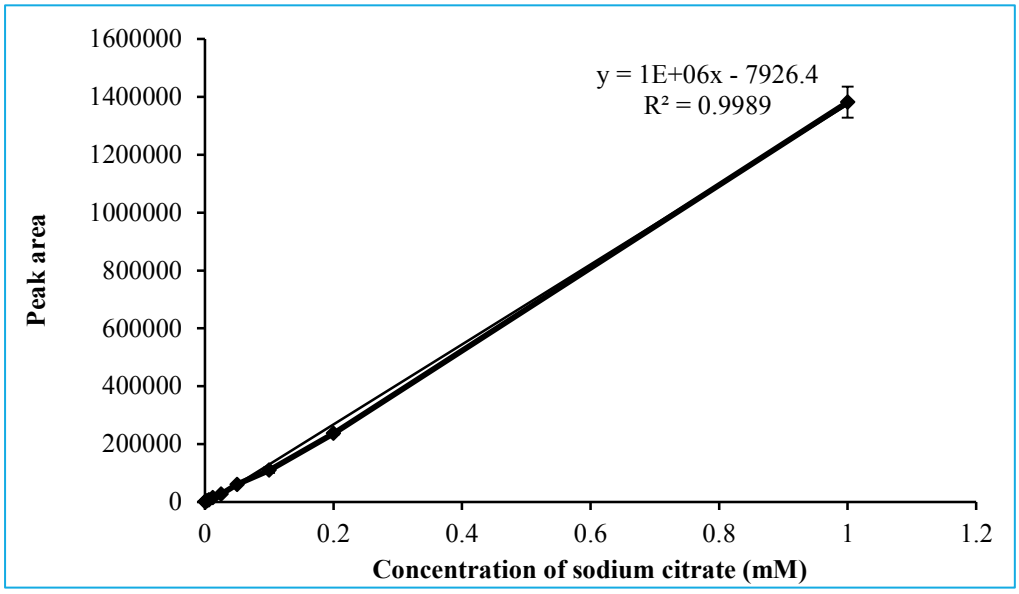

Figure A26 Standard curve of sodium citrate analyzed by GC-MS

24 GC chromatogram of trimethylsilyl of standard sodium succinate

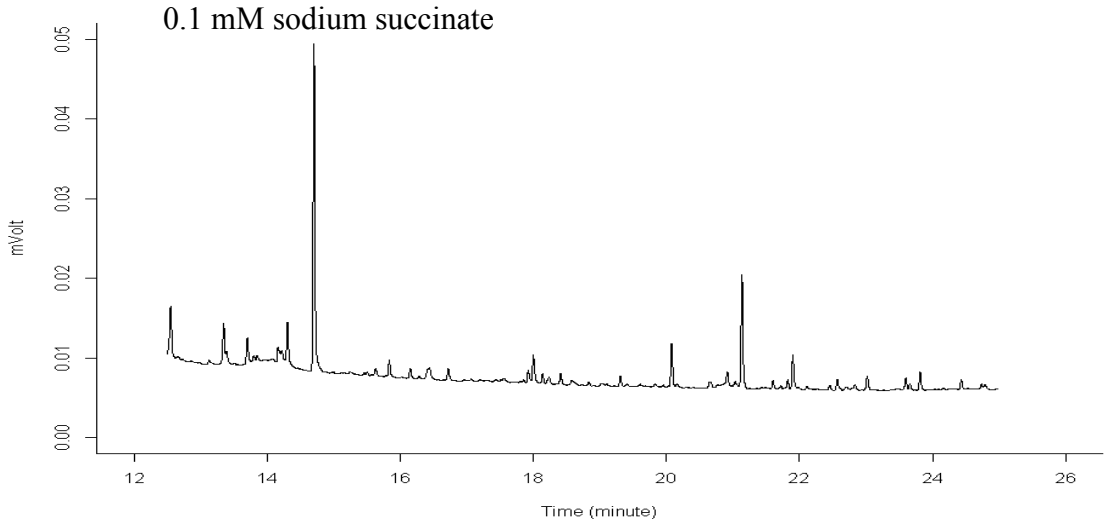

Figure A27 GC chromatogram of trimethylsilyl of standard sodium succinate

25 GC chromatogram of trimethylsily of standard sodium malate

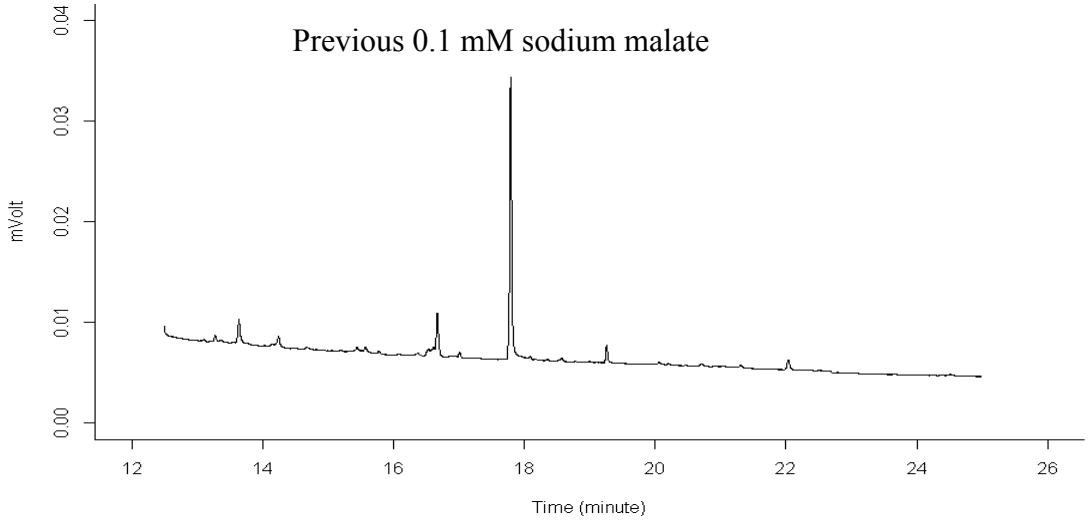

Figure A28 GC chromatogram of trimethylsilyl of standard sodium malate

26 GC chromatogram of trimethylsilyl of standard sodium citrate

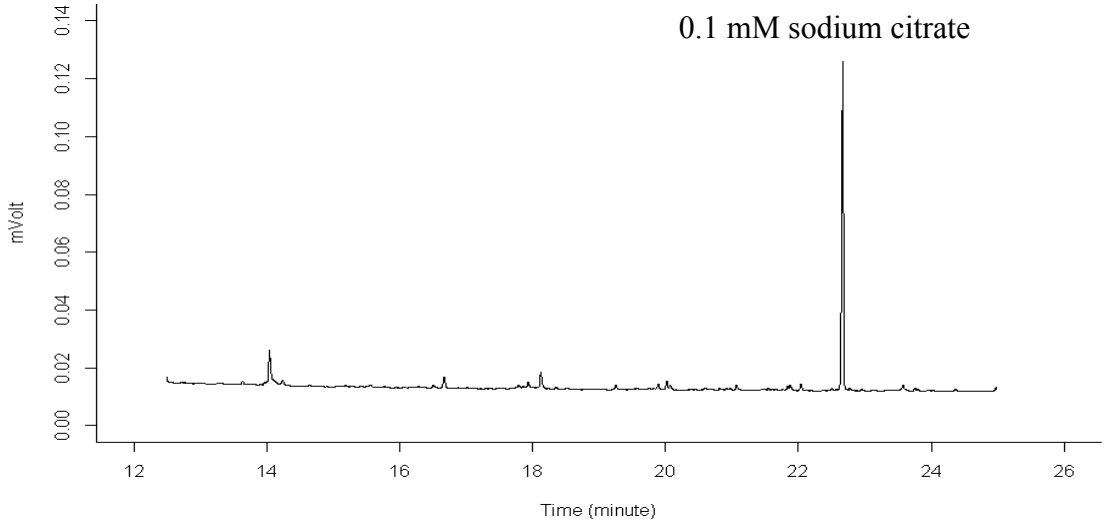

Figure A29 GC chromatogram of trimethylsily of standard sodium citrate

27 Mass spectrum of sodium succinate

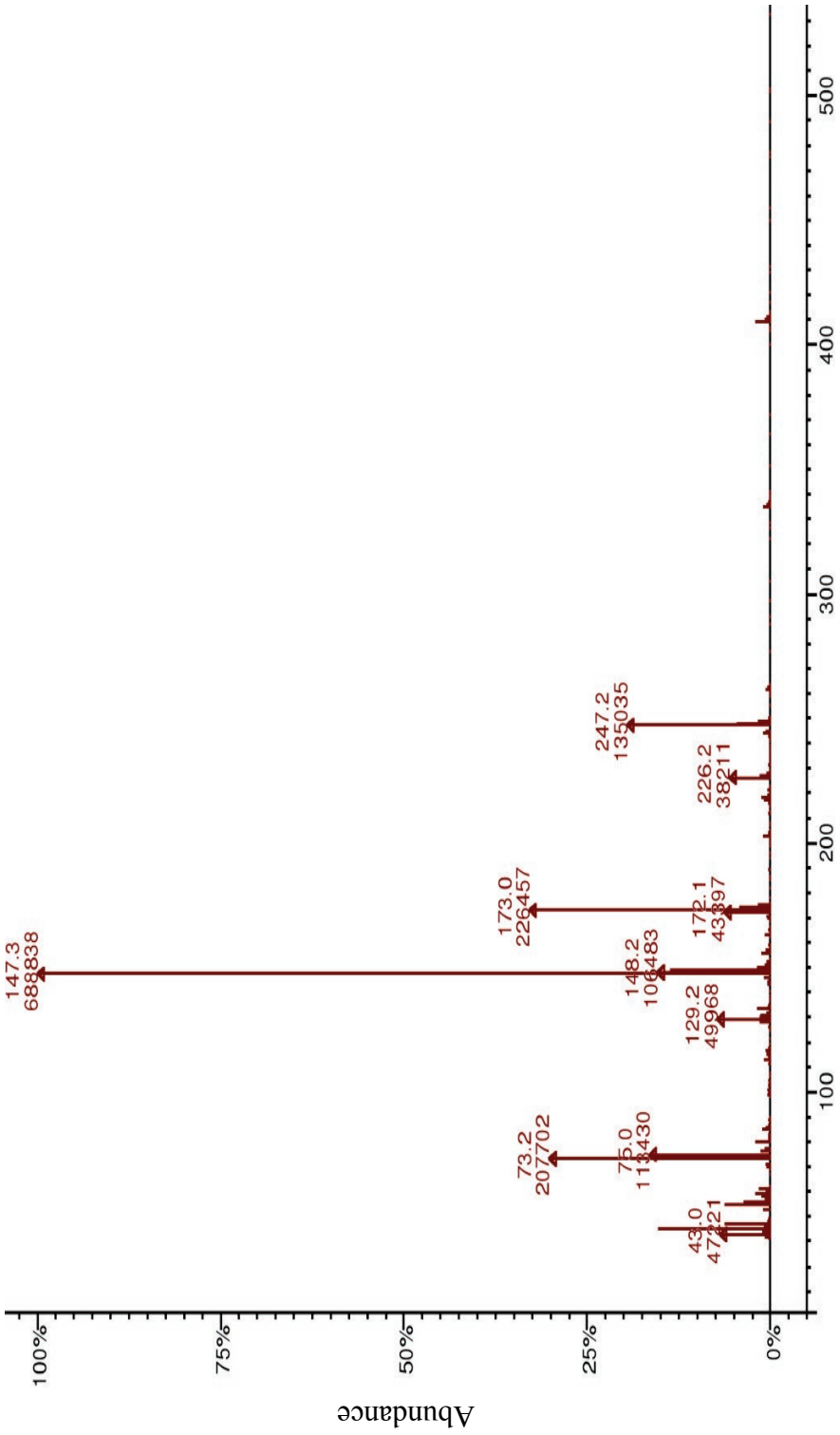

Figure A30 Mass spectrum of sodium succinate

28 Mass spectrum of sodium malate

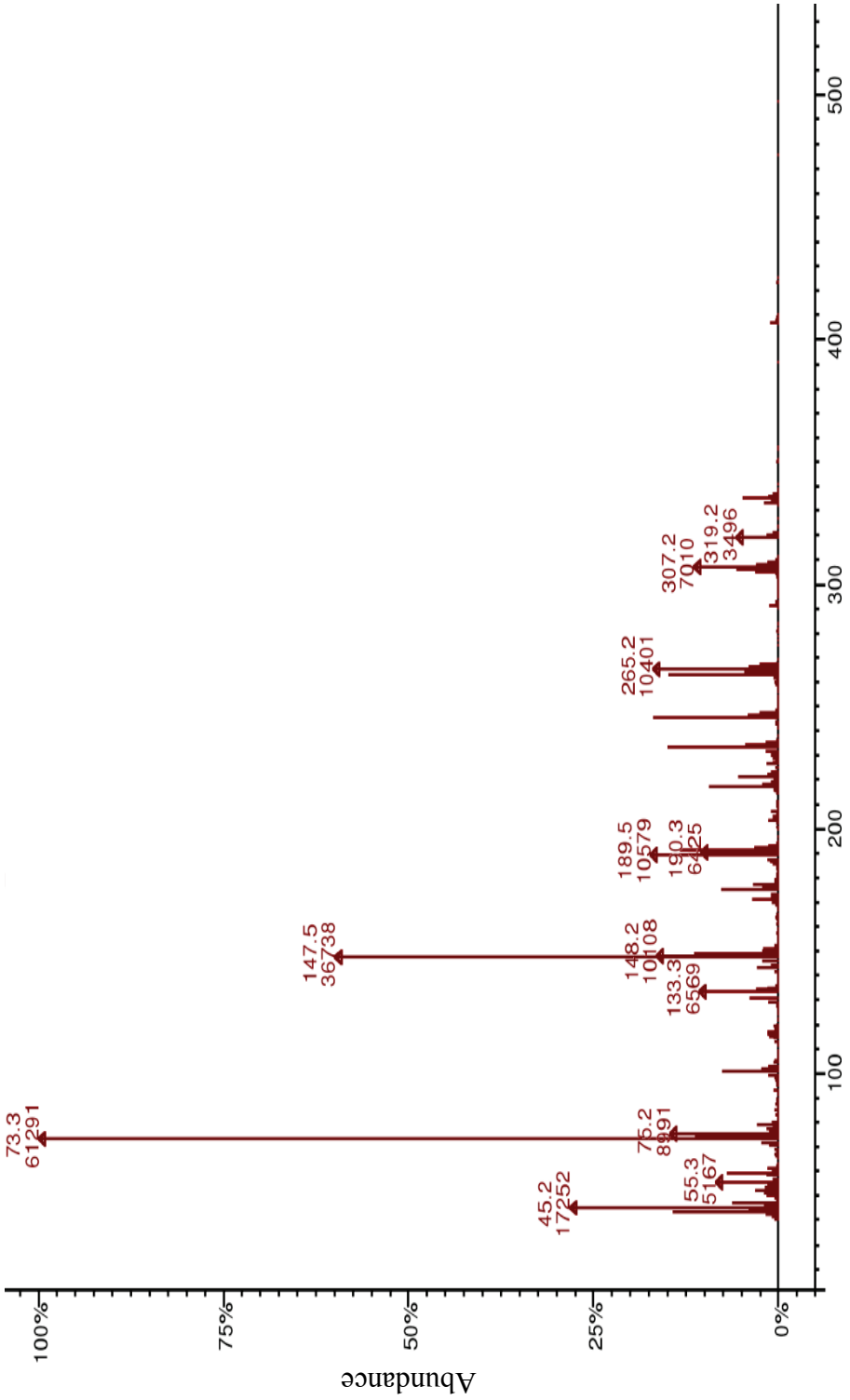

Figure A31 Mass spectrum of sodium malate

29 Mass spectrum of sodium citrate

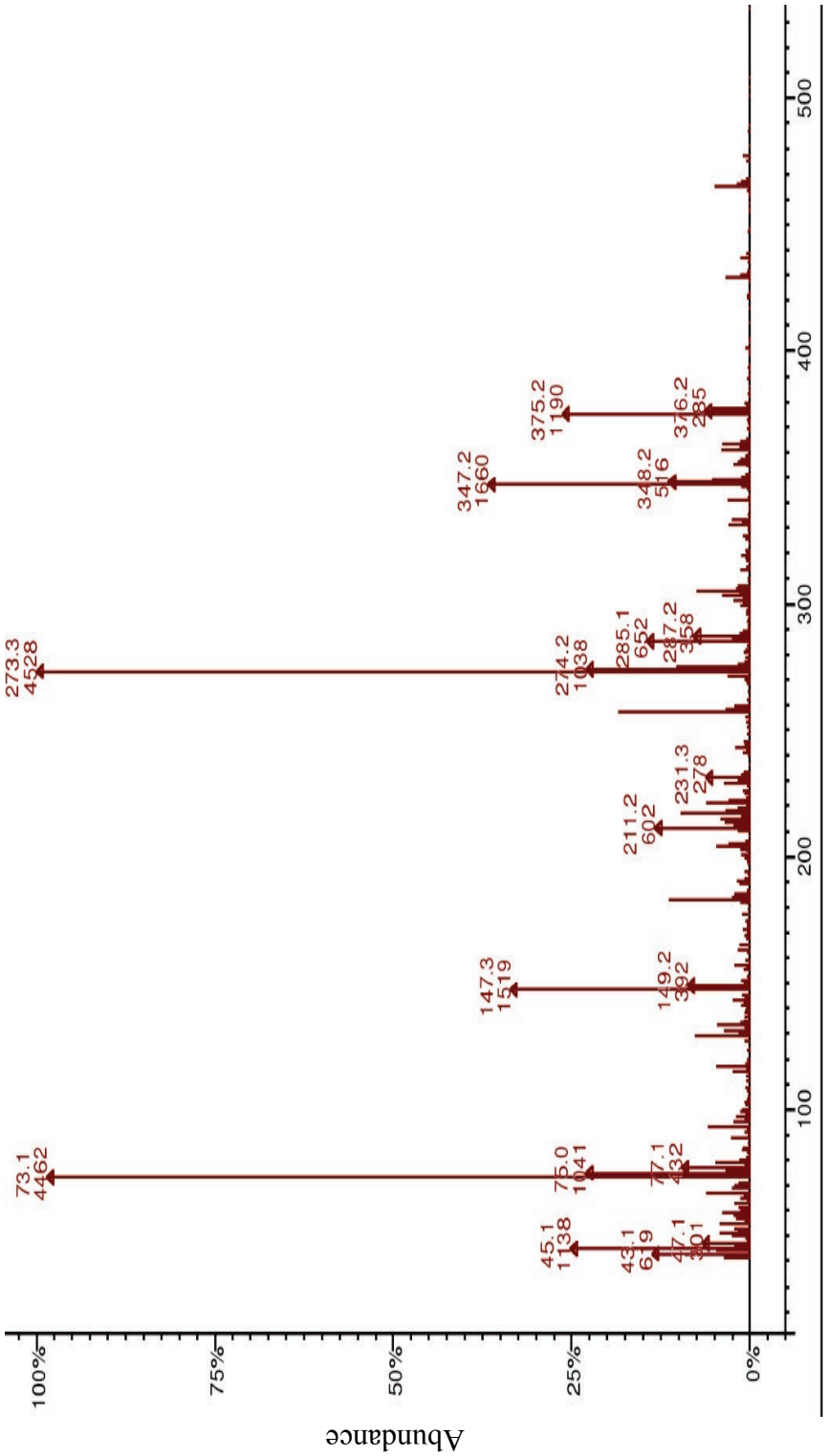

Figure A32 Mass spectrum of sodium citrate

30 GC chromatogram of trimethylsilyl derivatives of organic acids in scutellum

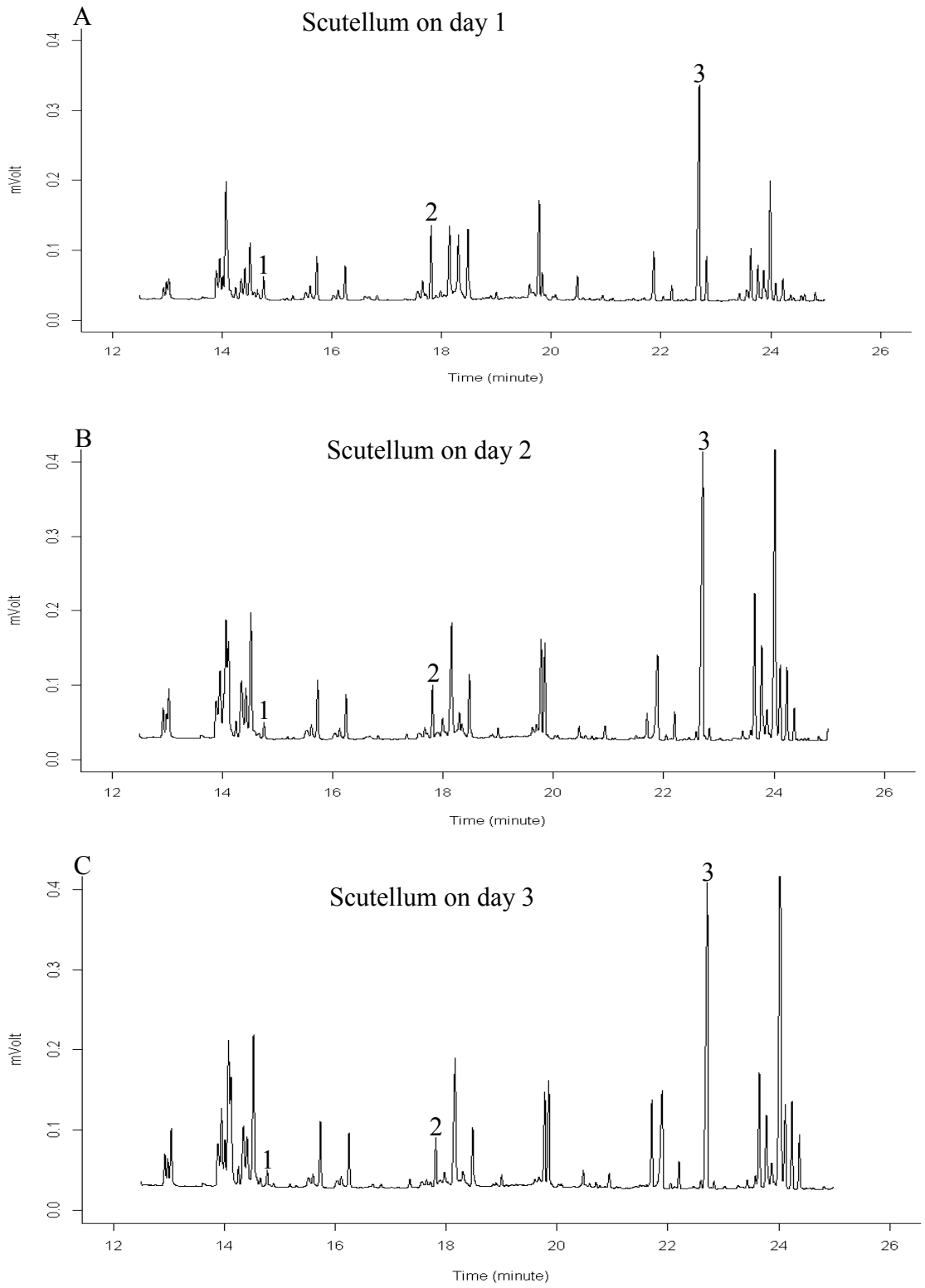

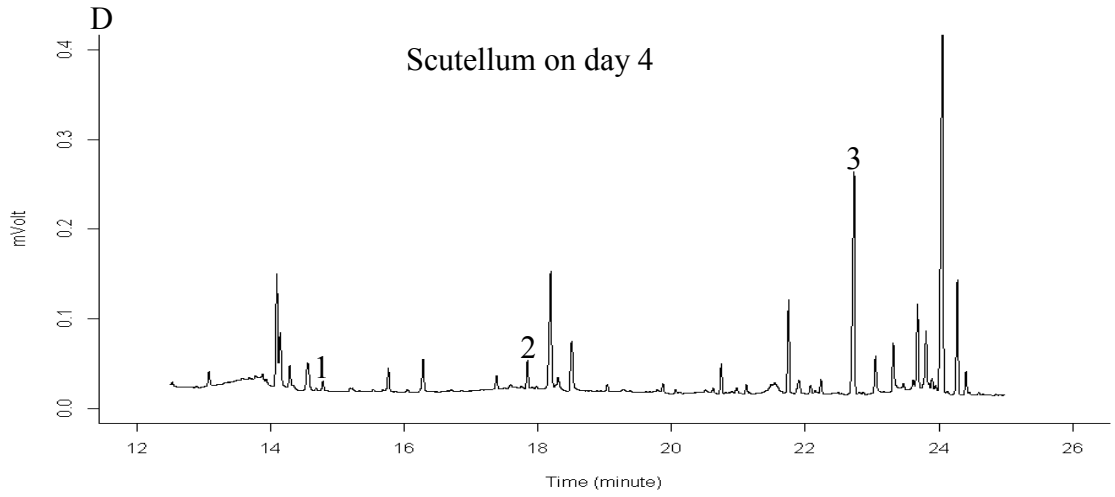
D
Scutellum on day 4
mVolt
Time (minute)
1
2
3

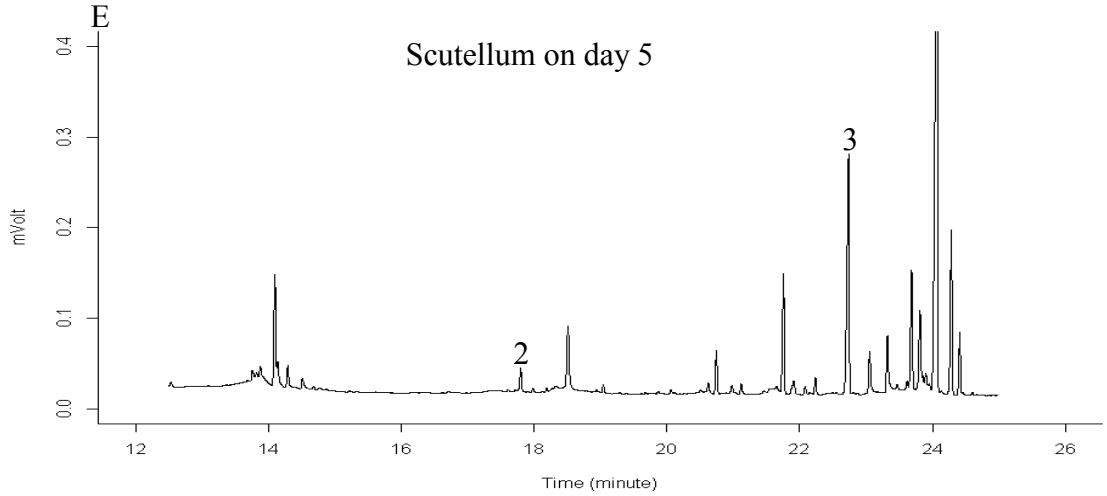
E
Scutellum on day 5
mVolt
Time (minute)
2
3

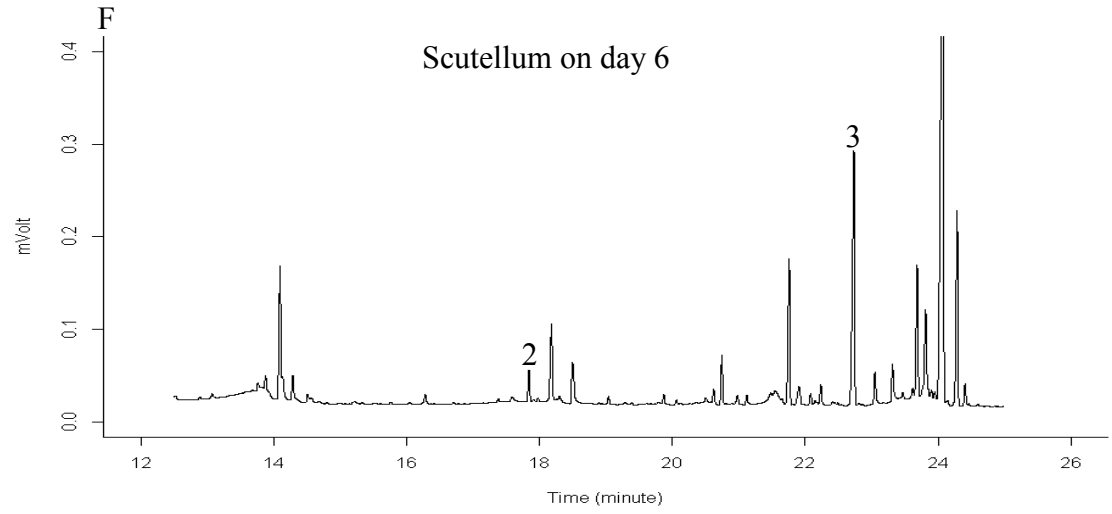
F
Scutellum on day 6
mVolt
Time (minute)
2
3

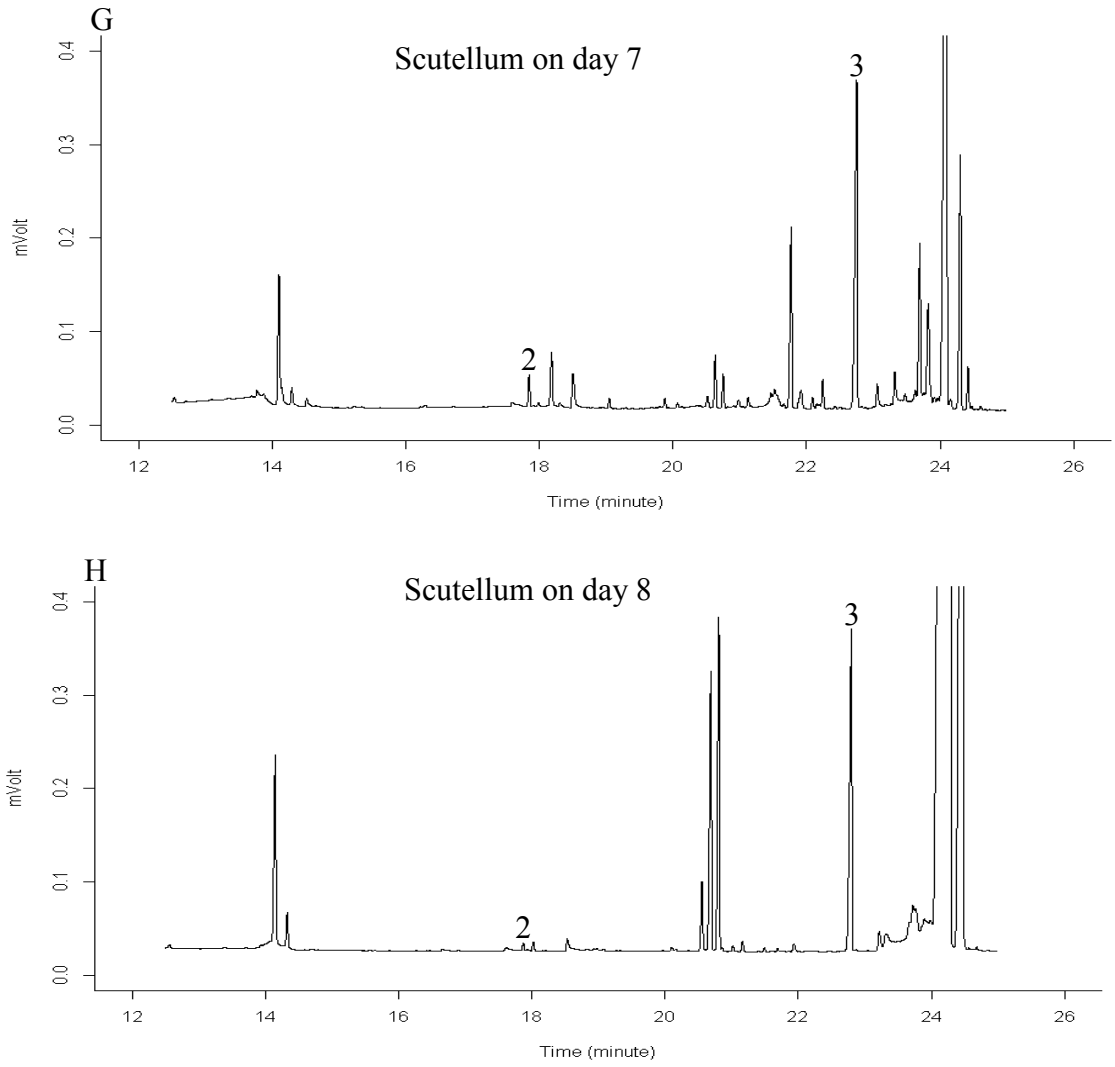

Figure A33 GC chromatograms of trimethylsilyl derivatives of organic acids in scutellum of barley seeds

1: the peak of trimethylsilyl derivatives of succinic acid, 2: the peak of trimethylsilyl derivatives of malic acid, 3: the peak of trimethylsilyl derivatives of citric acid; A, B, C, D, E, F, G, H: scutellum samples on day 1, 2, 3, 4, 5, 6, 7 and 8 respectively.

31 GC chromatogram of trimethylsilyl derivatives of organic acids in endosperm

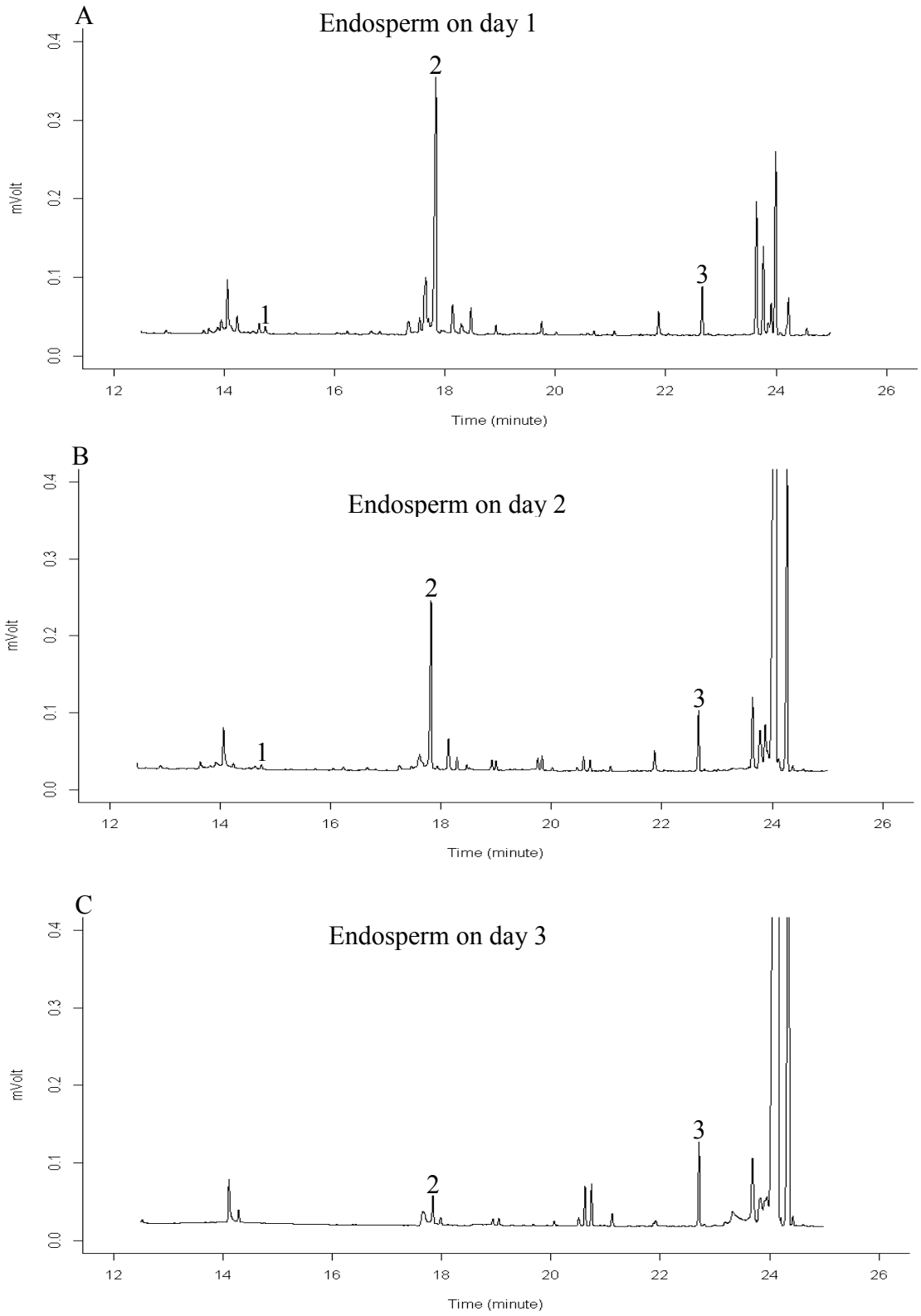

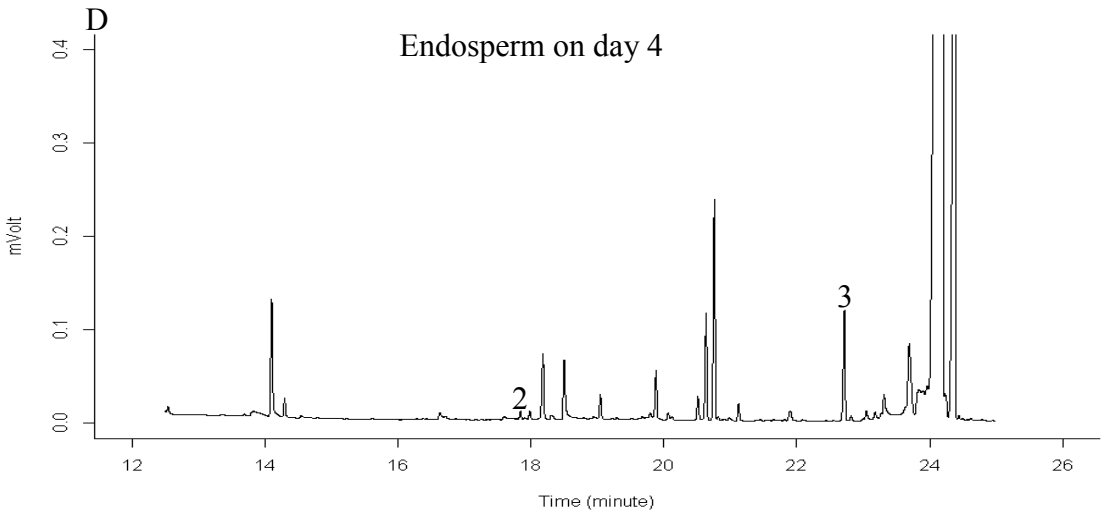
D
Endosperm on day 4
mVolt
0.0
0.1
0.2
0.3
0.4
2
3
12
14
16
18
20
22
24
26
Time (minute)

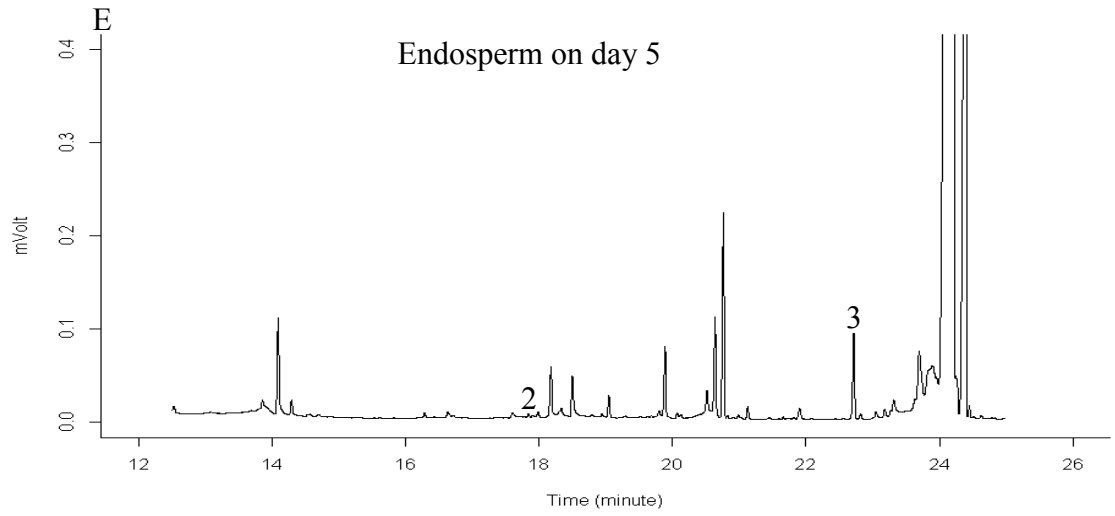
E
Endosperm on day 5
mVolt
0.0
0.1
0.2
0.3
0.4
2
3
12
14
16
18
20
22
24
26
Time (minute)

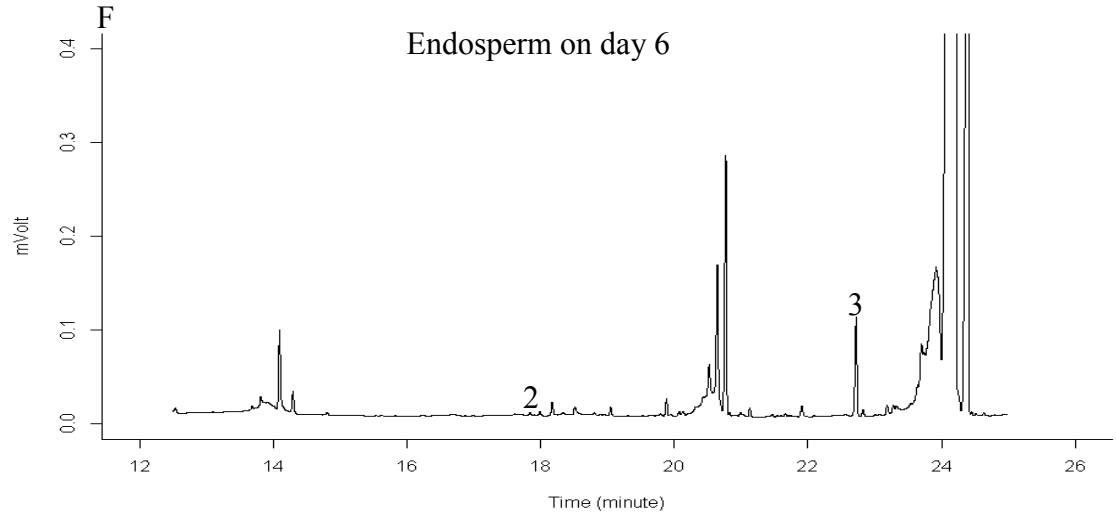
F
Endosperm on day 6
mVolt
0.0
0.1
0.2
0.3
0.4
2
3
12
14
16
18
20
22
24
26
Time (minute)

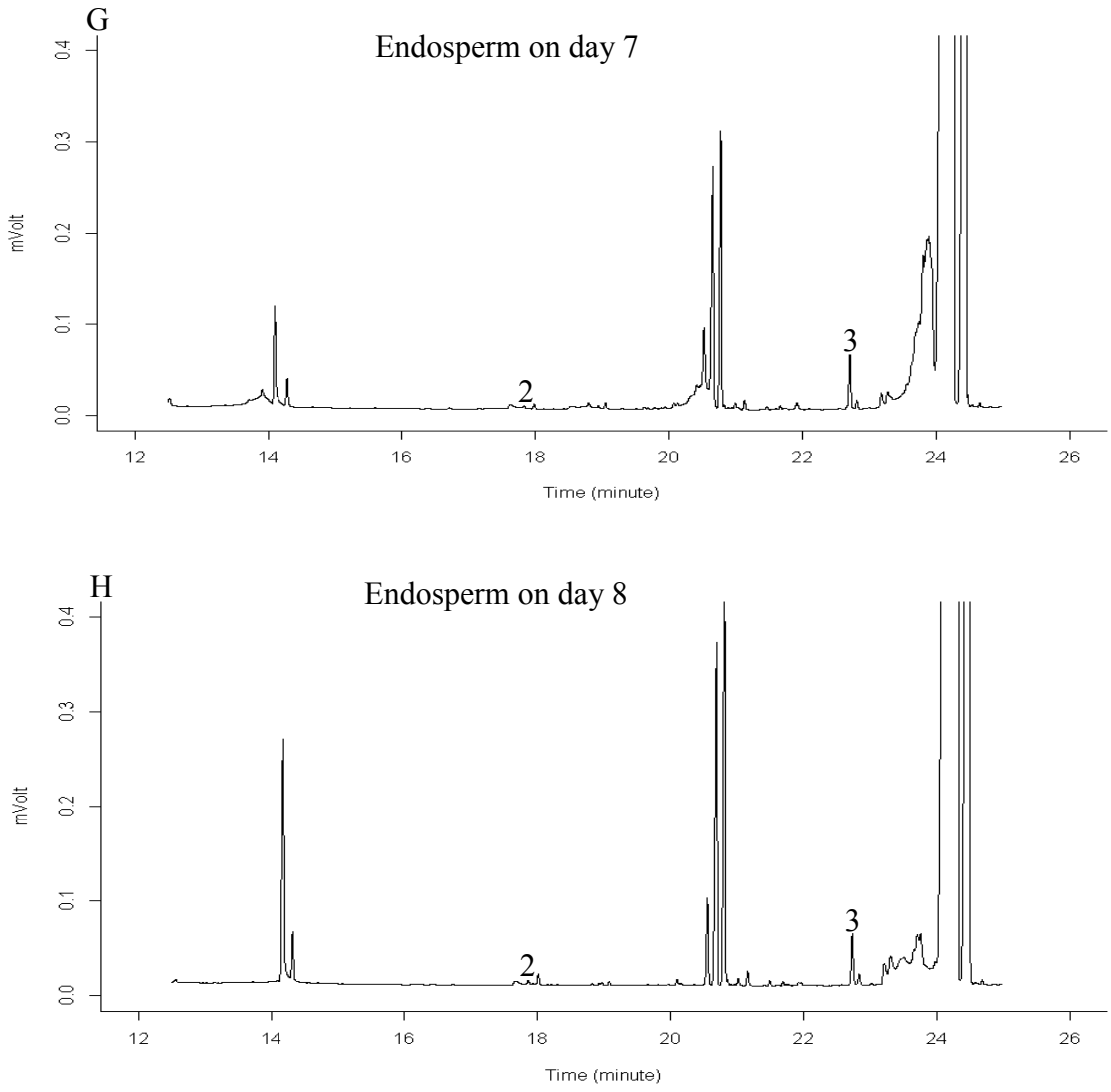

Figure A34 GC chromatograms of trimethylsilyl derivatives of organic acids in endosperm of barley seeds

1: the peak of trimethylsilyl derivatives of succinic acid, 2: the peak of trimethylsilyl derivatives of malic acid, 3: the peak of trimethylsilyl derivatives of citric acid; A, B, C, D, E, F, G, H: endosperm samples on day 1, 2, 3, 4, 5, 6, 7 and 8 respectively.